Understanding variation in tree mortality rates across the tropics

Nicoline Elizabeth Groot

Submitted in accordance with the requirements for the degree of
Doctor of Philosophy

The University of Leeds
School of Geography

August, 2020

The candidate confirms that the work submitted is her own and that appropriate credit has been given where reference has been made to the work of others.

Assertion of moral rights:

Acknowledgements

First and foremost I would like to thank my supervisor Tim Baker for all his support, motivation, patience and feedback, which has been invaluable to me. I am also most grateful for all the support and help provided by Nichola Wood. I owe a great deal of gratitude to Mark Vanderwel's for his helpful guidance and support during my internship and beyond, introducing me to Filzbach, C#, Visual Studio and hierarchical Bayesian analyses. I would like to thank Oliver Phillips, Simon Lewis, Manuel Gloor, and Drew Purves for introducing me to this topic, and for their guidance on the pan-tropical analyses. Mike Kirby, Stephen Sitch and Corinne Le Quere made the CRU data available to me. Andrew Smith has been amazing in trying to get Filzbach running in R.

This thesis would not have been possible without the tremendous fieldwork efforts of countless people, and I am most grateful to everyone who contributed to this in any way. I am thankful to Gabriela Lopez-Gonzalez for her assistance with access to the Forest-Plots.net database, and encouragement to learn SQL. I would also like to thank Georgia Pickavance for helping me to wrap my head around the preparations for and processing of fieldwork forms and data entry into the database. Ted Feldpausch was instrumental in providing me with the opportunity to conduct fieldwork in Guyana, and I am thankful for all his efforts and guidance, as well as his company during the start of the campaign. The fieldwork was made possible through the Guyana Forestry Commission and the Iwokrama International Centre for Rainforest Conservation and Development, and I would especially like to thank Mahendra Baboollal, Dave Kanoo, Marcia Gordon, Shuba Soamandaugh, Andrew Douglas, Mr. Orin Peters, for all their work and company both in preparation for and during the fieldwork, as well as Martijn van Berlo, who joined us for most of it.

Finally, I want to thank all of the amazing people who have made my time here in Leeds enjoyable, be it through visits, support from afar, and/or parcels from family and friends Jack, Liz, Roland, Monique, Wouke, Paul & Ella, Maaike, Ruben, Zita, Ton & Margje, and many others, or through mangoes, grammar lunches, dinners, cupcakes, games, music, hiking, camping, gigs, cycling, coding club, general discussions, and many other activities with housemates and friends, including, but not at all limited to, Sarah, James, Tom, Joey, Marie, Yi-Min, Chris, Julia, Chico, Rakesh, Samadhi, Lamprini, Yannis, León, Michelle, Brenda, Kamla, Jun-Woo, Zora, and most of all Antonio for all his encouragement and support.

I would like to dedicate this thesis to Will and Hellen Taber, who have always been a great inspiration in any way.

Abstract

Old growth tropical forests are an important carbon store, and currently function as a carbon sink. However, this sink capacity may already be declining and its future is highly uncertain, as patterns of tree mortality, one of the key processes shaping the future of tropical forest carbon, are still poorly understood. Accurate estimates of tropical tree mortality require substantial monitoring efforts across time and space, and analytical techniques that can account for variation at multiple scales. Here, I therefore develop Bayesian models to explore how tree mortality rates vary across the tropics and within Amazonia. Firstly, I derive recommendations for the sample size of plot monitoring networks to confidently detect short- and/or long-term changes in tree mortality rates. A key result is that forests with high baseline mortality rates require smaller plot sampling networks to detect a given change, compared to forests with lower rates. Secondly, using observations from an extensive long-term pan-tropical monitoring network, I derive mortality rate distributions at different, nested spatial scales: at the level of individual plots, biogeographical regions and continents. The results show that stem-based mortality rate distributions are best described at the scale of biogeographical regions: for example, forests in North Australia have lower mean mortality rates but suffer occasional larger-scale disturbances, whereas forests in western Amazonia have higher mean mortality rates but few large-scale disturbances. Finally, I test whether the long-term increase in tree mortality rates in Amazonian forests is related to long-term trends in cumulative water deficit. The results confirm a long-term increase in tree mortality rates, but indicate that this trend is not primarily driven by increasing drought stress. Overall, these findings are important for designing efficient national strategies for monitoring the impact of climate change on forests, calibrating vegetation models and predicting the future of tropical carbon under climate change.

Table of Contents

List of Tables

List of Figures

1 Introduction

1.1 Motivation

The terrestrial biosphere has functioned as an important carbon sink over the past half century, with an estimated net annual absorption of around a third (3.2 ± 0.6 GtC $year^{-1}$; ± 1σ) of the carbon dioxide (CO_2) emitted by fossil fuels in the period 2009-2018 (9.5 ± 0.5 GtC $year^{-1}$; Friedlingstein et al., 2019). This sink is the result of more CO_2 being fixed in vegetation during growth and regeneration than is released from land use change, respiration, or mortality events. Globally, the net sink in the terrestrial biosphere has been increasing on average since the 1980s (Friedlingstein et al., 2019). Recent estimates from the terrestrial tropical zone, range from the vegetation functioning as a slight net source of 425.2 ± 92.0 MtC $year^{-1}$ for 2003-2014 from woody carbon density changes estimates using MODIS (Baccini et al., 2017), through a range of estimates from a net vegetation source of 0.5 to a net sink of 0.3 GtC $year^{-1}$ using three atmospheric inversion models for 2009-2018 (Friedlingstein et al., 2019), to a net sink of 0.1 ± 0.4 GtC $year^{-1}$ using process-based models (Friedlingstein et al., 2019). Reducing uncertainty in these estimates to determine the trajectory of the carbon balance of tropical regions is an important research priority.

The carbon balance of intact forest landscapes is a particularly important component of the overall carbon balance of tropical regions. Intact tropical forests have functioned as a gross carbon sink over recent decades, with estimates ranging from 1.19 ± 0.41 GtC $year^{-1}$ for intact forests (1990-2007; Pan et al., 2011) to 1.4 ± 0.8 GtC $year^{-1}$ (1989-2003/7; Sarmiento et al., 2010). However, this sink is threatened by on-going climate change. For example, the observed carbon sink in aboveground biomass in Amazonian forests (Phillips et al., 1998; Baker et al., 2004a; Lewis et al., 2004b) already seems to have been decreasing in magnitude during the past two decades, due to losses from mortality outpacing gains from growth and recruitment (Brienen et al., 2015). The frequency and intensity of droughts has been increasing across Amazonia since the 1950s, and the dry season has increased in duration since 2005 (Marengo et al., 2011). During the 2005 El Niño drought, the old-growth Amazon forests turned from being a net carbon sink into a net carbon source, and released 1.2 to 1.6 GtC, due to increased losses from mortality (Phillips et al., 2009). Understanding the drivers of tree mortality is therefore crucial for predicting the future of the carbon stocks of tropical forests and to determine the effects of any feedbacks between vegetation and climate change.

Improved understanding of tree mortality has also been recognised as an important priority for modelling the future of tropical carbon. Within vegetation models, the mechanisms behind photosynthesis at the leaf level, carbon allocation to vegetation growth, losses through respiration, and their response to increasing temperatures at

different atmospheric CO_2 concentrations are relatively well represented (following e.g. Farquhar et al., 1980; Lloyd and Farquhar, 2008; see e.g. Galbraith et al., 2010; Friend et al., 2014). However, the large-scale processes resulting in aboveground carbon losses, which are mainly driven by the deaths of individual trees, is still largely modelled indirectly as being driven by growth, supplemented by age- and stress-induced mortality and prescribed stochastic disturbances to account for fires and wind throws (Cramer et al., 2001; Galbraith et al., 2013; Bugmann et al., 2019). A recent review has found that predictions of tree mortality in these dynamic vegetation models are the main determinant of the modelled response of forest dynamics to climate change (Bugmann et al., 2019). To improve these predictions, we need to quantify baselines of tropical tree mortality, provide insights into how mortality varies spatially, and ensure monitoring programmes can reliably detect on-going and future changes.

1.2 An introduction to tropical tree mortality

1.2.1 Longevity and death

In order to discuss tree mortality, it is important to first consider the perhaps surprisingly complex issue of when an individual tree can be considered to have died. Though an individual tree is only considered dead when all its cells have died, even in healthy, growing, adult trees, only a small proportion of their cells are alive (e.g. ca. 10 % in a live conifer; Franklin et al., 1987). For example, the interior heartwood might already be considered dead, and in some cases even have been decomposed partially or completely, despite the individual still being fully alive (Westing, 1964; Franklin et al., 1987). Furthermore, a live individual can lose significant portions of its overall biomass through loss of parts of its crown or stem(s), following disturbances (e.g. hurricanes; Bellingham et al., 1995), or the fall of neighbouring trees (Franklin et al., 1987). Trees also have remarkable regenerative properties, where just a remaining intact apical root or shoot meristem may suffice to ensure survival (Munné-Bosch, 2014). Despite this complexity, studies of tree mortality need to assign trees a binary “alive” or “dead” status, and therefore from a biomass perspective, the shift of its overall biomass from the living to the dead carbon pool is generally assumed to fully occur at the moment of the individual’s actual demise (Franklin et al., 1987).

There are various senescence-related factors that can contribute to eventual tree death, and these processes are best studied in the most long-lived trees. For example, through clonal propagation, individual clones of e.g. quaking aspen (*Populus tremuloides*) have managed to persist for over ten thousand years (Mitton and Grant, 1996) and non-clonal individual trees can also reach lifespans of thousands of years, with a record age of 5,062 years ascribed to a living bristlecone pine (*Pinus longaeva*; Munné-Bosch, 2014). Even in the tropics, the maximum estimated longevities for most species is in the order of

hundreds of years (Laurance et al., 2004), with some individuals reaching ages of 1,400 years (Chambers et al., 1998). If individual non-clonal trees can reach ages of thousands of years, what then could cause these individuals to eventually die? Westing (1964) proposed the following four mechanisms: the ratio of leaves to living mass to maintain becomes increasingly more unfavourable as a tree grows; through a build-up of inhibiting compounds or a lack of essential compounds over time; decay of heartwood can lead to a loss of structural integrity of the tree; or finally through meristem cells becoming increasingly damaged by background radiation. Any of these processes could reduce a tree's resistance to external mortality agents and disturbances. As such, there is still considerable debate about whether trees ever die of senescence alone (Mencuccini et al., 2005; Caswell and Salguero-Gómez, 2013; Munné-Bosch, 2014), and few studies address senescence explicitly, other than as an assumed decrease of overall tree 'vigour'.

1.2.2 Drivers of tree mortality

The causes of tree mortality, also known as mortality drivers, can be categorised in a number of ways. For example, one could distinguish between mortality resulting from endogenous or exogenous drivers, with the former encompassing mortality due to senescence and the latter covering, for example, mortality caused by environmental disturbances or attacks by biotic agents (Lugo and Scatena, 1996). It is also possible to split exogenous drivers into biotic (e.g. insect or fungal attacks, as well as competition and senescence) and abiotic processes, such as environmental disturbances and stresses (Franklin et al., 1987; van der Sande et al., 2017).

Tree mortality will generally be the result of various drivers acting consecutively or concurrently, even across these dichotomies (Franklin et al., 1987). For example, in a piñon-juniper woodland experiencing a drought lasting for 10 months, all piñon pines (*Pinus edulis*) that died had been infested by bark beetles (*Ips confusus*). The infestation did not occur until 8 months into the drought period (Breshears et al., 2009), leading some studies (e.g. Bendix et al., 2006; Hood et al., 2018) to make a distinction between the proximate drivers of mortality (i.e. the drought; see also Anderegg et al., 2012), and the ultimate drivers of mortality (i.e. the bark beetle infestation). While in this case the distinction seems straightforward, in other cases it might be much harder to disentangle which factor was mainly responsible for a tree's demise, or even impossible to separate the factors at all. As such, the "spiral of death" as proposed by Franklin et al. (1987) seems a more realistic representation of how drivers can collectively contribute to eventual tree mortality: any driver can weaken a tree, but at any point the tree has the opportunity to escape the spiral and recover; however as the tree progresses further down the spiral, these opportunities for recovery diminish.

How a tree dies, i.e. the "mode of death", can provide information on what might have caused the tree to die. Generally, the following main modes of tree mortality are distinguished: 'broken' (also crushed or snapped), 'uprooted', and 'standing' (Chao and Phillips, 2005; Martini et al., 2008). If a lateral force is exerted on a tree's crown or stem (e.g. through wind, rainfall, or the falling of a neighbouring tree), this can result in a tree dying broken or uprooted (Putz et al., 1983). When the stem of a tree is not strong enough to withstand the force, due to it having a smaller diameter, the heartwood having been weakened or partially decomposed by biotic agents, or the wood density being lower, the tree will break (Putz et al., 1983; Arriaga, 2000; Chao et al., 2009; Vozmishcheva et al., 2019). For example, in a forest in northern New York state, beech trees severely infected with beech bark disease were nearly twice as likely to die snapped than uprooted, following the 1995 storm (Papaik and Canham, 2006). However, if the stem can withstand the force, but the force exceeds the soil shear strength, or causes the roots to break or lose their grip on the soil, the tree will be uprooted (Putz et al., 1983). While the probability of this kind of event varies greatly among sites, according to local climate, soil type and topography, this tends to occur more on sandy soils, on slopes, when rooting depths are shallow, or when soils are waterlogged (Gale and Hall, 2001; Chao et al., 2009; Toledo et al., 2013). Furthermore, a broken or uprooted tree has the potential to crush or uproot other trees as well, leading to a multiple tree-fall event. For example, a study in Ecuador found 36 % of tree death events across four 2.5 hectare transects involved up to 14 trees (Gale and Barfod, 1999). Finally, various drivers, such as senescence, competition for nutrients and light, fire, lightning, drought or an attack by biotic agents, can result in a standing dead tree (Putz et al., 1983; Gale and Barfod, 1999; Gale and Hall, 2001). However, it can be challenging to correctly identify the mode of death, especially with long census interval lengths, because trees that have died standing can still get snapped or uprooted after death (Hennon and McClellan, 2003; Chao and Phillips, 2005).

Drought

During the 21st century, drought has arguably been the most pervasive catastrophic driver of tree mortality worldwide, with recent evidence from boreal (e.g. Peng et al., 2011; Ma et al., 2012; Searle and Chen, 2017; Hisano et al., 2019), and temperate (Villalba and Veblen, 1998; van Mantgem and Stephenson, 2007; Williams et al., 2010; Zhang et al., 2014; Moore et al., 2016; Klockow et al., 2018; Archambeau et al., 2020), as well as tropical forests (Condit et al., 1995; Williamson et al., 2000; Aiba and Kitayama, 2002; van Nieuwstadt and Sheil, 2005; Chazdon et al., 2005; Itoh et al., 2012; Aleixo et al., 2019). Furthermore, the frequency and severity of droughts, as well as the area affected by them, is expected to increase with a changing climate (Marengo et al., 2012; Dai, 2013; Trenberth et al., 2014; Duffy et al., 2015; Allen et al., 2015; Naumann et al., 2018). However, despite numerous studies of drought responses ranging from observations of elevated mortality

rates in the field, responses of potted plants, plants in greenhouse tunnels or in the Biosphere 2 vivarium (e.g. Adams et al., 2009; Anderegg, 2012; Garcia-Forner et al., 2017; MacAllister et al., 2019), to rainfall-exclusion experiments in the field (e.g. Nepstad et al., 2007; Misson et al., 2010; Plaut et al., 2012; Moser et al., 2014), the exact mechanism of how drought leads to mortality in some species, but not others, is still actively debated. This uncertainty is mainly due to the challenges of monitoring all potential pathways of drought stress in a non-invasive, non-destructive way in both those individuals that have managed to survive the drought and those that eventually succumb, as well as the degree of representativeness of such experiments, often conducted on saplings and seedlings, of how natural drought affects mature trees in the field.

For some years, the prevalent notion has been that there are two mechanisms of drought-induced tree mortality (Bréda et al., 2006; McDowell et al., 2008; Adams et al., 2009; Anderegg et al., 2012b; Mitchell et al., 2013; Sevanto et al., 2014; Garcia-Forner et al., 2017; Hartmann et al., 2018), with mortality occurring as a result of carbon starvation ("drought avoidance"), or hydraulic failure ("drought tolerance") due to cavitation in the xylem conduit or a hydraulic disconnect between the roots and the rhizosphere (Mackay et al., 2015). Isohydric species are generally presented as exhibiting a drought avoidance strategy, consisting of stomatal closure at a threshold water potential to minimize further water loss through transpiration. The suggested disadvantage of this strategy is that it might also limit the potential for carbon exchange, resulting in reduced carbon assimilation (McDowell et al., 2008). Combined with continued respiration costs, or even potentially increased respiration due to the higher temperatures, this strategy could eventually lead to death from carbon starvation, if the drought persists over a prolonged period of time (McDowell et al., 2008). In contrast, anisohydric species are believed to follow a drought tolerance strategy, which allows them to continue transpiration and carbon assimilation, despite reduced soil water availability (McDowell et al., 2008). However, this strategy is believed to carry the risk of cavitation in the xylem, if evapotranspiration causes xylem water potential to exceed critical cavitation thresholds. Cavitation results in air bubbles blocking stem water transport, and ultimately leads to desiccation of plant tissues (Bréda et al., 2006; McDowell et al., 2008).

A subsequent refinement of these two mechanisms (McDowell, 2011; McDowell et al., 2011) added more explicit interdependence and feedbacks between them. For example, a lack of non-structural carbohydrates might hamper refilling of embolized xylem conduits in a species with suspended carbon assimilation and can thus lead to hydraulic failure. Conversely, partial hydraulic failure in a species with continued evapotranspiration may lead to carbon starvation through reduced photosynthesis and reduced transport of water and carbohydrates to the relevant tissues. Although this interdependence between carbon starvation and hydraulic failure addresses some concerns (e.g. Sala, 2009; Sala et al., 2010),

overall, the original carbon starvation hypothesis as proposed by McDowell et al. (2008), where the size of the stored carbon pool determines how long the tree can survive before it succumbs to carbon starvation, is challenging to prove, and has still not been fully accepted (O'Grady et al., 2013; Meir et al., 2015; Hartmann et al., 2018).

In particular, it is unclear whether a tree can actually die of carbon starvation in a natural drought setting, since, when observed in an experimental setting, plants with depleted carbon stores had generally obtained adequate water to continue transport between tissues. This in contrast to hydraulic failure, for which evidence has been observed in field settings. For example, in a multilevel mixed effects model in a worldwide meta-analysis of drought- and heat-induced tree mortality, a narrow hydraulic safety margin and the xylem water potentials at which 50 % respectively 80 % of hydraulic conductivity is lost, were the only significant predictors of tree mortality across all species (Anderegg et al., 2016a). Similarly, a recent synthesis of evidence from experimental and observational studies found all trees which suffered drought-induced mortality to have lost of more than half of their xylem conductivity (Adams et al., 2017). In contrast, a lower presence of non-structural carbohydrates (NSC) in plant tissues was only found in 62 % of trees that died (Adams et al., 2017). However, when wanting to address potential depletion of carbon stores, it is important to take all plant tissues into account, since a localised effect might occur, especially if transportation between tissues is affected or reallocation towards other tissues like roots occurs (Nolan et al., 2017; Kannenberg et al., 2018). Evidence of a decrease in carbon stores in one or a few tissues, need not necessarily confirm a carbon starvation-induced mortality mechanism (Adams et al., 2017). For example, in an experimental set-up with Norway spruce trees, only root carbon stores were found to have decreased in trees that died, apparently as a result of impaired transport (Hartmann et al., 2013b). An experiment designed to specifically address carbon starvation versus hydraulic failure as a mortality mechanism, found that only well-watered individuals were able to exhaust carbon stores completely prior to death, and water-deprivation resulted in saplings dying faster, than when starved of carbon (Hartmann et al., 2013a). It therefore seems carbon might be used for maintaining transport under water-limited conditions (Sala et al., 2012). However, a role might also be reserved for carbon in the post-drought recovery ability of individuals (Sala et al., 2012), as evidenced by a significant recovery of hydraulic conductivity following rehydration in seven out of 12 broadleaf species (Trifilò et al., 2019).

Another point of contention stems from the proposed links between the different drought response mechanisms and species classified as being either isohydric or anisohydric (O'Grady et al., 2013; Sevanto et al., 2014; Garcia-Forner et al., 2017; Hochberg et al., 2018). Firstly, there seem to be various, sometimes conflicting, definitions concerning the classification of (an)isohydry (Nolan et al., 2017; Hochberg et al., 2018; Ratzmann et al.,

2019). Secondly, while genotype might play some role in the suite of hydraulic response mechanisms available to an individual, the environment seems to have a greater effect on whether an individual will display a more "(an)isohydric" response in a given environmental setting (Hochberg et al., 2018). In some cases, even individuals exposed to repeated droughts display a more (an)isohydric strategy, in response to an experimental drought, compared to individuals of the same species that have never previously been exposed to drought-like environmental conditions (Nolan et al., 2017). Furthermore, a study combining field observations and an experimental approach failed to identify differences in growth or carbon stores between species exhibiting supposedly opposing isohydric strategies (Garcia-Forner et al., 2017). This result is similar to the observed lack of differences in either growth or carbon stores between droughted and non-droughted trees in a long-term throughfall exclusion experiment (Rowland et al., 2015). Using different metrics might lead to less ambiguous hydraulic strategy classifications (Mencuccini et al., 2015; Nolan et al., 2017; Hochberg et al., 2018; Ratzmann et al., 2019; Martinez-Vilalta et al., 2019). At the very least, it seems that (an)isohydry represents a continuum of hydraulic control strategies both within and among species (e.g. Parolari et al., 2014; Roman et al., 2015; Skelton et al., 2015; Sperry and Love, 2015; Mencuccini et al., 2015; Nolan et al., 2017).

An alternative framework for considering how drought- and heat-induced water stresses can cause a tree to pass a threshold after which recovery is no longer possible, focuses on an individual's overall water resource use balance (Anderegg et al., 2012a; Martinez-Vilalta et al., 2019). Rather than explicitly addressing carbon starvation or hydraulic failure, this approach allows for both as consequences of any accumulated "water debt" or lower "relative water content". Using such a framework could help explain observations of lagged mortality following a drought (Drobyshev et al., 2007; Hiernaux et al., 2009; Suresh et al., 2010; Phillips et al., 2010; Anderegg et al., 2013; Aleixo et al., 2019), increased vulnerability to future disturbances (e.g. Mueller et al., 2005), and why trees have been observed to recover from droughts upon subsequent rewetting (e.g. Hartmann et al., 2013; Gu et al., 2015). Another perspective is that drought-induced mortality is a result of resource competition, with drought killing the competitively suppressed individuals in cases of resource scarcity. Some evidence for this ideas was found in Texan Ashe juniper woodlands where density-dependent parameters were the main predictors of crown death of the dominant species during drought (Crouchet et al., 2019). As such, future droughts would merely accelerate existing forest dynamics, rather than lead to catastrophic dieback. Finally, while most focus has been on carbon starvation and hydraulic failure as drought-induced mortality mechanisms, the high temperatures frequently accompanying droughts might also reserve a role for heat-induced tissue damage as a mortality mechanism (O'Grady et al., 2013; Teskey et al., 2015).

Fire

Carbon dating of charcoal from soil layers suggest that fire return intervals in tropical rainforests historically used to be hundreds or thousands of years, mostly corresponding to periods with drier climatic conditions (Sanford et al., 1985; Goldammer and Seibert, 1989). Increasing deforestation pressures, and burning of nearby agricultural land or pastures, means that concurrently with the increasing frequency and severity of droughts, the incidences of tropical rainforest fires have been increasing in magnitude and occurrence over the past few decades, and are expected to keep increasing (Cochrane, 2003). Over two decades ago the regional fire rotations in the "arc of deforestation" in the Brazilian Amazon had already been estimated to have decreased to 7-14 years, up to a few decades, or 125 years at most, except in the wetter, aseasonal part (Cochrane et al., 1999).

Normally, in an undisturbed tropical rainforest, only the drier fuel load present in local tree-fall gaps, generally representing less than 5 % of forest cover, becomes susceptible to burning after 16 days without precipitation (Cochrane, 2001). Deforestation causes a more open canopy, as well as an increased fuel load, that is able to dry out better, and as such allows fires to do much more damage, with increasing and drier fuel loads and decreasing canopy covers, upon each return (Uhl, 1998; Cochrane et al., 1999). During an initial fire, generally only circa 40 % of trees of over 10 centimetres diameter at breast height (dbh; corresponding to about 10 % of biomass) will be killed, since the fire will pass through the forest quickly enough to spare the larger trees with a slightly thicker bark (Cochrane, 2001). Upon a second burning, due to the increased fuel load and a reduction of around 40 % in original canopy cover (Cochrane, 2001), the fire can burn ten times more intensely (Cochrane, 2003) and for longer, thus also killing larger trees (with the same reduction of 40 % of trees now corresponding to 40 % of biomass), and reduce canopy cover to 35 % of its original levels (Cochrane, 2001). In Africa, Asia and Australia, due to the presence of species with thicker bark, these reductions might progress less rapidly (trees >10 cm dbh had around 8-15 % mortality in unlogged forests in West Africa and Kalimantan following fires (Wirawan, 1983 (unpublished) in Goldammer and Seibert, 1990; Swaine, 1992). With a bark thickness of 5.9 mm a tree has a 50 % chance of surviving a low-intensity fires, whereas for the same chance of surviving high-intensity fires it would need a bark of 9.1 mm (Hoffmann et al., 2012a). Nonetheless, the same process of canopy opening and subsequent warming and drying of the understory allows for invasion by highly flammable vegetation like grasses in all tropical forests (Jackson, 1968; Cochrane, 2001; Hoffmann et al., 2012b; Aubréville, 2013; Dwomoh and Wimberly, 2017). This invasion means that during subsequent fires, any remaining trees become susceptible to being killed too (Cochrane, 2001), while it also prevents successful reestablishment of higher wood density and shade-tolerant forest species (Jackson, 1968; Barlow and Peres, 2008; Aubréville, 2013; Dwomoh and Wimberly, 2017; Silva et al., 2018).

The most direct mechanism through which fire has been proposed to kill trees, is through cambium necrosis. Thicker-barked individuals have been found to be better protected against this process (e.g. Stephens and Finney, 2002; Cochrane, 2003; van Nieuwstadt and Sheil, 2005; Jones et al., 2006; Lawes et al., 2011; Balch et al., 2011; Brando et al., 2012; Poorter et al., 2014; Hood et al., 2018). With increasing fire intensity or flame residence time, the likelihood of heat-induced damage to, or death of, phloem and vascular cambium increases (Cochrane, 2003; Bova and Dickinson, 2005; Michaletz and Johnson, 2007). If the damage occurs around the entire circumference of a tree, effectively girdling the tree, no transport of photosynthates to the roots will occur (Cochrane, 2003; Michaletz and Johnson, 2007). As such the roots will eventually starve, which in turn will lead to hydraulic failure (Michaletz and Johnson, 2007). Recently, evidence has also been established for fire-induced decreases in xylem conductivity, through cavitation resulting from heat-induced decreases in sap surface tension, and heat-induced permanent deformations of xylem conduit walls (Michaletz et al., 2012; West et al., 2016). Furthermore, fire plumes could cause xylem cavitation, by increasing vapour pressure deficits so rapidly, that even trees with thicker bark might not be able to close their stomata to prevent the corresponding increased transpiration rates (West et al., 2016). This could potentially explain why a lagged mortality of up to three years has been observed for larger individuals following a fire (Barlow et al., 2003b; Baker et al., 2008), especially since evidence for a potential trade-off between thicker bark and embolism resistance has been identified (Resco de Dios et al., 2018).

Increased fire-induced tropical tree mortality has been observed during exceptional drought years (e.g. Barlow et al., 2003a; Aragão et al., 2007; Brando et al., 2012; Granzow-de la Cerda et al., 2012; Brando et al., 2014; Gatti et al., 2014; Anderson et al., 2015; Silva Junior et al., 2019), and with increasing deforestation and fragmentation (e.g. Cochrane et al., 1999; Cochrane, 2001; Brando et al., 2012; Grégoire et al., 2013; Brando et al., 2014; de Andrade et al., 2020). As such, future mortality from fires is expected to increase (Laurance and Williamson, 2001; Cochrane, 2003; Silva Junior et al., 2019). The moist forests in the seasonal parts of the Neotropics are amongst the most vulnerable to mortality from predicted future fires (Meir and Woodward, 2010; Pellegrini et al., 2017). At fire return intervals of 50-70 years, mainly shrub vegetation will dominate, and at 12-25 years, the vegetation will become completely open (Jackson, 1968), suggesting a possibility of rainforests transitioning to seasonal forests, savannahs or grasslands under increasingly fire-prone conditions (Laurance and Williamson, 2001; Malhi et al., 2009; Veldman and Putz, 2011; Aubréville, 2013; Brando et al., 2014; Dwomoh and Wimberly, 2017).

Lightning

While lightning is most prevalent in the tropics, the moist conditions of the air and fuel in tropical rainforests are generally not conducive to ignition of fires from lightning strikes

(Stott, 2000). Lightning will rarely result in a fire, unless it occurs towards the end of the dry season, when thunderstorms tend to be less accompanied by rainfall (Stott, 2000), and even then it might not affect more than a few trees. For instance, in Gabon, Tutin et al. (1996) observed that the locally tallest emergent tree (40 m tall, and 1.3 m wide at 1 m height) was struck by lightning, and caught fire, despite having high density wood and lacking flammable resins. However, its trunk and major branches were hollow, and host to both a large strangler fig and liana. Nonetheless, while the fire completely consumed the stricken individual, the main source of damage to the surrounding trees was from the collapse of its crown, killing one tree by snapping it and defoliating seven other neighbouring trees by 10-90 %. Combined with the heat from the fire, this resulted in the immediate death of another tree, with the largest of the remaining six trees dying broken five months later, at a point which had been exposed to the heat of the original fire. Interestingly, in general, through their lower resistivity, lianas might actually protect trees from lightning damage, with larger individuals and trees with greater electrical resistance predicted to benefit relatively more from this potential liana lightning protection mechanism (Gora et al., 2017).

Lightning with a high peak current can cause steam explosions in the vascular cambium, resulting in a lightning scar (Gora et al., 2017), though such lightning scars are rarely observed in the tropics (Price, 2017). As such, in the absence of these scars or lightning-induced fire, it has proved difficult to identify and thus quantify and understand the importance and mechanism of lightning as a driver of tree mortality in tropical forests (Yanoviak et al., 2017; Price, 2017). Lightning is believed to have resulted in the mortality of groups of circa 12-15 canopy and most of the understorey individuals of various sizes (up to 73 cm dbh) and from different species in a tropical forest in central Amazonia, creating gaps of 280, 600 and 680 m^2, across a range of soils and topographies (Magnusson et al., 1996). This result matches estimates from a recent study specifically investigating lightning damage in central Panama, which found that each of 32 registered lightning strikes directly (within 11-13 months) killed 3.5 trees on average (0.94 of which >60 cm dbh; cf. 2), and damaged a further 11.4, including 2.13 trees of over 60 cm dbh (Yanoviak et al., 2020), and another central Amazonian study which found lightning had killed 3 individuals of >10 cm dbh of more than one species, as well as most of the understorey trees (Fontes et al., 2018). An earlier study from Indonesia also identified numerous suspected lightning-induced tree mortality events, where multiple individuals in close proximity to each other from usually different species had mostly died standing, as well individual events where trunks did appear shattered, split or charred (Whittaker et al., 1998). The leaves of the canopy trees were observed to have fallen (Magnusson et al., 1996; Whittaker et al., 1998), with trees on the edge of the circle only having been defoliated on the side facing it (Whittaker et al., 1998). This result matches observations from a previous Panamanian study, which found that the only characteristic present in all

11 registered lightning strike events was flashover foliage damage (Yanoviak et al., 2017), and the more recent study identifying >50 % crown dieback in 14 % of damaged individuals, and 25-50 % crown dieback in a further 18 % (Yanoviak et al., 2020). Other commonly observed characteristics included damaged lianas (91 %, n=11); scorched, wilting and dying hemi-epiphytes (67 %, n=6) and at around 2-4 months following the lightning strike beetle infestations (55 %, n=11; Yanoviak et al., 2017). These patterns match observations from the suspected Indonesian lightning-induced mortality events, where, in addition to understory mortality, death of "stem creepers" had occurred too (Whittaker et al., 1998).

Combined with the fact that lightning strikes are common during the wet season in central Amazonian and Panamanian tropical forests (Magnusson et al., 1996; Yanoviak et al., 2017), it seems currently most tropical tree mortality from lightning strikes might be unaccompanied by fire, and might have previously been severely underestimated. The recent study of 32 lightning strikes suggests that at 40.5 % lightning is the most important direct driver of mortality of individual trees of over 60 cm dbh, and is directly responsible for the death of 4.5 % of all trees of over 10 cm dbh, increasing to 50.3 respectively 6.1 % if lagged mortalities observed after 11-13 months are taken into account (Yanoviak et al., 2020). Furthermore, lightning frequency in tropical forests might help explain continental differences in woody biomass turnover rates and large tree densities, with Africa and the Americas experiencing the highest frequency of lightning over tropical forests, followed by Asia and Australia (Gora et al., 2020).

Cloud-to-ground lightning is expected to increase along with a warming climate (Price and Rind, 1994), and smoke from fires has also been observed to increase the amount and intensity of positive polarity cloud to ground lightning strikes from thunderstorms (Lyons et al., 1998). Combined with the expected increasing drought severity and frequency, tree mortality from lightning-induced fires might start to become more prominent in the future.

Lianas

Lianas are woody vines that use trees for structural support and as a means to reach the canopy. High liana densities in forests or in individual trees (>75 % crown infestation) can result in tree mortality rates being twice as high (Ingwell et al., 2010; Tymen et al., 2016), with large lianas (≥10 cm diameter) even observed to have caused a threefold increase in basal area mortality rates of large trees (>50 cm dbh; Phillips et al., 2005). Due to not having to invest as much in tissues for structural support, lianas can maximise water transport and leaf investments (Paul and Yavitt, 2011), making them efficient above- and belowground resource competitors for trees. They also place a mechanical stress on host trees (Ingwell et al., 2010). This competition has been found to lead to trees in liana-infested forests to display lower stem growth rates (van der Heijden et al., 2015; Marshall

et al., 2017), and overall aboveground biomass (Laurance et al., 2001), and to increase their investments in leaves (van der Heijden et al., 2015). As such, lianas will likely affect the carbon and water balance of trees, and consequently their resilience to any other potential stressors. A pan-tropical review found no significant difference in the magnitude of the inhibiting effect of lianas on average tree stem growth rates (Marshall et al., 2017). However, the greatest contribution of lianas to elevated tree mortality rates might result from their effect on forest composition following disturbances (Laurance et al., 2001; Paul and Yavitt, 2011; Tymen et al., 2016).

Even at the individual tree level, liana infestations can be dynamic, with over 10 % of surviving trees with the highest crown infestation level in Panama observed to have become liana-free 11 years later, and, conversely, over 5 % of individuals which were previously liana-free, having become severely infested, regardless of their size class, pioneer-status or shade-tolerance (Ingwell et al., 2010). Furthermore, despite their more flexible structure and disturbance-recovery adaptation mechanisms (Paul and Yavitt, 2011), the falling of a large host tree proved fatal for two thirds of large lianas (Phillips et al., 2005). However, while they can still be responsible for at least 30 % of basal area tree mortality (Phillips et al., 2005), large lianas are generally restricted to relatively undisturbed forest interiors, probably due to their dependence on large host trees (Laurance et al., 2001; Phillips et al., 2005; Poulsen et al., 2017). Higher densities of predominantly small lianas (2-3 cm diameter) are often observed in disturbed forest gaps, fragments or edges (Laurance et al., 2001; Paul and Yavitt, 2011; Bakayoko et al., 2011; Tymen et al., 2016). Lianas can quickly reach and close any gaps in the canopy and prevent slow-growing shade-tolerant forest species from recruiting, favouring the establishment of faster-growing tree species with higher mortality rates (Paul and Yavitt, 2011; Tymen et al., 2016). This pattern is partly because some pioneer species are better able to avoid liana infestation (Putz, 1984; Laurance et al., 2001; Tymen et al., 2016). Liana-infested areas can be over 20 hectares in size, possibly establishing after large-scale disturbance like a micro-tornado (Tymen et al., 2016). Once established, the higher dynamics of these forests result in more gaps being created, which can create a positive feedback in these high-mortality liana-infested forests (Phillips et al., 2002), enabling a state of arrested forest recovery, which can last for over 20 years (Laurance et al., 2001; Paul and Yavitt, 2011; Tymen et al., 2016). However, the dense thickets created by lianas might also decrease tree mortality in hurricane-prone regions (Paul and Yavitt, 2011).

Several studies have found lianas to have increased in undisturbed forests in the neotropics during recent decades (Phillips and Gentry, 1994; Laurance et al., 2014), with increases observed in liana densities, basal areas and mean size (Phillips et al., 2002), as well as concurrent increases in the number of trees with crown infestations and the mean crown infestation level per tree (Ingwell et al., 2010). However, a tropical review found no

such changes in liana densities had been identified in any African studies (Schnitzer and Bongers, 2011). This could be related to variations in functional traits between lianas in the different biogeographical regions. For instance, lianas in the neotropics were found to have larger leaves (Gallagher and Leishman, 2012). It has been suggested that the most likely mechanisms for increasing liana densities in the neotropics are increases in evaporative demand, atmospheric CO_2 concentrations, and disturbances (Schnitzer and Bongers, 2011). Though lianas seem to be more adapted to drier environments with higher evaporative demands, and most species retain their leaves even in the dry season (Schnitzer and Bongers, 2011), they might be more vulnerable to prolonged drought conditions. Liana mortality increased by 70 % in a 4-year 60 % throughfall exclusion experiment (Nepstad et al., 2007), and the stems and leaves of lianas are more embolism-prone than those of their host trees (Johnson et al., 2013), with the leaves also potentially more vulnerable to overheating (Paul and Yavitt, 2011). As such, any expected continued increases in neotropical liana densities might be offset by increased drought-induced liana mortality, potentially resulting in no net difference in their overall contribution to future tropical tree mortality.

Wind

Apart from islands in the tropics (e.g. Samoa and other Polynesian islands, Puerto Rico and other Caribbean islands), which can suffer hurricane-induced tree mortality (e.g. Elmqvist et al., 1994; Franklin et al., 2004; Zimmerman et al., 2014; Webb et al., 2014; Eppinga and Pucko, 2018; Uriarte et al., 2019), northwest and central Amazonia also experience frequent severe disturbances by wind (Nelson et al., 1994; Espírito-Santo et al., 2014; Negrón-Juárez et al., 2018). Especially in the aseasonal northwest Amazon, this can lead to higher tree mortality rates from uprooting and mechanical breakage, most likely due to a combination of less deep rooting, rainfall events saturating soils, and lower wood densities (Negrón-Juárez et al., 2018; Fontes et al., 2018). This pattern has also been observed for lowland tropical forests in the more aseasonal parts of Asia (Ediriweera et al., 2020). Areas affected can range from a few individual trees up to 30 hectares (Negrón-Juárez et al., 2010). While not resulting in immediate mortality, defoliation of trees and loss of branches (Webb et al., 2014; Eppinga and Pucko, 2018; Silvério et al., 2019) can also affect post-disturbance survival. It has been suggested that wind disturbances might also contribute to elevated mortality rates of larger trees on forest edges (Laurance et al., 1997). Furthermore, elevated wind-induced mortality has been observed in previously burned forests (Silvério et al., 2019). After wind disturbances, light-demanding species with lower wood densities establish, leading to decades of elevated mortality rates from these faster turnover species following the initial disturbance event (Magnabosco Marra et al., 2018). Furthermore these species might be more vulnerable to breakage during future disturbances (Zimmerman et al., 1994; Magnabosco Marra et al., 2018). Under the

prediction of more frequent and severe wind disturbances in the future, forests in the central Amazonian region and Caribbean are expected to see an increase in tree mortality from wind (O'Brien et al., 1992; Negrón-Juárez et al., 2018).

Biotic agents

While biotic agents, like insects, bacteria, and fungi, can be important drivers of mortality, with the ability to wipe out stands of one species, either directly through damage to leaves, stems, or roots, or by allowing entry of a fungus (Papaik et al., 2005), there is generally a very specific host-pathogen relationship. As such, temperate and boreal forests composed of fewer species are more vulnerable to large-scale die-off from biotic agents than tropical forests. Furthermore it is challenging to detect evidence of tree mortality induced by biotic agents, since the damage might not be clearly visible from the exterior of the tree. Studies of biotic agents of tree mortality in the tropics are therefore limited. Three out of 67 dead trees in central Amazonia were found to have been infected by fungi known to affect the xylem (Fontes et al., 2018). A global review of how climate change might affect biotic, disease-causing agents, found a leaf blight fungus, currently affecting many tree species in Southeast Asia and Australia, might increase in prevalence, but that root rot incidence is expected to decrease across the tropics (Sturrock et al., 2011).

Flooding

Flooding makes trees more vulnerable to becoming uprooted when exposed to lateral forces, and oxygen depletion limits water uptake by roots, thus depleting carbon reserves (Moser et al., 2019). In a recent central Amazonian study mortality rates were observed to be highest during the wet months of the year, even during drought years, with pioneer species suffering elevated mortality rates during events with excessive precipitation (Aleixo et al., 2019). Additionally, flooding events can be accompanied by increased water currents, causing trees to become uprooted or broken even in the absence of wind (Damasceno-Junior et al., 2004). With excessive precipitation events predicted to increase, alongside increased droughts, tree mortality might be expected to increase concurrently as a result of flooding (Aleixo et al., 2019).

1.2.3 Background and catastrophic tree mortality

In most mortality studies, tree mortality is quantified as a rate corresponding to the absolute number or proportion of deaths observed in an area after a certain time interval. This is generally expressed in terms of absolute or relative losses of individual numbers of stems, or of aboveground biomass, though basal-area losses are also used occasionally. When trying to classify tree mortality rates, a distinction that is often made, is between "background" mortality, and "catastrophic" mortality. While catastrophic disturbances have the possibility to wipe out complete stands, when taking into account the recurrence

frequency of catastrophic events, more trees may die through "background" mortality over long timescales, than as a result of catastrophic disturbances. For example, over the course of 100 years, background mortality killed 4-5 times more trees in the Luquillo Experimental Forest in Puerto Rico than landslides and hurricanes combined (Lugo and Scatena, 1996). Similarly, an increase in insect outbreak-induced dieback resulted in less biomass lost through mortality over a 14-year period in the western U.S., than a 0.5 % per year increase in background mortality rates over the same period (Das et al., 2016). An increase in long-term background mortality rates, might therefore prove more disastrous for the continued functioning of forests as a carbon sink, than increased recurrences of catastrophic disturbance events. Based on the results from studies in tropical moist, wet and rain forests, which had an overall median mortality rate 1.6 % per year, where all 90th percentiles were under 3 %, and no individual observations exceeded 3.5 % per year, Lugo and Scatena (1996) proposed to designate mortality rates of under 5 % per year as background mortality, and anything exceeding that as catastrophic. However, expressing catastrophic events relative to a specific forest's long-term (background) mean would be more insightful, especially if taking into account that region's natural variability - for example through putting the threshold of catastrophic mortality at two standard deviations from the long-term mean (sensu Franklin et al., 1987).

1.3 Mortality rate analyses

1.3.1 Mortality rate measures

Mortality rate measures express how many trees have died during a certain time period. For this you need to know how many trees there were initially (N_0) and how many of those trees are still alive after a time period of *t* years (N_1). According to Sheil et al. (1995), the most common mortality measure, the exponential mortality coefficient (λ), assumes a constant mortality rate, leading to an exponential rate of population decline, such that:

$$N_1 = N_0 e^{-\lambda t} \quad (1.1)$$

From this the instantaneous exponential mortality coefficient λ is defined as:

$$\lambda = \frac{\ln(N_0/N_1)}{t} \quad (1.2)$$

However, constant exponential decline can also be expressed through the proportion of trees that die each year, by using the annual mortality rate (*m*):

$$N_1 = N_0(1-m)^{1/t} \quad (1.3)$$

This formulation essentially treats mortality as a discrete, rather than continuous, process (Sheil and May, 1996), with *m* determined as:

$$m = 1 - (N_1/N_0)^{1/t} \quad (1.4)$$

As such, *m* can be calculated from λ and vice versa as:

$$m = 1 - e^{-\lambda} \quad (1.5)$$

$$\lambda = -\ln(1 - m) \quad (1.6)$$

The two different mortality measures are similar at a low level of mortality (e.g. for annual mortality rates of between 0 and 5 % per year), but at greater values, the differences become quite pronounced (Sheil et al., 1995; see Figure 1.1).

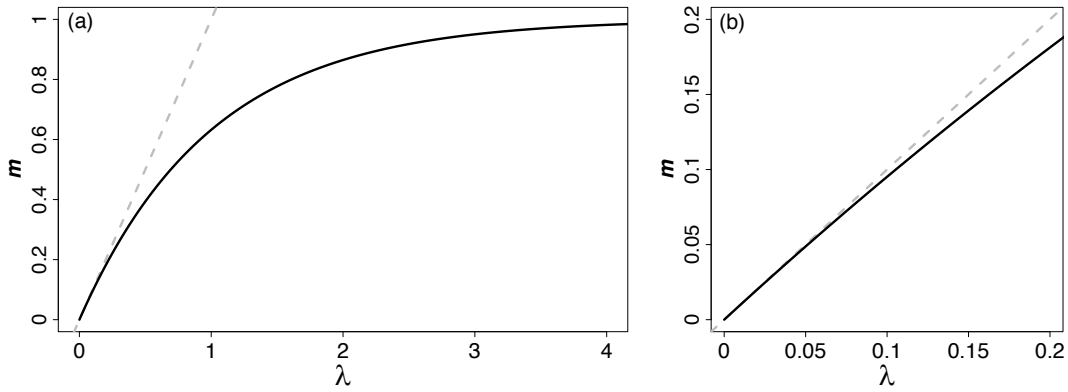

Figure 1.1. Relationship between the annual mortality rate (*m*) and the exponential mortality rate (λ). The dashed grey line represents a 1:1 relation for reference. (a) As *m* approaches 1, λ approaches infinity. (b) For smaller annual mortality rates (up to ca. 0.05), *m* and λ values are almost the same.

Despite the fact that λ is more widely used (e.g. Lieberman et al., 1985; Condit et al., 2004; Lewis et al., 2004a; Phillips et al., 2004; King et al., 2006; Madelaine et al., 2007; de Oliveira and Felfili, 2008; Poorter et al., 2008; Laurance et al., 2009), I agree with Sheil et al. (1995), that it is preferable to use *m* as a mortality rate measure over λ, since it is a truly annual mortality rate, and as such more intuitive. For example, if half the trees in a forest were to die over the course of one year, this would result in an *m* of 0.5 or 50 %, whereas the λ equivalent would be ln(2) ≈ 0.69. For annual mortality rates greater than $1\text{-}e^{-1} \approx 0.63$, as has been observed for example in the U.S. where 80 % of the non-seedling trees in a piñon-juniper woodland stand died over the course of 15 months (*m*=0.72) in New Mexico in 2002-2003 in response to a global change type drought and a concurrent bark beetle infestation (Breshears et al., 2005), λ will exceed 1. This also applies to census intervals that are shorter than 1 year, since the conversion between these two mortality rate measures is independent of the census interval length. Thus, as *m* approaches 1, corresponding to complete stand mortality over the course of a year, due to its exponential nature, λ approaches infinity.

Since the majority of annual mortality rates in the datasets I have used are relatively small, and consequently the difference between *m* and λ is small (1st quantile-3rd quantile range is 0.5118-1.996 %·year^{-1} for *m* and 0.5131-2.016 %·year^{-1} for λ), in this thesis I report only the findings obtained using *m*.

1.3.2 Census interval length

Ideally, in order to collect comparable annual mortality rate data from field plots, they should be revisited at regular intervals of preferably one year. However, this is often not feasible though, due to the costs and efforts involved with such plot censuses. As such, mortality rate data collected for various plots may correspond to intervals of different lengths, and even consecutive censuses for the same plot might have varying interval lengths. If a plot contains a completely homogeneous population, where all individual trees have the same probability of mortality, this is not an issue. However, if a plot is composed of a more heterogeneous population, some of which tend to be short-lived and some of which tend to live for a longer period of time, the length of the census intervals becomes of importance (Sheil and May, 1996). As the census interval becomes longer, the probability increases that some of the rapidly growing individuals might have grown to the diameter of interest and died, without them ever having been recorded in a census. Thus with an increasing census interval length, mortality rates are underestimated (Sheil and May, 1996).

To correct for this underestimation, Lewis et al. (2004b) developed a census interval effect correction factor using censuses from 14 long-term sample plots across Africa, Asia, Australia and Latin America:

$$\lambda_{corr} = \lambda * t^{0.08} \quad (1.7)$$

where λ is the exponential mortality rate as observed during a census interval length of *t* years, and λ_{corr} the corrected exponential rate.

Combining (1.5), (1.6) and (1.7), shows the annual mortality rate *m* can be corrected for the census interval effect in a similar fashion:

$$m_{corr} = 1 - (1 - m)^{t^{0.08}} \quad (1.8)$$

Through (1.4) and (1.8) it follows that the census correction factor can also be directly applied when using the census data to derive the census corrected annual mortality rate as follows:

$$m_{corr} = 1 - (N_1/N_0)^{1/t^{0.92}} \quad (1.9)$$

The census interval corrected annual mortality rate m_{corr} remains constrained by no (0 %) mortality and complete (100 %) mortality, and the conversion between λ and m, and vice versa, is maintained as per (1.5) and (1.6), independent of the census interval length (see Figure 1.2).

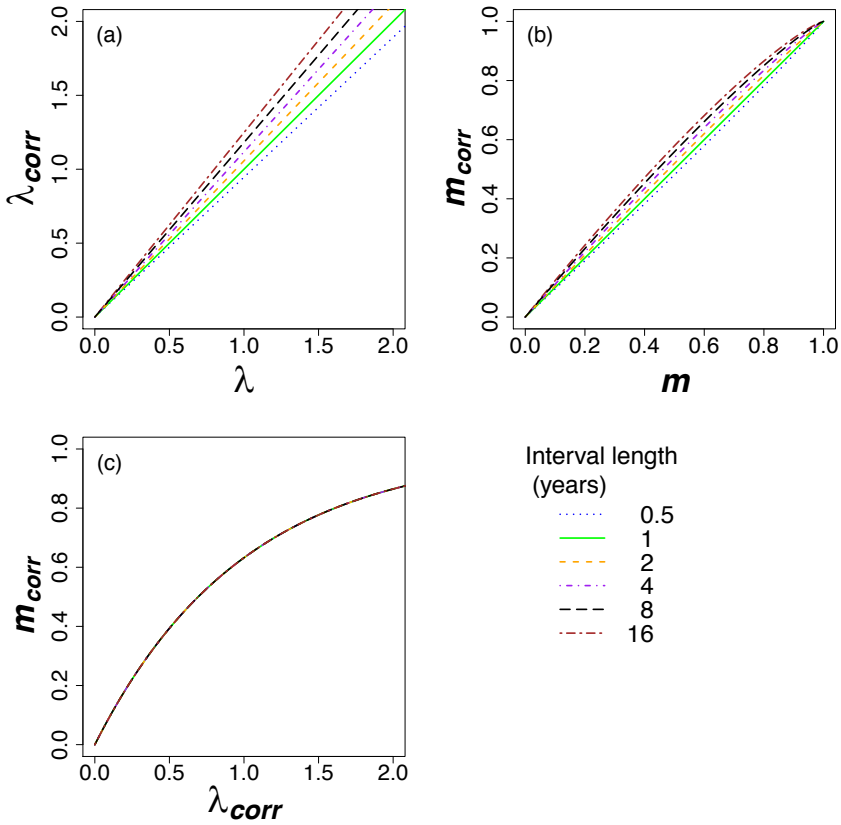

Figure 1.2. The effect of census interval length on the relationship between corrected and uncorrected mortality rates measures.
(a) The census interval length corrected (λ_{corr}) and observed (λ) exponential mortality rates.
(b) The census interval length corrected (m_{corr}) and observed (m) annual mortality rates.
(c) The relationship between m and λ is maintained, regardless of the correction for census interval length.

In large permanent sample plots, e.g. those of the CTFS-ForestGEO network (Anderson-Teixeira et al., 2015), which contains at least 12 plots of ≥50 hectares, with a median plot size of 25 hectares across all 59 plots, and where all woody stems ≥1 cm diameter at breast height (dbh) are censused, further issues may arise, as a census might take thus long to complete, that the census interval length will vary from stem to stem (generally the census date will be recorded per 20 x 20m quadrat, which might take several days to complete; Condit, 1998) within the plot. To deal with this (Condit et al., 1995) averaged the census interval lengths recorded for each individual stem of one species when calculating their species-specific mortality rates. However, Kubo et al. (2000) proposed to use maximum likelihood estimates for mortality, in a manner where this estimate collapses to Equation (1.1) in the case where the census interval length for all individual trees is equal. While they found the relative error between these two methods of within-census interval correction to be generally smaller than 3 %, they stress that the maximum likelihood estimation method will be more robust at handling greater within census variation in individual interval lengths, especially at overall higher mortality rates, or when deriving rates for species with few individuals. While these issues of varying census interval lengths

between individuals do not apply to the data analysed in this thesis, due to smaller plot sizes and a greater dbh threshold used, the Bayesian methods used in this thesis can also address inter-census interval length variations, as well as other sources of inter-census variation, in a similar fashion by incorporating them into the likelihood function.

1.3.3 Comparative studies

Comparative studies are central to understanding variation in tree mortality rates. Plot-level mortality rates are often compared between consecutive census intervals of the same (set of) plot(s), between different (sets of) plots, or across both space and time. This approach can be combined with comparing mortality rates among size classes or functional groups. When wanting to detect the effect of a "catastrophic" event or an experimental treatment on mortality rates, the rates observed for affected census intervals are generally compared to "background" mortality rates obtained during non-disturbed plot censuses. Furthermore, when trying to detect potential underlying drivers or explanatory variables of variations in (group-specific) mortality rates, mortality rates are generally compared across a range of variation in these driver values.

A range of statistical approaches have been used to compare plot-based estimates of mortality. For example, species- or dbh class-, or functional group-specific mortality rate comparisons may involve chi-square, Kruskal-Wallis or Wilcoxon paired-sample tests, (Condit et al., 1995; Davies, 2001; Damasceno-Junior et al., 2004; Vilanova et al., 2018). The effect of a catastrophic event on mortality might be determined using G-tests or Fisher's exact tests (Aiba and Kitayama, 2002; Nepstad et al., 2007), and comparison of mortality rates between census intervals or plots has been undertaken using Wilcoxon paired-sample or Student's t-test (Condit et al., 1995; Whittaker et al., 1998). The influence of explanatory variables on tree mortality may be done using (logistic or multiple) regression, principal component analysis, or generalised least squares models (Davies, 2001; Damasceno-Junior et al., 2004; de Toledo et al., 2011; Vilanova et al., 2018), or a Mann-Whitney U test if the explanatory variables are of a categorical nature (Condit et al., 1995).

However, comparative methods which simply compare plot-level estimates of mortality among sites or censuses can have two limitations. Firstly, they cannot effectively account for a range of sampling issues associated with data on tree mortality rates. For example, estimates of tree mortality rates are affected by comparing groups or plots with variation in census interval length, numbers of individuals, plot sizes, and census timing. Additionally, repeated censuses of the same set of trees are not independent of each other, just like measurements from plots within the same region are expected to be correlated to each other. Secondly, most approaches to comparative analysis essentially

cannot account for the fact that the drivers of mortality operate simultaneously at multiple scales.

In Bayesian analyses, these issues can be dealt with through the likelihood function, and inclusion as potential explanatory variables at different hierarchical levels, from the individual to the region. Furthermore, by nesting individual tree observations within hierarchical levels, temporal and spatial correlation can also be accounted for (McElreath, 2016). For example, repeated censuses of the same plot can be assumed to come from a plot level distribution, the parameters of which can be assumed to come from overarching levels of any of regional, continental, pan-tropical or even global distributions. Another advantage of hierarchical Bayesian analyses stems from the fact that within a hierarchical level, groups with more observations will automatically contribute more to the overall likelihood, without needing to explicitly weight for this, or losing data or variation through averaging (Kruschke, 2015; McElreath, 2016). The overarching distributions can even help constrain the estimates on regions with fewer observations (Kruschke, 2015). Finally, observations can be assumed to come from any distribution, and uncertainty estimates will be included on all estimated parameters (Kruschke, 2015; McElreath, 2016).

It is important to note that Bayesian parameter uncertainty estimates are fundamentally different to the confidence intervals obtained in frequentist analyses, which is due to the different nature of these analyses. In frequentist analyses, one is trying to infer a specific value of a parameter which is believed to exist in the field of interest. The “confidence interval” obtained in frequentist analyses, denotes the proportion (e.g. 95%) of a large number of repeated samples in which the confidence interval will contain this parameter value of interest (Kruschke, 2015; McElreath, 2016). With Bayesian analyses, on the other hand, one is trying to approximate such parameter values, while including the confidence in any posterior parameter estimates as a probability. Here, the “credible interval” of a parameter estimate will contain the parameter value with the specified posterior probability (e.g. 95%; McElreath, 2016).

As such Bayesian analyses offer a comprehensive analytical framework for exploring variation in mortality rates over time and space, that can account for the impact of tree-level variation in size, plot-level variation in sampling, and large-scale variation in climate, soils and biogeography.

1.4 Research aims and objectives

In this thesis I aim to further our understanding of tropical tree mortality rates using a combination of simulations and (hierarchical) Bayesian analyses of observations from a long-term pan-tropical forest monitoring network. Specifically, I address the following questions:

- What minimum permanent plot network size is required for detecting short- and long-term changes in tropical tree mortality rates? (Chapter 2).
- How does the relative importance of small-scale mortality rate events differ at various spatial scales across the tropics?(Chapter 3).
- Is regional variation in mortality rates in Amazonia related to variation in drought intensity? (Chapter 4).

These questions are addressed through the following objectives:

Chapter 2:

- Simulate tropical tree mortality dynamics in permanent sample plots
- Sample the simulated data to determine if a significant change in mortality rates has occurred
- Derive recommendations for the sample size of an optimal permanent plot network size capable of detecting a given change in tree mortality rates

Chapter 3:

- Derive pan-tropical mortality rates for each plot census in a pan-tropical dataset
- Use a hierarchical Bayesian model to quantify the probabilities of mortality rate events of different magnitudes at various nested spatial scales
- Asses at which spatial scale variation in tropical tree mortality rates are best expressed

Chapter 4:

- Using the mortality rates derived in Chapter 3, investigate regional trends in mortality rates in Amazonia, with both general linear analyses and Bayesian analyses
- Extract the precipitation data corresponding to the plot census intervals and use them to derive a measure of drought intensity
- Examine trends through time in these drought intensity measures, both in general linear analyses and using Bayesian analyses
- Investigate correlations between mortality rates and drought intensities, using both general linear analyses and using Bayesian analyses

1.5 Chapter outlines

In the first chapter, I highlighted the importance of tropical old-growth forests as an important carbon store and sink, and of tree mortality as one of the key dynamic processes that shapes this function. I detailed how tree mortality is still poorly understood and reviewed our current understanding of some of the main drivers of tropical tree mortality. I reviewed commonly used mortality rate metrics and computational issues involved with

their derivation. Finally, I showed that hierarchical Bayesian models are particularly appropriate for understanding variation in tree mortality rates.

In the second chapter I present the results from various forest dynamics simulation scenarios and use a power analysis to derive recommendations for the sample size of permanent plot networks to detect changes in mortality rates. The results can be used as a basis for the evaluation and expansion of existing monitoring networks at regional, national and international scales.

In the third chapter I present a hierarchical Bayesian model used to quantify mortality rate distributions at different, nested, spatial scales. I use the results from this analysis to recommend at which spatial scale mortality rates are best described, which can help inform research efforts into drivers of mortality, as well as provide a basis for improving modelling.

In the fourth chapter I identify potential trends in mortality rates and water deficits across South American biogeographical regions. I relate variation in an environmental driver to variation in tree mortality using both a linear and a Bayesian model approach.

Finally, in the fifth chapter, I synthesize the main findings from this thesis and highlight directions for future research.

2 Criteria for designing optimal sampling strategies for detecting changes in tree mortality rates in tropical forests

2.1 Introduction

Old-growth tropical forests have acted as a net carbon sink over recent decades, removing between circa 13 to 20 % of atmospheric CO_2 emissions from fossil fuel combustion and cement production from 1990 to 2007 at a rate of 1.19 ± 0.41 GtC $year^{-1}$ (Pan et al., 2011). However, the future of this sink under a changing climate is uncertain (Mitchard, 2018; Tagesson et al., 2020; Amigo, 2020). A key issue is whether increases in tree mortality rates, both due to more frequent short term spikes in mortality rates caused by "catastrophic" events like droughts (Allen, 2009; Brando et al., 2019), as well as long-term large-scale increases in community mortality rates, could cause the carbon sink of intact tropical forests to shut down (Brienen et al., 2015; Hubau et al., 2020). Increasing our understanding of both short-term and long-term trends in mortality rates is therefore important for understanding how climate change is affecting forest dynamics, for designing effective management and climate mitigation policies, and to help improve modelling efforts.

A key tool for understanding how tree mortality is changing are long-term inventories of permanent forest plot networks (e.g. Malhi et al., 2002; Lewis et al., 2009; Anderson-Teixeira et al., 2015). These networks track forest dynamics across numerous plots through repeated censuses over multiple decades. However, maintaining these networks is labour-intensive and expensive, and so national and international sampling networks need to be designed efficiently to detect both long-term and short-lived changes in forest dynamics. Most recommendations to date for efficient sample sizes for plot networks for policy-focussed questions have concerned uses focussed on silvicultural yields (Alder and Synnott, 1992), (national) carbon stock quantification (Köhl et al., 2011; Grussu et al., 2016) or biodiversity assessment (Grussu et al., 2016). At the same time, studies of plot network designs for ecological studies have mainly focussed on determining the most efficient plot size or shape to estimate biomass or species richness (Phillips et al., 2003). However, an optimal sampling strategy for one-off estimates of any of these parameters, will not necessarily capture the variability over time of a stochastic forest dynamic property such as tree mortality. As such, it is crucial to have monitoring strategies for tree mortality that can determine whether identified rates and the presence of any trends therein are a true representation of the ecosystem being studied, and are related to specific drivers such as a drought, or whether they are simply chance observations.

Monitoring changes in forest dynamics like tree mortality is complex, since tree death occurs stochastically, and events can be clustered both in time and space. In particular, the design of a monitoring strategy needs to account for variability over time, whereas sampling strategies that are used for understanding static properties only need to account for variation in space. As a first step, we need to understand the minimum network sample size that will allow detection of the phenomena that we are interested in studying. The magnitudes and timescales of these trends in mortality vary greatly, and consequently the extent of the monitoring network required to detect them also varies.

To address this issue, here, the sample size for detecting long-term and short-term trends in mortality rates will be evaluated. In terms of long-term trends, across the tropics, increases of up to 3 % in mortality rates have been observed over a period of three decades using 50 plots (Lewis et al., 2004b). Monitoring networks need to be able to detect this magnitude of change over these relatively long decadal timescales. In addition, we also need to be able to detect short-term elevated mortality rates from catastrophic disturbances. For instance, the 1997 El Niño drought was found to increase mortality rates in 12 plots by 71 % over a period of just over one year (Williamson et al., 2000).

Confidence in detecting sustained or one-off changes in mortality rates will also be affected by census interval length, the overall average mortality rates, and the magnitude of change that is observed. For example, as census interval length increases, and the overall monitoring period increases, we will be more confident of detecting any changes

between two consecutive census intervals. Additionally, if a forest has higher initial mortality rates, a proportional increase would more easily stand out against that forest's natural range of mortality rates. Consequently, it should require fewer plots to detect an increase of the same relative magnitude in relatively more dynamic forests, compared to less dynamic forests. Finally, as any increase or decrease in mortality rates becomes larger, fewer plots will be required to detect the change with confidence. Overall, increases in the census interval length, mean mortality rates and the magnitude of change are all expected to reduce the number of plots required to detect alterations in mortality rates. Understanding how sampling intensity is affected by these parameters will assist the design of efficient strategies for monitoring changes in forest mortality rates.

Here, a power analysis is conducted, by simulating and sampling various short- and long-term increases in mortality rates in permanent sample plots, in order to answer the following questions:

- What is the minimum number of 1-hectare plots and the sampling strategy required for confidently identifying a long-term change of 1 to 3 % in annual stem-based mortality rates?
- What is the minimum number of 1-hectare plots required for confidently detecting a short-lived increase of 5 to 100 % in annual stem-based mortality rates caused by a one-off "catastrophic" (e.g. drought) event?

2.2 Methods

This chapter aims to identify the number of 1-hectare permanent sample plots required to detect long-term (see Section 2.2.1) or one-off short-term "catastrophic" (see Section 2.2.2) increases of various magnitudes in annual mortality rates between two consecutive census intervals for a range of mortality rate distributions. This is achieved by sampling a series of simulations of the impact of a change in tree mortality rates on tree populations with varying characteristics.

A change in mortality rates between two consecutive intervals can be determined in a number of ways:

- Do the mortality rates observed during the first and second census interval come from distributions with significantly different means?
- Do the absolute differences between the mortality rates observed during the first and second census interval significantly differ from zero?
- Do the relative annual increases (where e.g. a doubling of mortality rates over the course of a year, corresponds to a relative annual increase of 100% per year)

between the mortality rates observed during the first and second census interval significantly differ from zero?

Here, the smallest number of plots required to confidently detect a change, based on each of these metrics, is evaluated.

All simulations and analyses were performed using R 3.4.4 (R Core Team, 2019) in RStudio 1.1.463 (RStudio Team, 2016).

2.2.1 Identifying increases in long-term mortality rates

Extensive plot networks were simulated for a set of hypothetical forests that represent various underlying scenarios:

Firstly, the "no increase", or "baseline", scenario represented forests with stable dynamics and stable population sizes, with no increase in annual mortality and recruitment rates (henceforth abbreviated as 'm0r0'). Here, mortality balanced recruitment, and thus the overall population size remained the same on average through time. This represents a long-term equilibrium scenario.

Secondly, an "increasing dynamics" scenario was simulated. Here, the annual mortality rates still balanced the annual recruitment rates, and the overall population size thus also remained the same on average through time, but both the annual mortality rates and the annual recruitment rates increased continually by either 1 % or 2 % each year (scenarios 'm1r1' and 'm2r2' respectively). Such a scenario has been observed for example in West and South Amazonia, where raw mortality and recruitment rates increased by 2.15 respectively 2.12 % per year between 1983 and 2001 (Phillips et al., 2004).

Finally, in the "increasing population" scenario, the annual increase in recruitment rates outpaced the annual increase in mortality rates, and therefore the stem density per unit area increased each year. Three different variations of this scenario were simulated (see Table 2.1). The first version represents a forest with no increase in annual mortality rates, but where the annual recruitment rates increased by 1 % each year ('m0r1'). In the second version, annual mortality rates increased by 1 % each year, while annual recruitment rates increased by 2 % each year ('m1r2'). Lastly, a third version increased annual mortality and recruitment rates by 3 and 4 % each year respectively (variation 'm3r4' for short). Relative annual increases of a similar magnitude (mortality 3.08, recruitment 4.25 % per year) were identified across 50 South American plots by Lewis et al. (2004b) for the period 1971-2002.

Next, the sensitivity of the results to variation in the distribution of mortality rates was examined. Since annual mortality rates represent the proportion of trees that have died per year, which are bounded by 0 (no mortality) and 1 (complete mortality), both the beta distribution and the logistic normal distribution were evaluated for modelling their distributions. However, due to these annual mortality rate distributions being strongly

positively skewed, with many small mortality events and few larger mortality events, the probability of annual mortality rates of zero was estimated as infinity in some of the Bayesian parameter estimation runs of Chapter 3 when using the beta distribution. Thus, the logistic normal distribution was found to provide a consistently better fit, and has been used throughout this thesis to model tree mortality probability distributions, which is in line with other studies (e.g. Hamilton Jr. and Edwards, 1976; Lines et al., 2010; Vanderwel et al., 2013).

Table 2.1. The simulated scenarios of changes in annual mortality and recruitment rates.
All variations were run for all mortality rate distributions (see Table 2.2), except for the baseline scenarios (corresponding to a 0 % increase in annual mortality rates, denoted by *), which were not run for the $N(-4.75, 0.75^2)$ distribution.

Forest population scenario type	Annual mortality rate increase (%)	Annual recruitment rate increase (%)	Mortality/recruitment increase abbreviation
No increase	0*	0*	m0r0
Increasing dynamics	1	1	m1r1
Increasing dynamics	2	2	m2r2
Increasing population	0*	1*	m0r1
Increasing population	1	2	m1r2
Increasing population	3	4	m3r4

As such, for each variation of the previously described scenarios (see Table 2.1), mortality rates were drawn from normal distributions in logistic space which varied in their mean and standard deviation. The chosen values ($N(-4.5, 0.5^2)$, $N(-4.5, 0.75^2)$, $N(-4.5, 1.0^2)$, $N(-4.25, 0.75^2)$, $N(-4.75, 0.75^2)$) correspond to mortality rate distributions with means of 1.2, 1.4, 1.7, 1.8 and 1.1 % per year respectively (see Table 2.2). These distributions were chosen to represent tropical forests with a range of mean base mortality rates from as low as 1.1-1.2 % per year, e.g. as identified for East-Central (Phillips et al., 2004) and Central Amazonia (Williamson et al., 2000), to 1.7-1.8 % per year, e.g. as identified for Sabah, Malaysia (Newbery et al., 1999) and as a mean pan-tropical turnover estimate (Stephenson and van Mantgem, 2005).

A three-step procedure (see Figure 2.1, Appendix A) was followed to determine the minimum number of plots required to detect different levels of long-term increase in annual mortality rates with increasing census interval length. In the first step, plot censuses datasets were generated for each of these scenarios and their corresponding annual rate distributions. The second step consisted of repeated sampling from these datasets. The final step consisted of analysing the results from the repeated sampling of these data.

Table 2.2. The parameters of the distributions from which all simulated annual mortality rates were drawn: means and standard deviations of the normal annual rate distributions in logistic space.
Including the estimated median and mean mortality rates (in %·year^{-1}) of the corresponding logit-normal distributions.

Mortality distribution in logistic space		Corresponding mortality rates	
Mean	**Standard deviation**	**Median** *(%·year^{-1})*	**Mean** *(%·year^{-1})*
-4.50	0.50	1.1	1.2
-4.50	0.75	1.1	1.4
-4.50	1.00	1.1	1.7
-4.25	0.75	1.4	1.8
-4.75	0.75	0.86	1.1

Step 1. Generating the plot censuses datasets

Plot censuses were simulated for sets of 100 plots and a unique plot identification number was assigned to each individual plot. For every plot, an initial census was simulated to have taken place in 1970, with annual re-censuses up until and including the year 2020. At the first census, all plots were initialised with 581 trees, which was the mean number across the permanent sample plots analysed by Lewis et al. (2004). Each tree was assigned a unique tree identification number, to track their status as 'alive' or 'dead' across the following re-censuses. Each tree was also assigned an "intrinsic mortality probability", which determined the probability of that individual tree dying during the census interval.

For the 'baseline' scenario, where there is no increase in annual mortality rates, the intrinsic mortality probabilities (p) were all drawn from a normal distribution in logistic space with base mean (μ) and standard deviation (σ) as follows:

$$\log \frac{p}{1-p} \sim N(\mu, \sigma^2) \qquad (2.1)$$

For the scenarios where the mortality rates increased with time, the increase in the corresponding annual mortality rate was compounded accordingly. For example, in the case of a relative annual increase in mortality rates of 0.01 (1 %; as in variations 'm1r1' or 'm1r2'), the annual mortality rate m after t years was derived as $m_t = m_0(1 + 0.01)^t$ where m_0 is the median of the annual mortality rate distribution at the start of the simulation period in 1970 (t = 0).

The probability of an individual tree surviving (s) the 1-year census interval is equal to one minus the probability that it will die; s = (1 - p). These survival probabilities were used in Bernoulli trials, to determine for each individual tree whether they had survived that census interval or not. If the trial was a "success", that individual tree was considered to have survived the census interval; if not, it was assumed to have died since the last census.

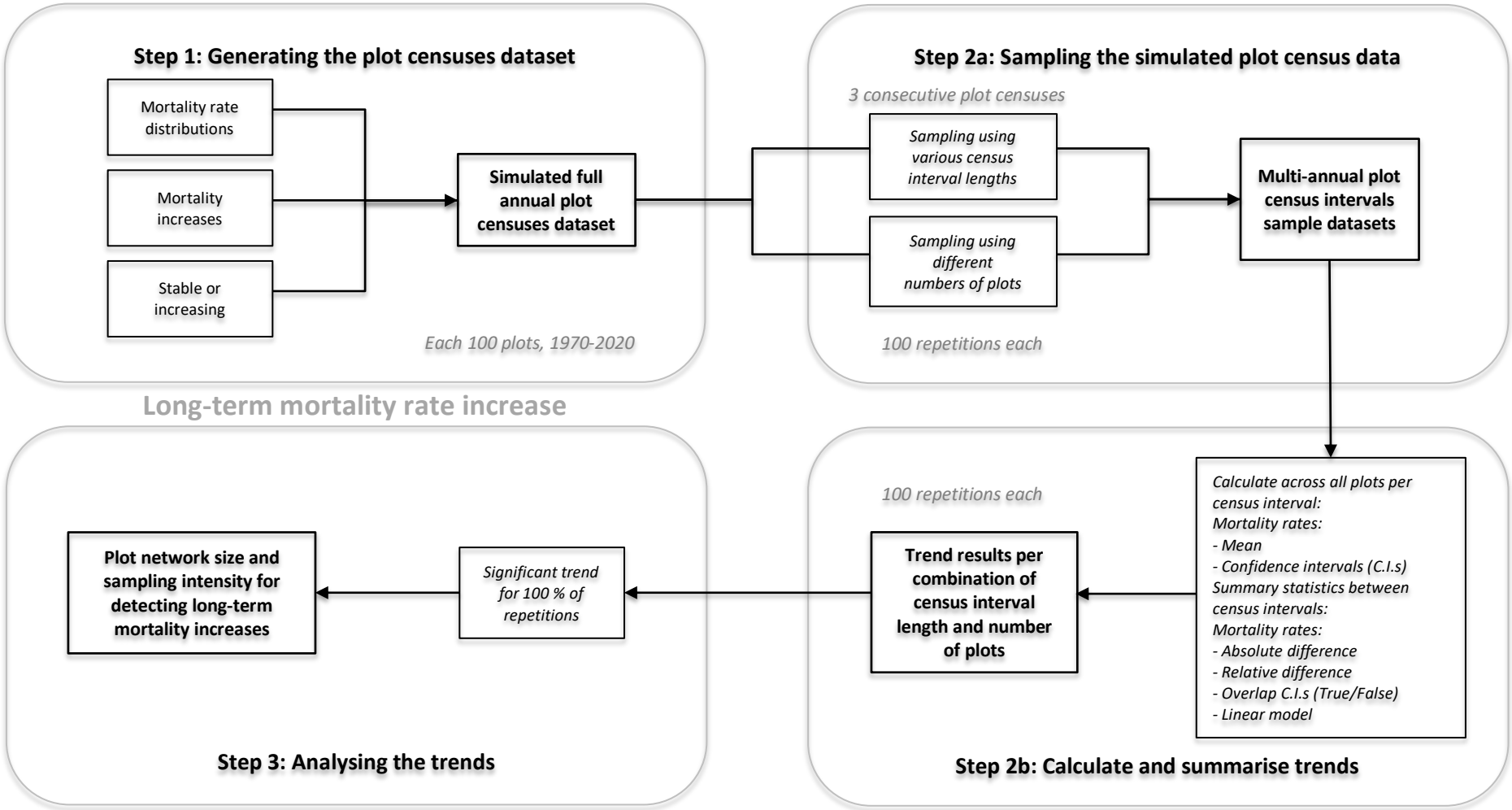

Figure 2.1. Flowchart of the process for determining the recommended plot network size for detecting long-term mortality rate increases.

For the individuals that died, the 'alive' status was changed to "0" and their individual tree IDs were removed from future census inventories. The alive trees maintained their 'alive' status of "1" and their IDs were retained for the next re-census. In addition to the possibility of trees dying in the interval between two censuses, new recruits could also pass the minimum size threshold during any given census interval. In order for recruits to numerically balance the deaths in the stable populations, or outpace the deaths in the increasing population scenarios, the number of recruits to be added during the re-census was also drawn from a normal distribution in logistic space (rounded up to the next integer value), whose mean increased in a similar fashion as described above. Each recruit was assumed to be 'alive', assigned a unique tree ID number, and an intrinsic mortality probability.

Finally, during each plot's re-census, a tally was made of the number of trees that were alive in that plot at the start of the preceding census interval (N_0), the number that survived the census interval (N_t), and the number that died during the census interval (N_d). These values were used to calculate the annual mortality rate (m) for that census interval of length t = 1 year (sensu Sheil et al., 1995) as:

$$m = 1 - (\frac{N_0 - N_d}{N_0})^{\frac{1}{t}} \quad (2.2)$$

This process was applied to all 50 consecutive re-censuses of the 100 plots for each scenario.

The different scenarios represented in these hypothetical forest populations translate to distinct trajectories in the actual numbers of dead and alive trees encountered at each plot census. The number of alive trees found at each (re-)census, is constant for the "no increase" and "increasing dynamics" scenarios (Figure 2.2a). In contrast, the number of alive trees increases through time for the forests with "increasing population" dynamics, which is the scenario where the relative increase in annual recruitment rates always outpaces the increase in annual mortality rates (Figure 2.2a).

The number of dead trees found at each re-census (Figure 2.2b), is only constant through time for the "no increase" ('m0r0') scenario. The rate of increase being equal, the "increasing population" scenarios show higher numbers of dead trees, compared to the "increasing dynamics" or "no increase" scenarios, due to the overall population increasing in size. Since the increase in annual mortality rates is relative, there is no difference between the trend of the increasing annual mortality rates of the "increasing dynamics" scenario or that of the "increasing population" scenario (Figure 2.2.c) at the same rate of increase (e.g. 'm1r1' versus 'm1r2').

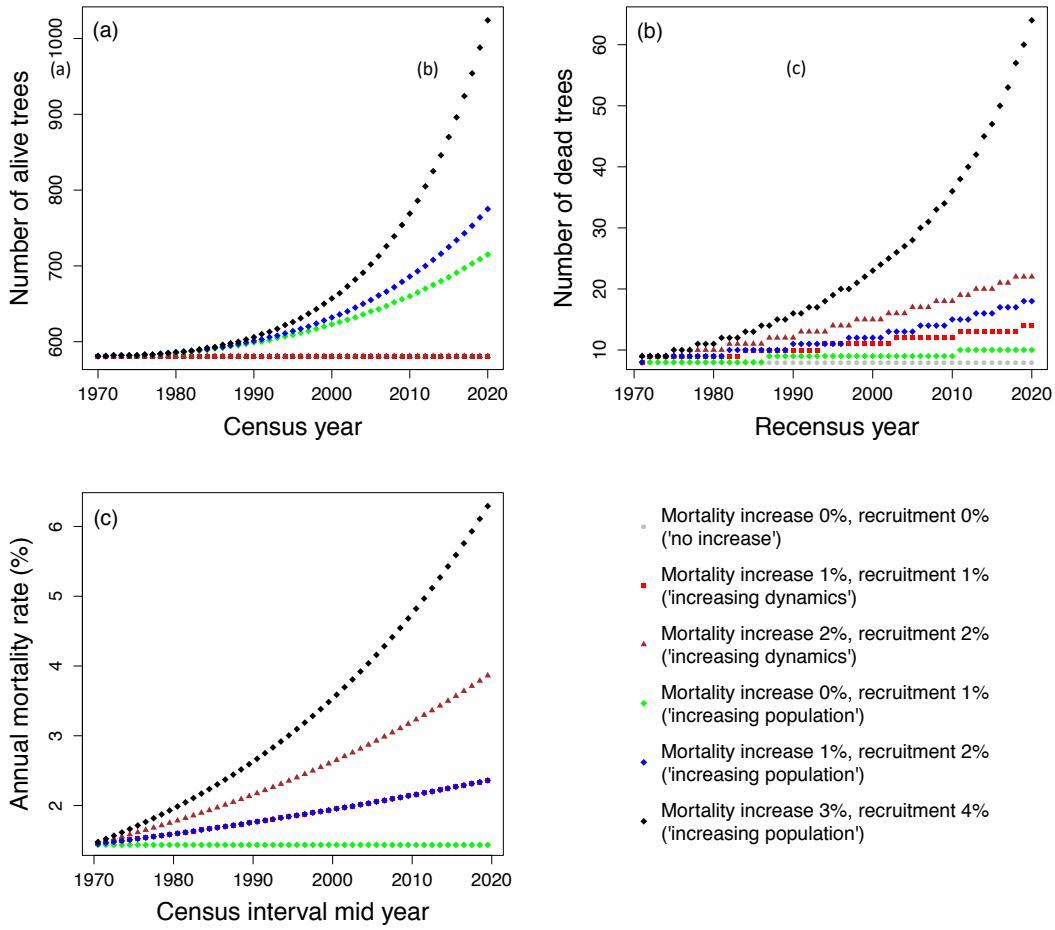

Figure 2.2 Trends in (a) the number of alive trees in each plot at the census year; (b) the number of dead trees per plot at the re-census year; (c) the annual mortality rate (%) at the mid year of the census interval. Results for six scenarios are shown: "no increase", "increasing dynamics", and "increasing population", with variations for different magnitudes of increase in mortality rates. All trends are for the same mortality rate distribution with a median base mortality rate of 1.1 %·year^{-1}.

For the two "baseline" variations, draws were only made from four mortality rate distributions. For the remaining four variations, five distributions were drawn from (see **Error! Reference source not found.**). The different standard deviation (0.5, 0.75, and 1.0) of three of the distributions (all with mean -4.5), was used to test the effect of variation in mortality rates for the number of plots required to detect an increasing trend. The distributions with different mean values (-4.25, -4.5, and -4.75; all with SD 0.75), were used to identify whether a greater number of plots might be needed for detecting a change in the annual mortality rates in forest with low, compared to high, mortality rates.

The result of this first step was a dataset of 28 plot census tables, each with 3-3.5 million rows, for all the trees encountered annually in 100 plots over the simulated overall census period from 1970 to 2020 (see Appendix A: Figure A.1). These plot census tables form the dataset from which random samples were drawn in step 2.

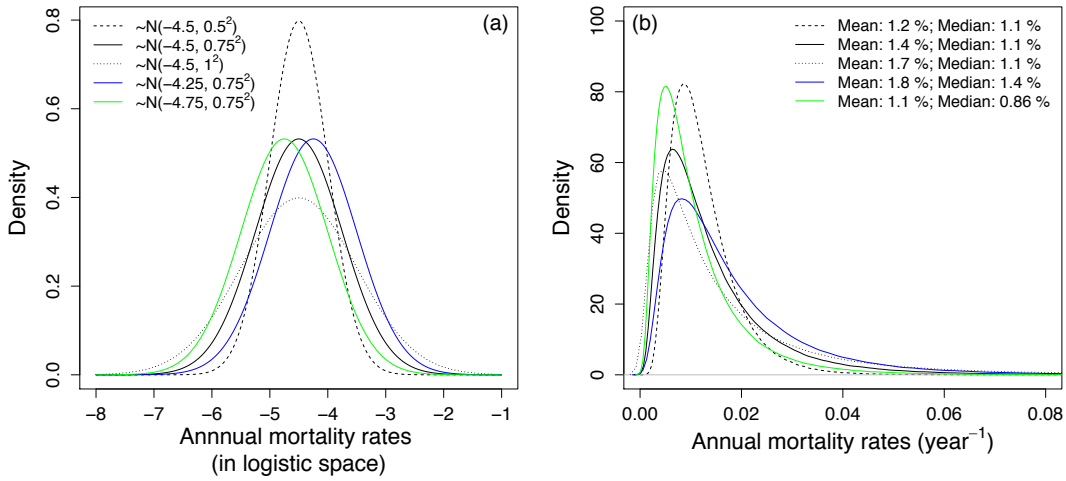

Figure 2.3. The distributions from which mortality rates were drawn.
(a) The probability density of the annual mortality rates in logistic space.
(b) The probability density of the annual mortality rates for the equivalent logit-normal distributions.

Step 2a. Sampling the simulated plot census data

Random samples were drawn from the plot census datasets of 50 re-censuses of 100 plots each generated in step 1, at increasing census interval lengths and for an increasing number of plots. Each set of samples consists of three consecutive censuses. These three censuses were treated as being the initial census and the first and second re-census of that plot. The annual plot re-censuses were then consolidated, ignoring "missed dead recruits", and thus focussing only on the trees that were alive at the start of the consolidated interval and recruits that appeared during this interval and were still alive at the time of the re-census. This procedure resulted in a new set of tallies for N_0, N_t, and N_d for each new census interval length. This time, when calculating the annual mortality rate (m) as per Equation (2.2), t was equal to the consolidated census interval length in years (e.g. Figure 2.4).

This sampling and consolidation procedure was repeated for interval lengths of 2, 5, 10 and 20 years, and for an increasing number of plots (10, 20, 30, 40, 50, 60, 70, 80, 90, 100 plots). The sampling of each of these combinations of consolidated interval length and number of plots from the plot census dataset was repeated 100 times (e.g. see Figure 2.5).

This resulted in 112,000 consolidated plot census tables (derived from 28 plot census tables, resampled for 4 different consolidated interval lengths, for 10 different numbers of plots, repeated 100 times; see Appendix A: Figure A.2).

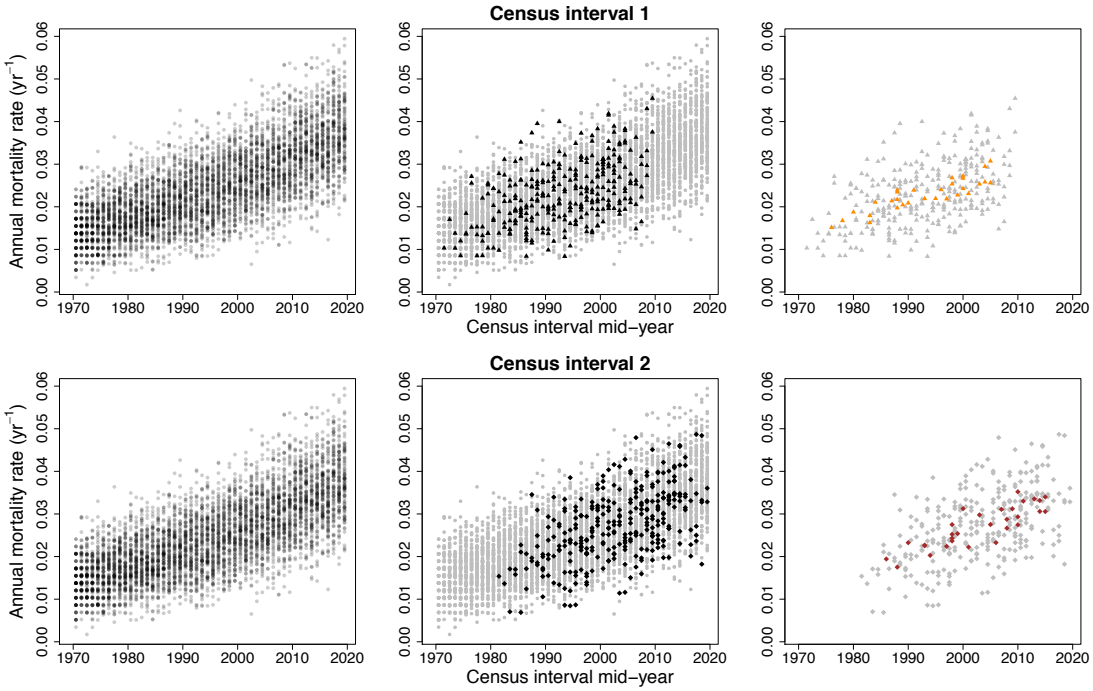

Figure 2.4. Example output of the plot census interval mortality rate generation and consolidation steps. Output generated for steps 1 (left panels) and 2a (middle and right panels) for distribution $N(-4.25, 0.75^2)$, under the 'm2r2' scenario, for a consolidated interval length of 10 years, repetition #6/100. Left: the annual mortality rates generated for 100 plots with 50 annual re-censuses each from 1970-2020. Darker parts correspond to more plot censuses with a similar rate at that point in time. Middle: from the total number of plot censuses, two sets of consecutive censuses are selected to be consolidated (top: black triangles = the first set; bottom: black diamonds = the second set; both: grey circles = all the plot censuses generated), for, in this case, a total of 30 plots. Right: the annual mortality rates of the plot censuses to be consolidated (grey) and their consolidated rates (top: orange triangles = the first set; bottom: brown squares = the second set).

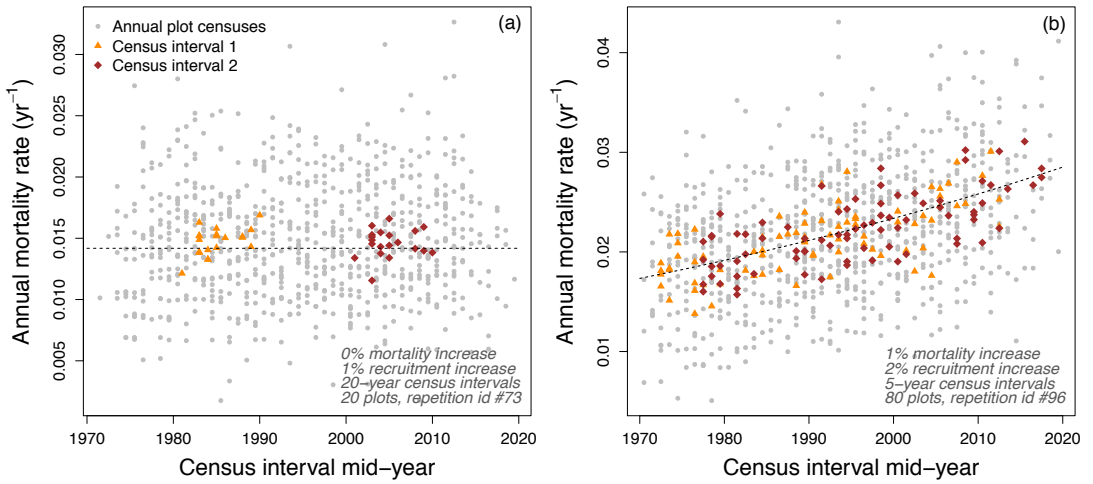

Figure 2.5. Two examples of the results of the simulated annual plot census intervals consolidation process. Annual mortality rates versus (consolidated) census interval mid-year for two different distributions (a: $N(-4.5, 0.75^2)$, b: $N(-4.5, 1.0^2)$), different population dynamics variations (a: m0r1, b: m1r2), different numbers of plots consolidated (l: 30, m:20, r:80), different consolidated interval lengths (a: 20 years, b:5 years), for different repetitions of the consolidation process (a:#73/100, b:#96/100). Grey dots are the observed annual plot census rates, which are consolidated into a first (orange triangles) and second (brown squares) consecutive interval set of the specified length. The dashed line shows the increase in the relative annual mortality rates for that variation through time.

Step 2b. Calculating and summarising the trends

The samples of two consecutive consolidated plot census intervals were used for generating and summarising various trend detection metrics, to identify how many plots are required to detect a given increase in annual mortality rates.

For trend detection, both the absolute difference ($ppDiff$, in percentage points) and the annual relative difference ($relDiff$, in %) between the annual mortality rates (in % per year) of the second and first consecutive set of consolidated plot re-censuses was calculated.

The absolute difference ($ppDiff$) in annual mortality rates (m_x) of the consolidated set IDs (x) was calculated as:

$$ppDiff_{m_2,m_1} = m_2 - m_1 \quad (2.3)$$

The annual relative difference ($relDiff$), i.e. the proportion by which the annual mortality rates increased each year, was calculated using the census interval mid-years (t_x) of the first and second consolidated sets as:

$$relDiff_{m_2,m_1} = \left(\frac{m_2}{m_1}\right)^{\frac{1}{t_2-t_1}} - 1 \quad (2.4)$$

In addition to these absolute and relative comparisons between the first and second set of consolidated census intervals, summary statistics of the two sets were also generated across all plots for a given combination of number of plots and consolidated interval length. These summary statistics used were:

- The mean annual mortality rates of the first and second set of consolidated intervals;
    - their corresponding lower and upper 95 % and 99 % confidence interval bounds and whether there was an overlap between these confidence intervals.
- The absolute (ppDiff) and relative (relDiff) differences between the annual mortality rates of the two consecutive intervals;
    - their corresponding lower and upper 95 % and 99 % 2-tailed confidence intervals;
    - their corresponding lower 95 % and 99 % 1-tailed confidence intervals (since an increase is expected);
    - and whether these confidence intervals overlapped with zero.
- A linear model of the relative differences in annual mortality rates of the two consecutive consolidated intervals versus the overall census period mid-year, where:
    - it was noted whether a significant intercept was identified ($p \leq 0.05$ and $p \leq 0.01$).

Using these summary statistics, the 112,000 consolidated plot census tables generated in step 2a. were condensed into 28 trend result tables (e.g. middle and right panels of Figure

2.4). These trend result metrics tables have 4000 rows each, with one hundred random resampling repetitions for each unique combination of the four consolidated interval lengths and ten different numbers of plots (Figure A.2; e.g. Figure 2.5).

Step 3. Analysing the trends

In order to identify trends in the annual mortality rate metrics generated in step 2b above, and separate them from patterns which might merely have resulted from random variation in the plot census data, trend result metrics were compiled across the 100 repetitions of each combination (Figure 2.1, Figure A.3). The different combinations assessed the effect of the number of plots, consolidated interval length, relative annual increase scenario, and annual mortality rate distribution parameters.

A number of different metrics were evaluated for their ability to detect the persistence of trends across the repetitions. A metric which needs fewer plots to detect the same increase is preferred. These metrics included:

- the proportion of sample repetitions in which the 95 or 99 % confidence intervals of the mean annual mortality rates of the first and second set of consolidated intervals overlap;
- the proportion of repetitions where the one- or two-tailed 95 or 99 % confidence intervals of the absolute (*ppDiff*) or relative (*relDiff*) difference between the mean annual mortality rates of the first and consolidated second set contain zero;
- the proportion of cases in which the intercept of the linear model of the relative differences in annual mortality rates versus the census period mid-year was found to be significant at the 95 and 99 % level.

Both *ppDiff* and *relDiff* had normal distributions, enabling the utilisation of their parametric confidence intervals.

The result of this final step was a table of 1120 rows (for the 28 mortality rate dynamics variations, 4 consolidated interval lengths, 10 different numbers of plots), denoting the proportion of the total 100 repetitions where a metric of interest was observed (Figure A.3). From this table, the most efficient trend result metrics were identified.

2.2.2 Identifying short-term mortality rate increases

For answering the second research question, which aims to identify the number of forest sample plots required for detecting an increase in annual mortality rates caused by one-off short-term “catastrophic” events, a similar three-step approach was applied (see Figure 2.6). Firstly, an extensive plot census sample dataset was generated for disturbances of various degrees of magnitude from which repeated random samples were drawn using an

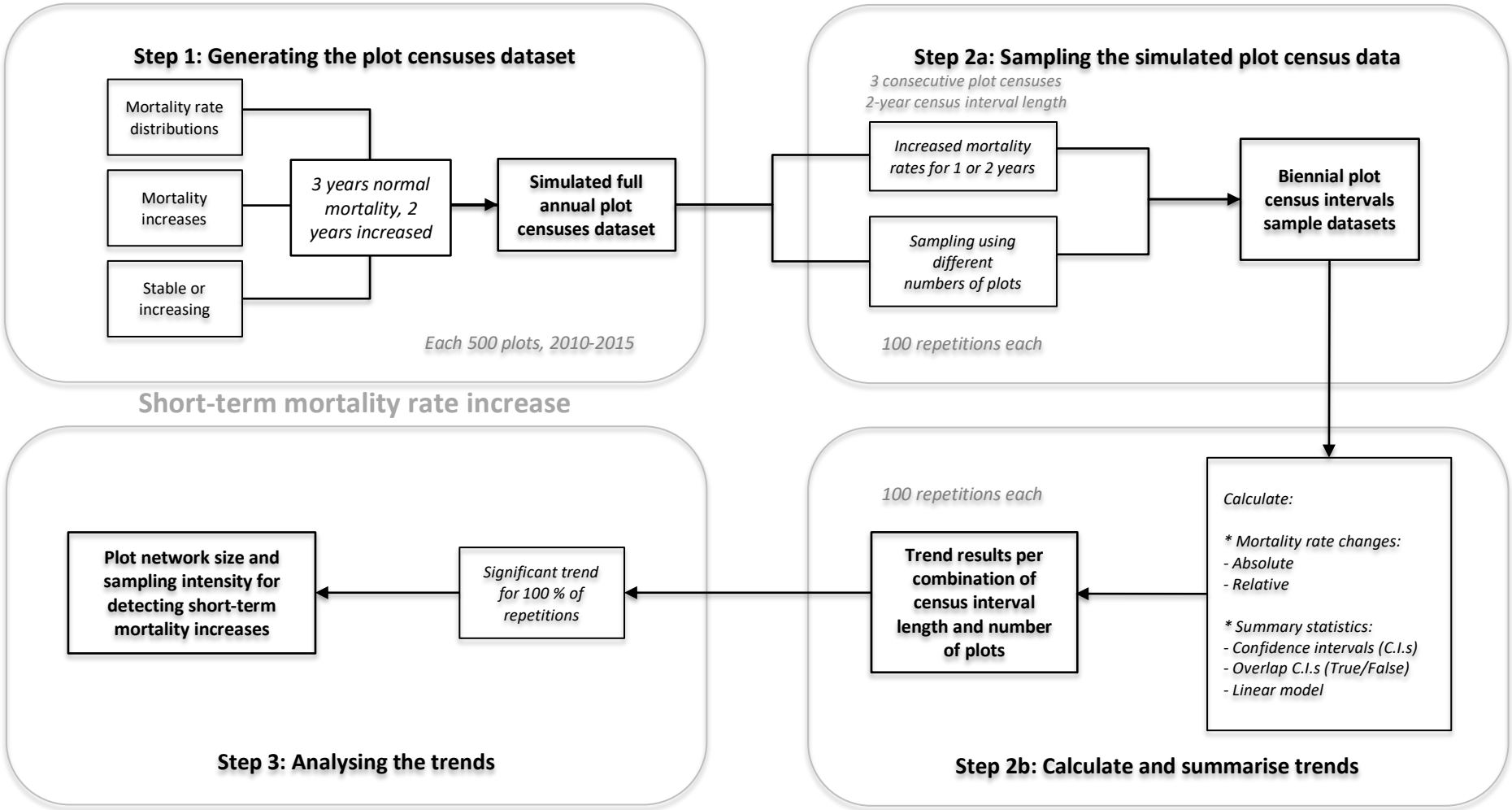

Figure 2.6. Flowchart of the process for determining the recommended plot network size for detecting short-term mortality rate increases.

increasing number of plots. The trend results were then also evaluated for their consistency in detecting increases of varying magnitudes using a specified number of plots. The main differences, compared to the process for detecting a long-term increase in mortality rates as described in Section 2.2.1, concern a greater magnitude of sudden increases in mortality rates, simulated as occurring over a shorter period of time, the inclusion of more plots in the first step, and a different sampling strategy in step 2a as detailed below.

For simplicity, here, only one mortality rate distribution ($N(-4.5, 0.75^2)$, corresponding to median and mean mortality rates of 1.1 and 1.4 % per year respectively; see Table 2.2) was used to generate the sample plot censuses dataset. In addition, since the focus here is to detect potential increases in annual mortality rates associated with short-lived one-off catastrophic events, only a consolidated census interval length of 2 years was used. However, since intra-census interval variation might be greater than inter-census interval variation with just a 2-year census interval length and a low rate of increase in annual mortality rates, a larger number of plots (500) was simulated in step 1, to allow for random sampling up to a greater number of plots in step 2a (see Figure 2.6).

Firstly, a sample dataset was generated simulating a one-off known increase in mortality rates. Simulated plots were initialised in 2010 and subjected to three years of (increasing) "background" annual mortality and recruitment rates under the m0r0, m2r2, m2r3 and m4r4 dynamics scenarios (2010-2013), after which the (relative increase in) "background" annual mortality rate was increased by either 5, 7.5, 10, 15, 20, 30, 40, 50, 75, or 100 % for two years (2013-2015).

In step 2a, an increasing number of plots (10 to 250, in increments of 10) were randomly drawn from the dataset generated in the first step, with 100 draws made for each replicate. The plot censuses from these plots were consolidated in two ways, each representing a different post-disturbance tree mortality measurement scenario.

The first scenario represents a short-lived mortality event, resulting only in elevated annual mortality rates for the duration of a single 1-year census interval, or where plots were re-censused one year after the event, but which had already undergone a year of background mortality since the last re-census prior to the event. For these plots the consolidation process combined two "background mortality" census intervals into the first consolidated set (2010-2012), and one census interval with "background mortality" and one with "elevated mortality" into the second consolidated set (2012-2014).

The second scenario represents a mortality event resulting in prolonged elevated mortality rates throughout the entire second 2-year census interval, with the timing of the mortality event immediately following the first census interval. This scenario can also be used to evaluate instances where the post-disturbance re-census has been made after a year. In

this scenario, the first set consisted of consolidation of two census intervals under "background mortality" (2011-2013), and the second set consisted of two census intervals under "catastrophic mortality" (2013-2015).

Step 2b was the same as has been described for determining the number of plots required for detecting long-term increases in forest dynamics in Section 2.2.1: metrics of trends between the first and second consolidated set were compiled, across all plots for each of the 100 repetitions.

In the third and final step, trend results were again compiled across all repetitions, for each combination of number of plots and magnitude of the catastrophic event (see Figure 2.6). These proportions were used to determine the number of plots required to detect a one-off catastrophic event of a given magnitude in forests that are re-censused at a 2-year census interval length.

Unless mentioned otherwise, all results focus on the number of plots required to detect an increase using the two-tailed 95 % confidence interval of the absolute (*ppDiff*) or relative (*relDiff*) difference in annual mortality rates between the two consecutive census intervals for the distribution with a mean base annual mortality rate of 1.4 % per year (Table 2.2). While all metrics at all levels of significance are provided in Appendix B, here only results which held across all repetitions are presented. For an evaluation of the various trend result metrics see Appendix C.

2.3 Results

2.3.1 Identifying long-term mortality rate increases

Census interval length

The number of plots required to detect an increase in annual mortality rates decreased as the consolidated census interval length increased (see Figure 2.7, Appendix B).

For example, when using two consecutive census intervals of 2 years each, 100 plots are not enough to detect a mortality rate increase of up to 3 % per year for any of the mortality rate distributions. However, when using 5-year census intervals, a 3 % long-term increase in annual mortality rates can be detected using at least 30 (*ppDiff*) or 40 (*relDiff*) plots. For a 2 % increase, at least 90 plots were required to detect it confidently (both for *ppDiff* and *relDiff).*

With a 10-year census interval length, only 10 plots were required to detect a 3 % increase in mortality rates, and 20 plots sufficed for detecting a 2 % increase. With this consolidated interval length, even increases of 1 % in annual mortality rates were detectable with just 40 plots.

Finally, using 20-year census intervals, only 10 plots were required to detect an increase of 1 % in annual mortality rates .

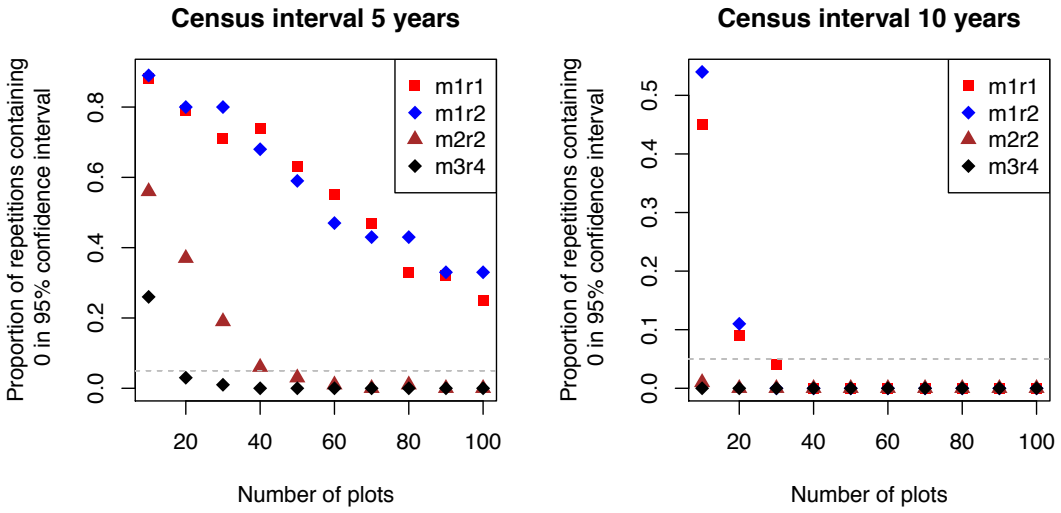

Figure 2.7. The number of one hectare plots required for detecting a long-term increase of annual mortality rates decreases with increasing levels of forest dynamics and increasing census interval length.
The dashed grey horizontal line demarcates where 5 % of repetitions generate confidence intervals on the estimate of change that contain zero: any points below this line represent sampling intensities that would confidently detect the specified change. Results shown here for consolidated intervals of length 5 (left) and 10 years (right) for the non-baseline population dynamics variations, where m# and r# denote the relative increases in annual mortality and recruitment rates respectively for the different scenarios.

Annual mortality rate distribution parameters

In general, the mortality rate distributions with a higher mean value needed fewer plots to detect an increase of the same magnitude (see Appendix B). This pattern was more pronounced at longer census interval lengths and for greater long-term increases in mortality rates. For example, the annual mortality distribution with a mean of 1.8 % (-4.25 in logistic space; median 1.4 %) needed only 60 plots to detect a 2 % increase using *ppDiff*; for the distribution with mean of 1.7 % (-4.5 in logistic space; median 1.1 %), this value increased to 90 plots, and with a mean of 1.1 % (-4.75 in logistic space; median 0.86 %), even 100 plots were not sufficient to detect this increase.

While slightly less pronounced, it appears that mortality rate distributions with a higher standard deviation (SD) also needed fewer plots to detect the same long-term increase in mortality rates. For example, with a 10-year census interval length, for the distribution with a standard deviation of 1.0, just 30 plots were required to detect a 1 % increase in long-term mortality rates using *ppDiff*, while for a standard deviation of 0.75 this increased to 40, and for a standard deviation of 0.5, it was 70 plots. This same general trend was again observed for *relDiff* too (see 'm1r1' in Appendix B; for 'm1r2' 40, 40 and 60 plots were required respectively).

Population dynamics scenario

The greater the long-term mortality rate increase, the fewer plots were needed to detect the change for any given distribution and consolidated interval length (see Figure 2.8). For example, for a census interval length of 10 years, only 10 plots were required to detect a 3 % increase in annual mortality rates (using *ppDiff*), whereas detecting a 2 % increase required 20 plots, and detecting a 1 % increase required 40 plots (both for 'm1r1' and 'm1r2'; see right panel in Figure 2.7). As such, within a given distribution, the mortality rate increase mainly determines the number of plots required for detection, irrespective of whether the overall population is stable (equal increases in recruitment and mortality) or increasing (the increase in recruitment outpaces the increase in mortality). The same finding held for *relDiff*.

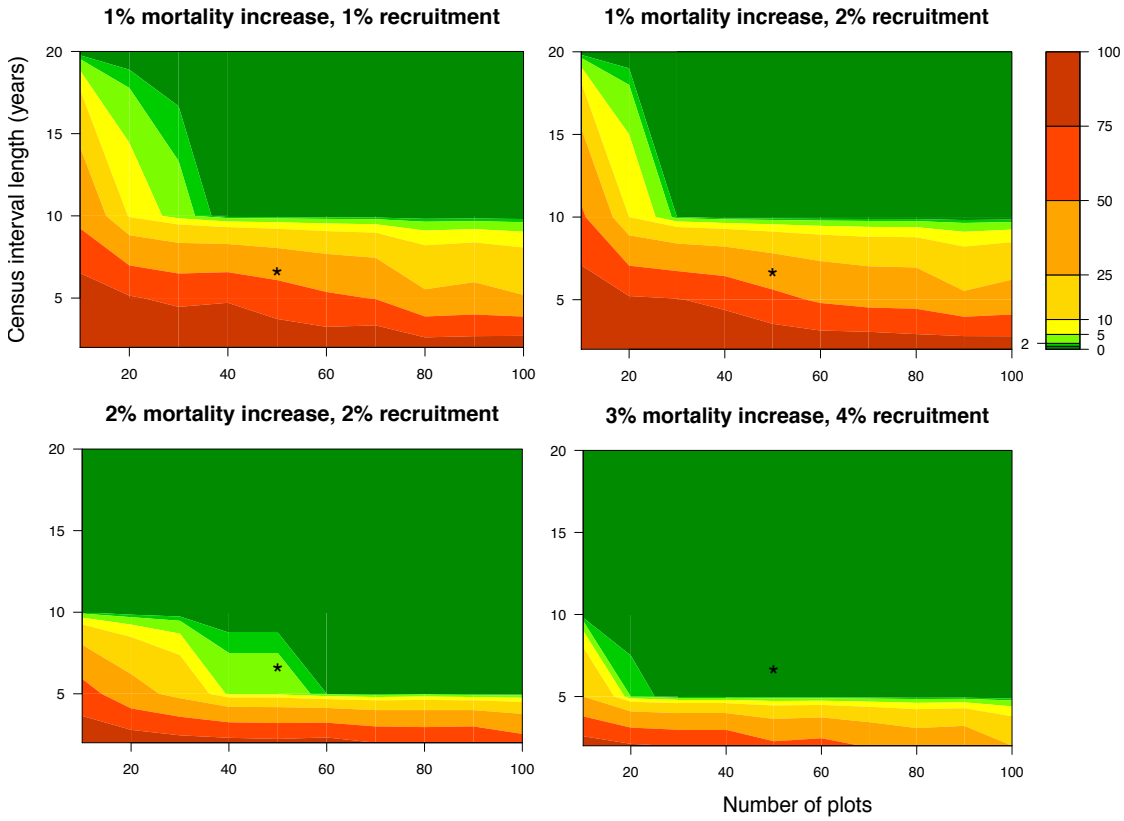

Figure 2.8. The required sampling intensity for confidently detecting a long-term increase in mortality rates decreases with increasing forest dynamics and increasing census interval lengths.
Detection confidence levels are defined as the proportion of repetitions where the two-tailed 95 % confidence interval of the percentage points difference between the two consecutive sets of annual mortality rates overlap with zero (from 0 % in dark green to 100 % in dark red; ≤5 % for all shades of green). These results are for a mortality rate distribution defined as $N(-4.5, 0.75^2)$, corresponding to a distribution with median and mean annual mortality rates of 1.1 and 1.7 % per year respectively. The asterisk (*) denotes the sampling intensity associated with the observed 3 % increase in mortality, and 4 % increase in recruitment reported by Lewis et al. (2004).

2.3.1 Identifying short-term mortality rate increases

At a 2-year census interval length, the intra-plot census variation can equal or exceed the inter-plot census variation in annual mortality rates, and, as a result, a relatively high number of plots were required to detect relatively small increases caused by one-off mortality events (see Figure 2.9, Appendix D).

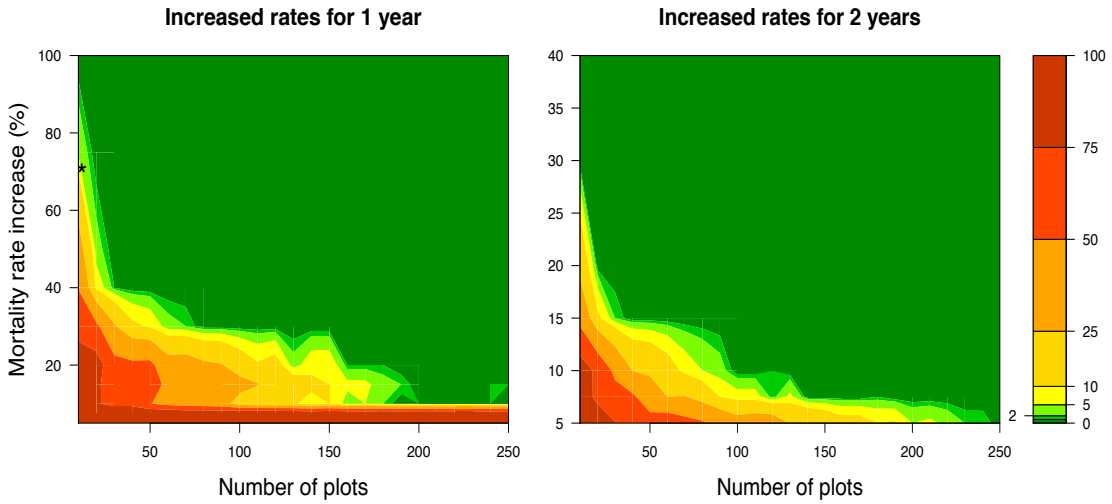

Figure 2.9. The required sampling intensity for confidently detecting a one-off catastrophic increase in mortality rates decreases with increasing magnitude of the disturbance event.
The impact of sample size on the proportion of repetitions (from 0 % (darkgreen) to 100 % (darkred); ≤5 % for the three shades of green) where overlap with zero is observed for the 95 % confidence intervals of the relative difference between the "background" annual mortality rates (drawn from distribution $N(-4.5, 0.75^2)$, corresponding to a distribution with median and mean annual mortality rates of 1.1 and 1.7 % per year respectively, under variation 'm0r0' (no increase)), and those following a "catastrophic" event of varying magnitudes (relative annual mortality rate increase in %). Census interval length is 2 years, and the elevated "catastrophic" annual mortality rates persisted either for one year (left), or two years (right). The asterisk (*) denotes the observed relative increase in mortality rates (71 %) for 12 plots over a 1-year census interval reported by Williamson et al. (2000).

The results from two different mortality event scenarios are presented here: firstly, the number of plots required to detect a "short-lived" mortality event, where the increased mortality rates persisted only for 1 year (left panel in Figure 2.9), and secondly, the number of plots required for detecting a "prolonged" mortality event, where the mortality rates increased at the specified relative increase rate throughout the 2-year census interval (right panel in Figure 2.9).

For the first "short-lived" scenario, detecting a 10 % increase in annual mortality rates over a 2-year census period required 250 plots. As the relative annual increase in annual mortality rates for the catastrophic event year increases from 20, through 30, 40, 50, 75 to 100 percent, the number of plots required to detect this increase drops from 190, through 80, 40, 30, 20, to 10 (see Appendix D, left panel Figure 2.9).

These results mean that 40 plots are sufficient to detect a 40 % increase in mean annual mortality rates, from 1.4 % to effectively 1.7 % during the consolidated census interval of length 2 years (with one year at 1.4 % $year^{-1}$ and one at the 40 % increased "catastrophic"

rate of 2.0 % year^{-1}). Ten plots are sufficient to detect an increase to effectively 2.2 % year^{-1} in the case of one year with relative increase in mortality of 100 % (equivalent to elevating annual mortality rates to nearly 2.9 % year^{-1} during the year with the catastrophic mortality event).

For the second scenario, where the "catastrophic" event resulted in two consecutive years of elevated mortality rates, fewer plots were needed to detect the increase in mortality rates caused by the event. Detecting a 5 % increase in annual mortality rates was possible with 250 plots, a 7.5 % increase was detectable with 190 plots, and 10 % increase with 130 plots (see Appendix D, right panel Figure 2.9).

As observed before, in forest plots with increasing mortality (and recruitment) rates through time, fewer plots were required to detect a relative increase of the same magnitude. For example, the second scenario required 130 plots to detect a 10 % increase in annual mortality rates over a 2-year period under the 'm0r0' population dynamics variation. However, if the forests that were experiencing a concurrent long-term 2 % increase in mortality rates (variations 'm2r2' and 'm2r3') only 50 plots were required to detect this same increase, and 30 plots sufficed in forests experiencing a 4 % long-term increase in mortality rates (see Appendix D).

2.4 Discussion

2.4.1 Identifying long-term mortality rate increases

Overall, these results provide a range of conclusions for designing monitoring networks for detecting the impacts of climate change on forests. For identifying long-term sustained increases in annual mortality rates between two consecutive census intervals, an overall monitoring period of at least 10 years is recommended, though 20 years is preferable (see Figure 2.8). With an overall monitoring period of 20 years, a network of 40 one-hectare plots will allow for confident detection of increasing forest dynamics, even when the increases are relatively small (1 % annual increase in mortality rates, and 1-2 % annual increase in annual recruitment rates; see Figure 2.7, Appendix B). However, a minimum of 60-70 plots is recommended if wanting to detect such small increases in forests with a relatively low overall base mortality (average annual mortality rates of 1.1 to 1.2 %·year^{-1}; see Appendix B). A network of 60-70 plots will also enable detection of greater increases in forest dynamics (2 % increase in annual mortality and recruitment rates) for forests with a minimum average annual mortality rate of 1.4 %·year^{-1} using just a 10-year monitoring period, with two consecutive census intervals of 5 years each.

In general, the results from published studies that report the presence of a long-term trend in mortality rates are based on sampling strategies that are consistent with the findings of this study. For example, Lewis et al. (2004) reported an increase in annual mortality and

recruitment rates of 3 and 4 % respectively based on 50 plots monitored for an average overall period of 13.25 years (see asterisk in Figure 2.8). The results here suggest that this kind of trend can confidently be detected with a network of just 30 plots and an overall monitoring period of 10 years, with comparable mean annual base mortality and recruitment rates to this study of 1.5 % $year^{-1}$.

Similarly, Phillips and Gentry (1994) used turnover times (the mean of mortality and recruitment rates), to report an average relative annual increase of 3.7 % using 19 non-disturbed plots (mean 604 stems/ha, median 575), with an average census interval length of 8 years, where observed values of turnover rates increased from 1.54 to 2.04 %·$year^{-1}$. The mortality rates for the overall monitoring period (mean 1.85 %·$year^{-1}$, SD 0.75) were very similar to the turnover rates (mean 1.81 %·$year^{-1}$, SD 0.71; Phillips and Gentry, 1994). When comparing their increase with the results from the similar 'm3r4' forest dynamics variation here, we find that detecting an increase of this magnitude using 19 plots corresponds to the highest level of confidence (see Figure 2.8). Furthermore, using an increased dataset of 27 pan-tropical forest plots, an increase of 3.93 % in annual turnover rates from 1.49 to 2.01 %·$year^{-1}$ was identified over two consecutive censuses with an average interval length of 8.7 years. This sampling intensity again corresponds to such an increase being detected at the highest level of confidence using the 'm3r4' variation here (see Figure 2.8).

In a study of the long-term dynamics of Amazonian mortality rates, various significant ($p<0.05$) long-term trends in annual mortality rates were identified (Phillips et al., 2004). When relating their reported increases (from 1.26 to 4.83 % per year) to the corresponding simulations, this study assigns a similar level of confidence to these increases. Equally, for the non-significant increase observed in the plots in East & Central Amazon (1.43 % per year for the raw data (n = 12, 14; 12 years; p=0.23), 0.91 % per year for corrected (n=28; 10 years; p=0.33); Phillips *et al.*, 2004), the results here agree that more plots with a longer overall monitoring period would be required in order to confidently assess that these trends are not merely due to natural variation. Due to the East & Central Amazon's relatively low mean base annual mortality rates of 1.1-1.2 %, detecting an increase of 1 % at the highest level of confidence would require at least 50 (mean 1.1 %; median 0.86 % per year; Appendix B) or 70 (mean 1.2 %; median 1.1 % per year) plots with a 10-year census interval length.

Finally, a long-term monitoring study of mortality rates in a Sri Lankan mixed-dipterocarp rainforest (Ediriweera et al., 2020), again helps to illustrate how even relatively minor changes can be confidently detected if the overall monitoring period is long enough. Significant changes in annual mortality rates were identified along a gradient of elevations, with a decrease of 0.70 % observed for the plots at lowest elevations over 40 years (from 2.08 % to 1.81 % per year at an elevation of 335 m, using 16 plots), an annual increase of

2.38 % for the intermediate plots (from 1.23 % to 1.98 %·year^{-1}, at 560m, for 18 plots), and an increase of 1.39 % in the highland (from 1.62 % to 2.14 %·year^{-1}, at 915m, 16 plots). Despite the relatively small changes, we also find that increases of 1 % can be confidently detected with 10 plots with a census interval length of 20 years.

In contrast, at first glance, the results here seem to conflict with those from a recent study addressing sampling efforts required for detecting changes in long-term mortality rates (McMahon et al., 2019). Their study found a substantially higher number of plots would be required to detect a given increase, with more re-censuses during a longer overall monitoring period, based on the overall time it would take at the specified sampling strategy to detect the increase in 80 % of the simulations using a changepoint analysis. Their models represented forests experiencing 50 years of stem mortality rates of 2 %·year^{-1}, which then linearly increased over the course of 10 years, to 50 years at 4 %·year^{-1} mortality rates. When using a 1-hectare permanent sample plot network, they found 120 plots would be required, re-censused at least every three years for 30 years preceding and following the shift, and annually during the actual 10-year period when mortality rates increased, in order to confidently detect this increase.

However, the intention of their study was to only detect shifts in mortality rates of large individuals (e.g. ≥60 cm dbh), or of one particular species, and thus their simulated plots had only 25 trees per hectare: as a result 120 plots in McMahon et al. (2019) correspond to just five of the plots modelled in this study. Assuming a similar overall census period of 70 years, the relative annual increase between the average community mortality rates observed in the two consecutive 35-year census intervals would have been 1.82 %, which would be very confidently detected, at a community level, with just 5 fully sampled plots and three censuses. Furthermore, while McMahon et al. (2019) advocate that sampling of random individuals is the most efficient approach for detecting a shift to increased mortality rates of larger individuals or one species, due to these individuals being much further apart, this strategy might not necessarily cut down on overall fieldwork monitoring effort. More importantly however, permanent forest sample plots that measure and track all trees can serve to concurrently monitor much more than merely shifting mortality rates of some species through time, including for example recruitment rates, growth rates and forest species composition (e.g. Taylor et al., 2008). If mortality rates are found to be shifting, it is important to see how they are changing concurrently with these other variables, especially after any potentially catastrophic events (e.g. Fauset et al., 2012).

As such, while change-point analyses and sampling of random individuals are useful for determining whether a linear shift has occurred between two consecutive series of baseline rates, and can pinpoint the timing of this shift, and as such help identify any potential causes, the recommendations presented here will help provide a more complete picture of any on-going dynamics and compositional changes, while also still allowing

evaluations of changes in mortality rates per size class, taxon, or functional group (e.g. Condit et al., 1999; Nakagawa et al., 2000; Sheil et al., 2000; Laurance et al., 2009).

2.4.2 Identifying short-term mortality rate increases

Detecting an increase of annual mortality rates caused by a catastrophic event is most efficiently done with a network of at least 40 plots (Figure 2.9). This will allow detection of increases of 40 %, if the event occurs a year after the last re-census, or 15 %, if it immediately follows the re-census, for a forest with a mean "background" mortality rate of 1.4 %·year^{-1} and a 2-year census interval length (Figure 2.9).

Published studies, which were able to identify significant short-term trends in mortality rates, appear generally to have used sampling strategies that are consistent with the recommendations from this study. For example, Williamson et al. (2000) used only 12 plots to detect the impact of the 1997 El Niño drought event on annual mortality rates in 1-hectare central Amazonian old-growth rainforest permanent sample plots. While they identified a significant substantial relative increase (71 %, from 1.12% to 1.91%, p=0.004) in mortality rates for the droughted census intervals of merely 12-16 months, they found no significant difference between the mortality rates of the pre-drought and the 12 -13 months long post-drought census intervals. As such, had these post-drought rates been included in an overall droughted census interval of circa 2 years, the number of plots would have been too few to have confidently detected the short-term increase, rather requiring closer to 20 plots (left panel of Figure 2.9). However, due to the short duration of the droughted census interval, and by effectively excluding non-droughted mortality rates from it, even 10 plots would have sufficed to detect an increase of this magnitude (right panel of Figure 2.9).

Similarly, in an Atlantic tropical moist forest, the effect of the 1987 and 1999 El Niño-Southern Oscillation (ENSO) effects were detected using just five plots (Rolim et al., 2005). The large magnitude of the increases, from the 17-year long-term average of 1.4 % per year (average census interval 2.1 years) to 3.8 % (relative annual increase of 39 %) for the 1987 event and to 4.9 % (61 % annual increase) for the 1999 event, shows that events of a severe magnitude can still be confidently detected, even with a small sample size.

The increases reported by Williamson et al. (2000) and Rolim *et al.*, (2005) illustrate that if the catastrophic event is large enough (i.e. ≥30 % increase in annual rates over a 2-year period in the case of the former), a network of 5-10 plots can suffice to identify it. These studies however also highlight the importance of relatively frequent re-censuses when wanting to detect the impact of catastrophic events, since the event might otherwise occur several years after the last plot census, and thus include years experiencing only background mortality in the "catastrophic" census interval. This effect would substantially decrease the observed overall rates.

2.4.3 Limitations and further work

The forest dynamics variations as simulated here did not evaluate the scenario where the trend in mortality rates outpaces that in recruitment rates, as observed for example by Murphy *et al.* (2013) for the long-term dynamics of tropical rainforests in Australia. These forests were frequently disturbed by cyclones at various degrees of severity, and there was a long-term mortality increase of 2 % per year , and a 1 % per year increase in recruitment rates across their 20 plots monitored for 40 years. However, the number of plots required for confidently detecting a relative annual increase in annual mortality rates of 1 %, varied very little between the scenario where the population was stable (increases in recruitment rates equalling those of mortality at 1 %; 'm1r1') and the scenario where the overall population was increasing (recruitment rates increasing at 2 %; 'm1r2'). As such, no substantial differences in results are expected for scenarios where mortality outpaces recruitment (e.g. 'm2r1' as identified by Murphy *et al.*, 2013) compared to the corresponding "stable population" scenario 'm2r2' simulated here.

Despite the focus of this study being on detecting increases in mortality rates between consecutive census intervals, using the same monitoring efforts, a decreasing trend could also be detected. As such the method can also be applied to detect any potential eventual "levelling off" of currently observed increasing trends.

Though the effect is not expected to substantially alter the number of recommended plots required, future studies could address detecting changing rates in declining populations, linear increases in forest dynamics and the effect of variable interval lengths across plot censuses. Furthermore, the method used here could be adapted to provide estimates for required monitoring efforts in non-rainforest forests in- and outside of the tropics and assess if the numbers of plots required are similar when focussing on biomass losses.

2.4.4 Recommendations

Most studies identifying changing forest dynamics focus on changes in biomass, but stem-based mortality was found to be a key driver of size stand structure and above-ground biomass in Amazonia (Johnson et al., 2016). Here, we show that a permanent sampling network of 40 plots can be used to detect changes in long-term stem-based mortality rates of 1 %, with three censuses over a period of twenty years. In addition, with biennial censuses, a network of this size can also detect one-off increases of one year at 40 % and one year at the normal background mortality rate, or an increase 15 % if the disturbance immediately follows the last re-census and the elevated mortality is sustained until the next re-census. A network of at least 60 plots will detect annual increases ≥2 % in background mortality rates with three censuses over just ten years. A network of 100 plots, with censuses conducted every two years, will detect one-off catastrophic increases (where the census includes one year at background mortality rates) of 20 % for forests

with increasing mortality rates through time, or where the mean background annual mortality rate is ≥1.8 %.

These results indicate that recommendations for an optimal minimum sampling network size will therefore differ depending on the underlying level of forest dynamics of the region. For example, in regions with more dynamic forests like the Western Amazon (Johnson et al., 2016), it is advised to have a minimum sampling network of at least 40 plots, censused biennially, with an earlier re-census of approximately a year after the occurrence of any catastrophic event. However, in forests with relatively low mean mortality rates, like those on the Guiana Shield (Johnson et al., 2016), establishing a network of 70 plots is recommended, to detect similar small changes in background mortality rates. In general, for confidently identifying short-term catastrophic increases of over 15 %, (or over 40 % if including one year at background mortality rates), like in eastern Amazonian forests during El Niño drought events (e.g. Williamson et al., 2000), a sampling network of at least 40 plots is recommended. If wanting to detect both long- and short-term changes in mortality rates reliably, through setting up an extensive monitoring network, it could be advised to resample a proportion of the plots each year. This would ensure that the overall longer census interval length would allow for detection of any long-term trends, while still providing a recent re-census for that proportion of the plots for the detection of any short-term increases. Overall, the findings presented here will help national governments and environmental agencies design sampling strategies to detect changes in forest dynamics that are appropriate for their region (Vicuña Miñano et al., 2019). The robust statistical basis for these decisions will enhance confidence and help to support long-term investment in forest monitoring.

3 Tree mortality rates vary among biogeographical regions across the tropics

3.1 Introduction

Tree mortality shapes the standing biomass and structure of forests, returns nutrients to the soil, and provides a habitat for insectivorous birds in snags and for macrofauna in deadwood (Franklin et al., 1987). Though they have the potential to be long-lived, most trees die relatively young through an external cause of tree mortality, or a combination of causes, which can include a lack of resources (e.g. light, nutrients, water), biotic agents (e.g. parasitic insects, lianas, fungi, strangler figs) and adverse environmental conditions (e.g. flooding, fires, heat waves, landslides, blow-downs, volcanic eruptions, air pollution; Mueller-Dombois, 1986; Franklin et al., 1987). These processes operate at varying spatial and temporal scales, affecting from one individual tree to entire stands. Characterising variation in pan-tropical tree mortality rates can aid insights into whether and how mortality rate distributions vary at different spatial scales, and the relative importance of mortality drivers in different locations. Furthermore, since stem-based mortality rates have been identified as a key predictor of aboveground biomass (Johnson et al., 2016), understanding how these rates vary across the tropics might help understand controls on variation in biomass.

Existing studies that have examined tropical tree mortality rates at large spatial and temporal scales show there can be pronounced regional differences in mortality rates across the tropics. For example, western Amazonia, with its more fertile and shallow soils, has more dynamic forests than eastern Amazonia (Phillips et al., 2004; Quesada et al., 2012), and woody biomass residence times differ amongst all three tropical continents (Galbraith et al., 2013). These studies show that mortality rates are not constant at large spatial scales across the tropics and highlight the need for further understanding of mortality as a key ecological process. However, most tropical tree mortality studies to date have focussed on mortality dynamics at local scales, over relatively short periods of time, and use different protocols, thus making inter-comparison a challenge.

A large number of observations, through both time and space, is required for accurately characterising mortality dynamics (e.g. Lloyd *et al.* 2009). In this chapter, tree mortality rate distributions are therefore derived from a unique, long-term pan-tropical dataset spanning decades of measurements in hundreds of plots in the forests of all four tropical continents. This dataset enabled us to determine at which spatial scale tree mortality rate distributions can be best described. Following Feldpausch et al. (2012), we distinguish nine biogeographically distinct regions in the four continents with tropical forests (Figure 3.1). Based on the various edaphic, climatic and compositional processes in each of these biogeographical regions, we expect different regional mortality rate characteristics.

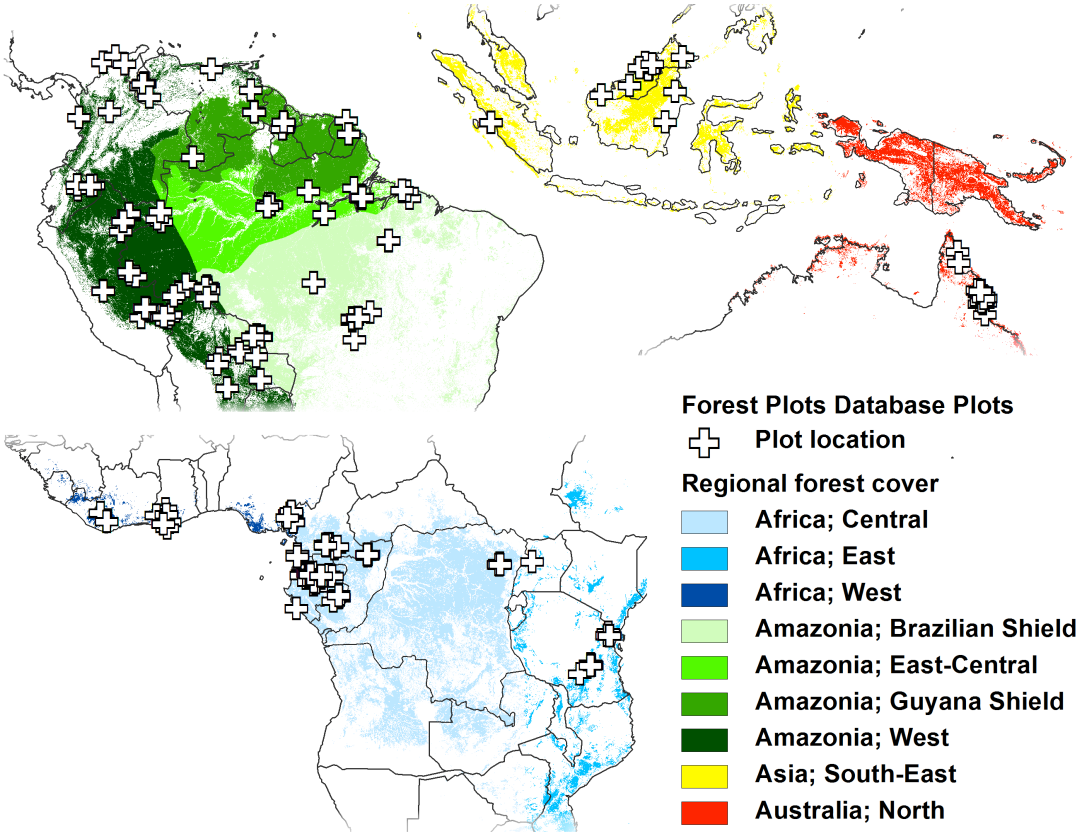

Figure 3.1. Location of the permanent sample plots within their corresponding biogeographical regions. Forest cover: European Commission, Joint Research Center 2003. Regions: Feldpausch et al. (2012). Plot locations: Lopez-Gonzalez *et al.* 2013.

Lower mortality rates are expected in North Australia, and Central and East Africa; intermediate mortality rates in West Africa, the Brazilian and Guyana Shields, and East-Central Amazonia; and higher mortality rates are expected in Western Amazonia and South-East Asia. The variability of mortality rates in these regions is mostly expected to follow the average mortality trends, except in West Africa and the Guyana Shield, where a greater variability in mortality rates is expected. We expect mortality rate distributions to vary among biogeographical regions, rather than merely among continents. We test this prediction by characterising mortality rate distributions at different scales (plot level, biogeographical, continental and pan-tropical), using nested hierarchical Bayesian models (Kruschke, 2015; McElreath, 2016).

The Bayesian models that are used in this chapter to derive estimates of tropical tree mortality are based on a logistic function, as has been applied in other studies estimating probabilities for dichotomous events like a tree dying (e.g. Hamilton Jr. and Edwards, 1976; Lines et al., 2010; Vanderwel et al., 2013). This distribution allows the skewed nature of mortality rates, where the large majority of tree deaths are concentrated in small events, to be accounted for. For example, in Amazonia, individual tree deaths and small disturbances of less than 0.1 hectare in area account for approximately 88.3 % of 1.88 Pg of carbon lost annually through natural disturbances (Espírito-Santo et al., 2014). Thus, since

most observed tree mortality events tend to involve only a few trees at a time, and larger-scale mortality events are rare, especially in the tropics, stem-based mortality rate distributions are expected to be long-tailed, as has been observed at the continental scale for pan-tropical woody residence times (Galbraith et al., 2013).

3.2 Materials and methods

3.2.1 Data

We derive mortality rates from tree measurements in a selection of long-term permanent sample plots of the RAINFOR (e.g. Phillips *et al.* 2004), AfriTRON (Lewis et al., 2009), Asian and Australian networks, as collated in the Forest Plots Database (Lopez-Gonzalez et al., 2013). The permanent sample plots are distributed across undisturbed old growth mixed forests in the tropics, and have a minimum plot area of 0.2 ha.

The 411 plots are typically one ha in size (1st quantile (25 %): 0.72, Q2 (median): 1.0; Q3 (75 %): 1.0). All trees with a diameter at breast-height (dbh; generally at 1.3 m) greater than or equal to 10 cm are tagged with a unique identification number, identified to the lowest possible taxonomic level and the dbh is measured. The plots have been re-censused 4.6 times on average (range 2-22, median 2), and have a mean census interval of 3.6 years (Q1: 1.6, Q2: 2.8, Q3: 5.0), resulting in a total of 1514 re-censuses during the period 1953-2012 (mean 1997). There are 26 unique plot census intervals in East Africa, 103 in Central Africa, 63 in West Africa, 69 in the Brazilian Shield (Amazonia), 246 in East-Central Amazonia, 262 in the Guyana Shield (Amazonia), 476 in West Amazonia, 183 in South-East Asia and 175 in North Australia, with a mean overall monitoring period of 14.1 years (Q1: 6.2, Q2: 11.9, Q3: 18.1). When plots are re-censused, it is noted whether the tagged trees have survived the census interval. New recruits are tagged and also checked for their status as dead or alive in the following census. There were no plots where no tree deaths had been observed during the entire monitoring period of the plot.

3.2.2 Mortality rates

Tree mortality rates can be expressed using the numbers of stems lost during a census interval. Following Sheil *et al.* (1995) we consider a stand of trees with a constant annual mortality rate of m (year^{-1}). The number of trees in our hypothetical stand that will survive (N_1) a census interval of T years, out of the original number of trees that were alive (N_0) at the start of the census interval, is given by:

$$N_1 = N_0(1-m)^T \qquad (3.1)$$

The annual stem-based mortality rate (the fraction of stems dying per year) can thus be expressed using the fraction of surviving trees as:

$$m = 1 - (N_1/N_0)^{1/T} \quad (3.2)$$

(Sheil et al., 1995). Our analysis sought to estimate and compare the magnitude of variation in m within plots through time, and among plots within biogeographical regions, continents, and across the tropics as a whole. To do so, we developed a set of hierarchical Bayesian models that each characterized the probability distribution of m at different spatial scales.

3.2.3 Hierarchical Bayesian Analyses

The structure of our hierarchical Bayesian models mimic the hierarchical nature of the tree measurement data collected in the permanent sample plots, where measurements are nested both temporally (various censuses over time per plot) and spatially (plots are located within biogeographical regions, contents and across the tropics). Here, the basic unit of mortality is one census interval in one plot, where the annual mortality rate during that census interval is derived from the number of trees that survive the census interval. We can further distinguish four scales of variation that describe the distribution of mortality rates among plots and census intervals:

1. Since climatic conditions in the same spatial location can vary from year to year, the first hierarchical level is the plot-level, which contains the mortality rates during all the census intervals for a given plot. This level therefore represents variation of the mortality rates in that location through time.
2. Plots within a biogeographical region are expected to exhibit more similar mortality rate distributions, due to similar geomorphologic and phylogenetic conditions. Biogeographical regions therefore form the next hierarchical level, with all the mortality rates of all the census intervals of all the plots in a biogeographical region contributing to the large-scale variation in mortality rates across space in that region. The biogeographical regions defined here (sensu Feldpausch et al., 2012) are Central Africa, East Africa, West Africa, the Brazilian Shield (Amazonia), East-Central Amazonia, the Guyana Shield (Amazonia), West Amazonia, South-East Asia and North Australia.
3. As the main phylogenetic differences in composition across the tropics are at the continental scale, neighbouring biogeographic regions were grouped together into their corresponding continents for the next level in the analysis: Africa, Asia , Australia and South-America.

4. The highest hierarchical level is comprised of the tropics as a whole, capturing the variation in both space and time across all measured plot census intervals in an attempt to characterise pan-tropical spatiotemporal variations in mortality rate distributions.

In this study, we define several variations on a basic statistical model. These model variations are each hierarchically structured, such that we can formally describe the probability distribution of mortality rates in different ways. By varying the spatial extent that these probability distributions represent, insight can be gained about the spatial scale that best describes variation in mortality rates and thus what processes may drive these differences. A full description of the distinctions of all tested models is provided in Appendix E.

For the first level in the hierarchy, we describe the annual rates for each census of a plot with a logit-transformed normal distribution of all annual mortality rates of that plot. Models with just one hierarchical level (HL1), assume the variation in mortality between plots is the same as that within a plot over time (i.e., there is no plot-specific mortality effect). Models with two hierarchical levels (HL2) overcome this, by allowing for plot-specific parameter estimates, nested within a regional level. While the mean mortality rate is plot-specific, the variance in mortality through time is shared across each region. At this second hierarchical level, the location parameters (mean) of these plot distributions are again assumed to be described by logit-normal distributions for the corresponding spatial region. This spatial region can either be the bio-geographical region, the continent or pan-tropical, resulting in nine, four and one estimated regional distribution(s) respectively.

Each of these three HL2 models is parameterised using a Bayesian Markov Chain Monte Carlo (MCMC) sampling approach with non-informative priors using Filzbach, a parameter estimation package (Purves and Lyutsarev, 2011). Three independent Markov chains are used for each model, to decrease the risk of finding a local maximum likelihood optimum. Each of these chains are run for a burn-in period of 500,000 iterations, with a further 500,000 iterations for parameter estimations. Overall chain convergence is assured by $\sqrt{\hat{R}}$ values of less than or equal to 1.20. In this fashion estimates, including uncertainty, for all relevant model parameters (see Appendix E, Table E.2) and Deviance Information Criterion (DIC) values were obtained for each of the three models. The DIC is most appropriate for comparing hierarchical models (Spiegelhalter et al., 2002).

Starting at the lowest level of the hierarchy, we estimate the annual mortality rate $m_{x,t}$ (year^{-1}) during census interval t in plot x. However, since mortality rates are bounded by 0 (no mortality) and 1 (complete mortality), and generally quite close to 0, this does not allow for an efficient sampling of the parameter space of interest. To ensure correct estimates are obtained, all model parameters are estimated as real numbers ($k_{x,t} \in \mathbb{R}$)

and only logistically transformed when compared to mortality observations. In this case $m_{x,t}$ is the logit of its corresponding model parameter $k_{x,t}$ (year^{-1}):

$$m_{x,t} = \frac{1}{1 + e^{-k_{x,t}}} \quad (3.3)$$

The probability of an individual tree dying during census interval t (of length T years) in plot x, which has an estimated mortality rate of $m_{x,t}$ per year, is:

$$P(died_{x,t}) = 1 - (1 - m_{x,t})^T \quad (3.4)$$

and the log-likelihood function for observing $N_0 - N_1$ dead and N_1 surviving trees for that plot's census interval, given $m_{x,t}$ and assuming a constant mortality rate during any given census interval, equates to:

$$LL(N_0, N_1 | m_{x,t}) = \underbrace{(N_0 - N_1) * \log\left(1 - (1 - m_{x,t})^T\right)}_{\substack{\textit{probability of } N_0\text{-}N_1 \textit{ trees dying during} \\ \textit{census interval } t \textit{ of length } T \textit{ in plot } x}} + \underbrace{N_1 * \log\left((1 - m_{x,t})^T\right)}_{\substack{\textit{probability of observing} \\ N_1 \textit{ surviving trees}}} \quad (3.5)$$

Moving up to the first level of the hierarchy, it is assumed that the logit-transformed mortality rates $k_{x,t}$, for each census interval t of length T in a given plot x, are drawn from a normal distribution with a plot-specific mean k_x (year^{-1}) and a region-specific standard deviation σ_c (year^{-1}):

$$k_{x,t} \sim N(k_x, \sigma_c) \quad (3.6)$$

Considering the full dataset, at the highest level of the hierarchy, the plot-specific mean k_x is drawn from a regional-scale (bio-geographical, continental or pan-tropical) normal distribution with a region-specific mean $k_{\mu,c}$ (year^{-1}) and standard deviation σ_c (year^{-1}):

$$k_x \sim N(\mu_c, \sigma_c) \quad (3.7)$$

The overall likelihood thus becomes:

$$LL = \underbrace{LL(N_0, N_1 | m_{x,t})}_{\substack{\textit{likelihood for one plot} \\ \textit{census interval}}} + \underbrace{LL(k_{x,t} | k_x, \sigma_c)}_{\substack{\textit{likelihood for all} \\ \textit{census intervals of} \\ \textit{one plot}}} + \underbrace{LL(k_x | \mu_c, \sigma_c)}_{\substack{\textit{likelihood for all} \\ \textit{plots in one region}}} \quad (3.8)$$

For each region, census mid date and plot size parameters were included as linear predictor variables.

3.3 Results

The spatiotemporal variation in our observed pan-tropical mortality rates is found to be described well using a normal distribution in logit-space. All models converged well, with the maximum $\sqrt{\hat{R}} \leq 1.20$ for all parameters of each model, ≤1.05 for all parameters of models with one hierarchical level (HL1), and ≤1.01 for all regional parameter estimates of HL2 models.

The Deviance Information Criterion (DIC) scores of the different models were compared to assess their performance. The biogeographical HL2 model had the lowest DIC score ($32.0 \cdot 10^4$), which was lower than both that of the HL1 plots only model and the HL0 model without any hierarchical levels ($32.3 \cdot 10^4$ vs $32.3 \cdot 10^4$ respectively). This HL2 biogeographical model assumes that the spatiotemporal distributions of mortality rates vary among biogeographic regions, rather than among continents or across the tropics as a whole, suggesting that intra-continental variation is greater than inter-continental variation.

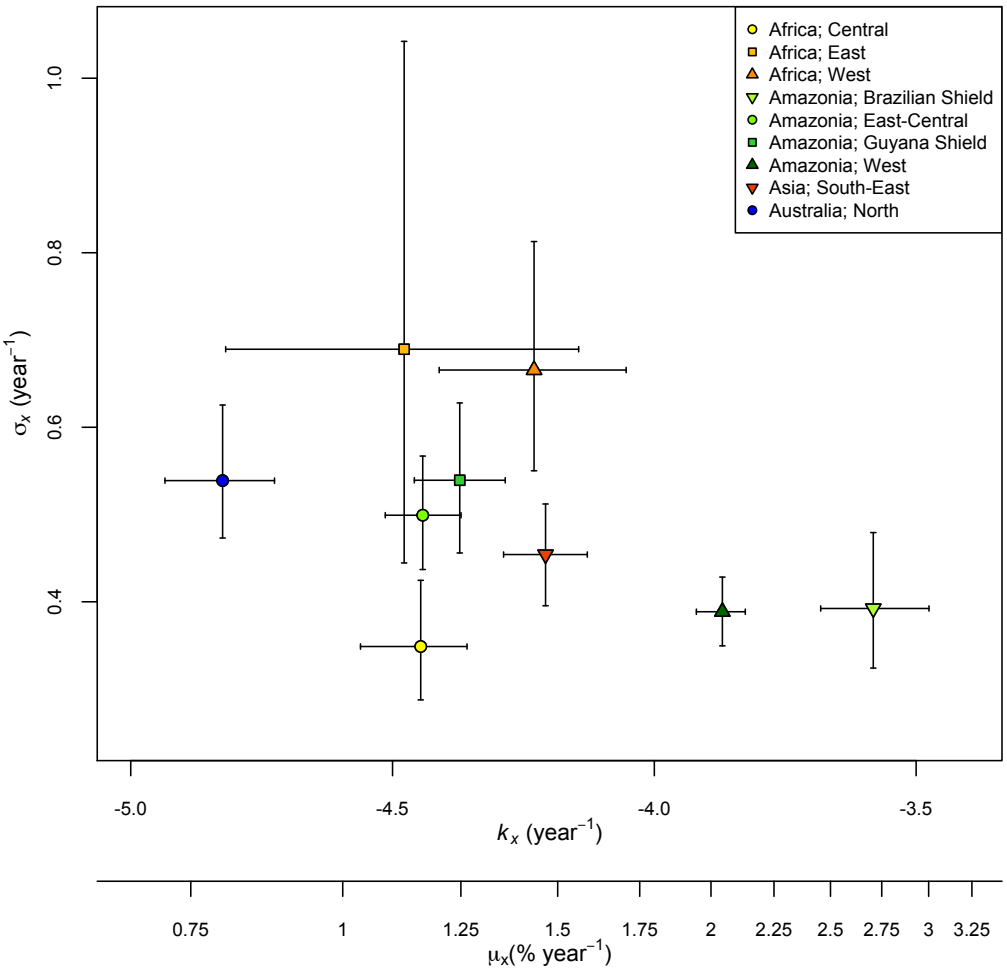

Figure 3.2. Mortality rate distribution parameter estimates for each biogeographical region. Estimates include 95 % credible intervals for the regional means μ_c (k_x in figure) and standard deviations σ_c (σ_x in figure) of the normal distributions in logit-space (including back-transformed mean annual mortality rate estimates $m_{x,t} - \mu_x$ in figure) describing the regional mortality rate distributions of observed annual mortality rates for each biogeographical region.

All biogeographical back-transformed μ_c values and their corresponding σ_c estimates in logit-space, are presented including 95 % credible intervals (Figure 3.2, Table 3.1). Northern Australia is the biogeographical region with the lowest median mortality rate (0.80 %·yr^{-1}; mean 0.92·yr^{-1}), which is significantly lower than the median of all other biogeographical regions, except for East Africa (1.12 %·yr^{-1}; mean 1.40 %·yr^{-1}), possibly due to the plots in East Africa only being represented by 26 plot census intervals. East Africa thus only has a significantly lower median than the two regions with the highest median

mortality estimates: West Amazonia (2.04 %·yr^{-1}; mean 2.19 %·yr^{-1}) and the Brazilian Shield (2.71 %·yr^{-1}; mean 2.90 %·yr^{-1}).

Table 3.1. Parameter estimates of the annual mortality rate distributions for the various regions at the biogeographical (BG), continental (C), and pan-tropical (PT) level.
Estimates include their 95 % credible intervals in brackets. The back-transformed regional estimates μ_c (%·year^{-1}), correspond to the medians of the logit-normal distributions, and the standard deviations are for the distribution in logit-space σ_c (year^{-1}). Using both of these parameters, the corresponding equivalent regional mean annual mortality rates m_c (%·year^{-1}) have been derived. To enable comparison with values from other studies, the standard deviations of the logit-normal distribution sd_c (year^{-1}) are included. The coefficients of variation cov_c show the same trend as the original σ_c estimates.

Region		μ_c	σ_c	m_c	sd_c	cov_c
BG	Central Africa	1.16 (1.03-1.26)	0.35 (0.29-0.42)	1.23	0.44	0.35
BG	East Africa	1.12 (0.80-1.56)	0.69 (0.44-1.04)	1.40	1.05	0.75
BG	West Africa	1.43 (1.20-1.71)	0.67 (0.55-0.81)	1.77	1.28	0.72
BG	Brazilian Shield	2.71 (2.45-3.00)	0.39 (0.32-0.48)	2.90	1.14	0.39
BG	East-Central Amazonia	1.16 (1.08-1.25)	0.50 (0.44-0.57)	1.31	0.69	0.52
BG	Guyana Shield	1.25 (1.14-1.36)	0.54 (0.46-0.63)	1.44	0.82	0.57
BG	West Amazonia	2.04 (1.95-2.13)	0.39 (0.35-0.43)	2.19	0.86	0.39
BG	South-East Asia	1.47 (1.35-1.59)	0.45 (0.40-0.51)	1.62	0.75	0.46
BG	North Australia	0.80 (0.71-0.88)	0.54 (0.47-0.63)	0.92	0.53	0.57
C	Africa	1.24 (1.15-1.35)	0.54 (0.47-0.61)	1.42	0.81	0.57
C	South America	1.63 (1.57-1.70)	0.54 (0.50-0.57)	1.87	1.05	0.56
C	Asia	1.46 (1.35-1.57)	0.46 (0.40-0.52)	1.62	0.76	0.47
C	Australia	0.80 (0.72-0.88)	0.54 (0.46-0.62)	0.92	0.53	0.57
PT	Pan-tropical	1.43 (1.39-1.48)	0.57 (0.55-0.59)	1.66	1.00	0.60

The median mortality rate estimate in Central Africa (1.16 %· yr^{-1}; mean 1.23 %·yr^{-1}) is virtually identical to that of East-Central Amazonia (1.16 %· yr^{-1}; mean 1.31 %·yr^{-1}) and similar to that of the Guyana Shield (1.25 %· yr^{-1}; mean 1.44 %·yr^{-1}), though its standard deviation in logit-space (0.35 yr^{-1}) is significantly lower. The μ_c estimates of West Africa (1.43 %·yr^{-1}; mean 1.77 %·yr^{-1}) and South-East Asia (1.47 %·yr^{-1}; mean 1.62 %·yr^{-1}) are also similar to one another. Frequent high-mortality events observed in West Africa are likely to be responsible for its standard deviation estimate (0.67 yr^{-1}) being significantly higher than that of South-East Asia (0.45 yr^{-1}).

Overall, after translating these biogeographical μ_c and σ_c estimates into their corresponding mortality rate distributions (Figure 3.3), they are found to approximate the observed plot census interval rates reasonably well (Figure 3.4).

While the variation in mortality rate distributions was found to be best described at the biogeographical scale, there is also evidence for differences among continents (DIC = 32.5·10^4): the median mortality estimates μ_x differ significantly between most continents,

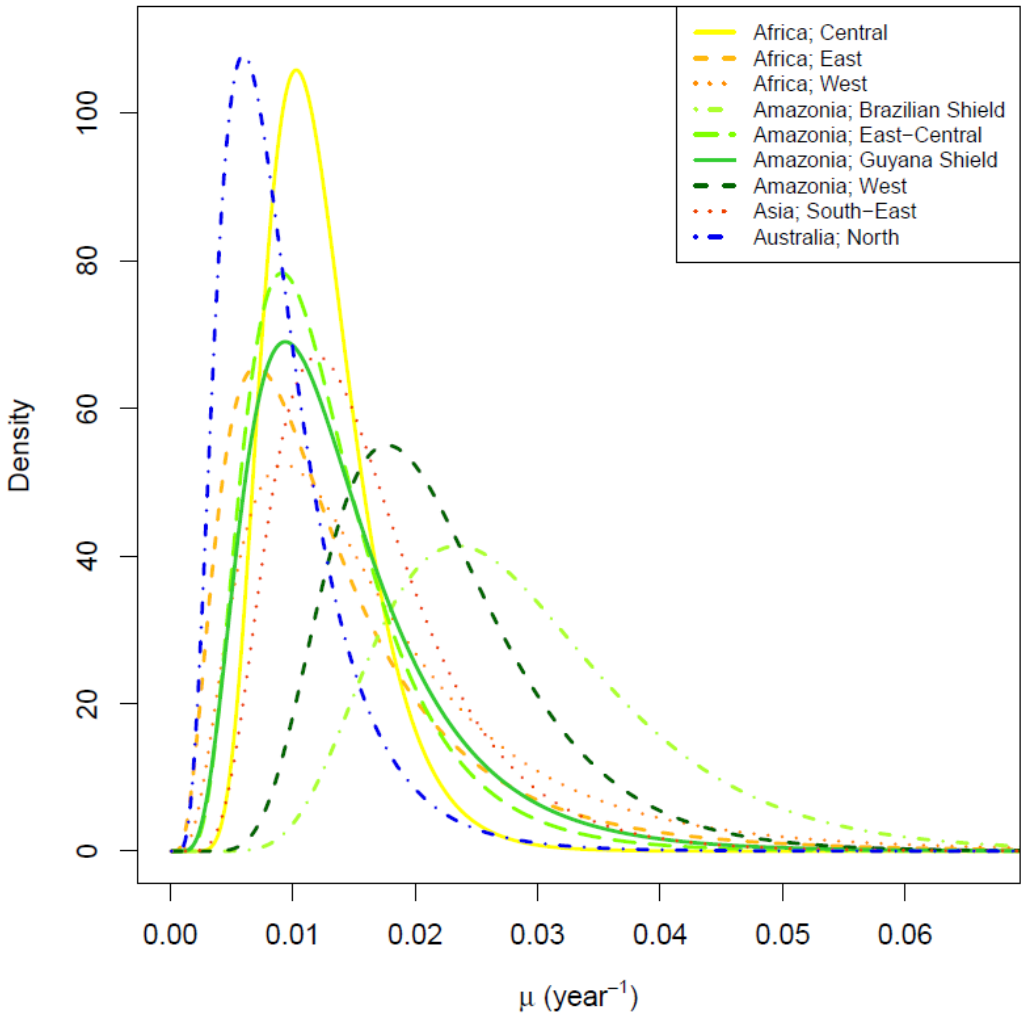

Figure 3.3. The estimated annual mortality probability density distributions for all biogeographical regions. These distributions describe the relative probabilities of observing a given annual mortality rate *m* (μ in figure) in each of the biogeographical regions, back-transformed to a logit-normal distribution from the corresponding region's μ_c and σ_c estimates in logistic space.

based on a lack of overlap between the 95 % credible intervals of the parameter estimates (Table 3.1). Australian forests have the lowest median mortality rates (0.80 %·yr^{-1}; mean 0.92 %·yr^{-1}). Median annual mortality rates in African forests are just significantly lower at 1.24 %·yr^{-1} (mean 1.42 %·yr^{-1}) than those of South-East Asian forests (1.46 ; mean 1.62 %·yr^{-1}). The credible intervals for South-East Asian forests slightly overlap the higher median rates of 1.63 %·yr^{-1} for plots in South America (mean 1.87 %·yr^{-1}). This overlap is expected, since at the continental scale, the South American region includes forests from both the East-Central and Guyana Shield regions, which have a significantly lower estimates of μ_c than South-East Asia in the biogeographical regions model.

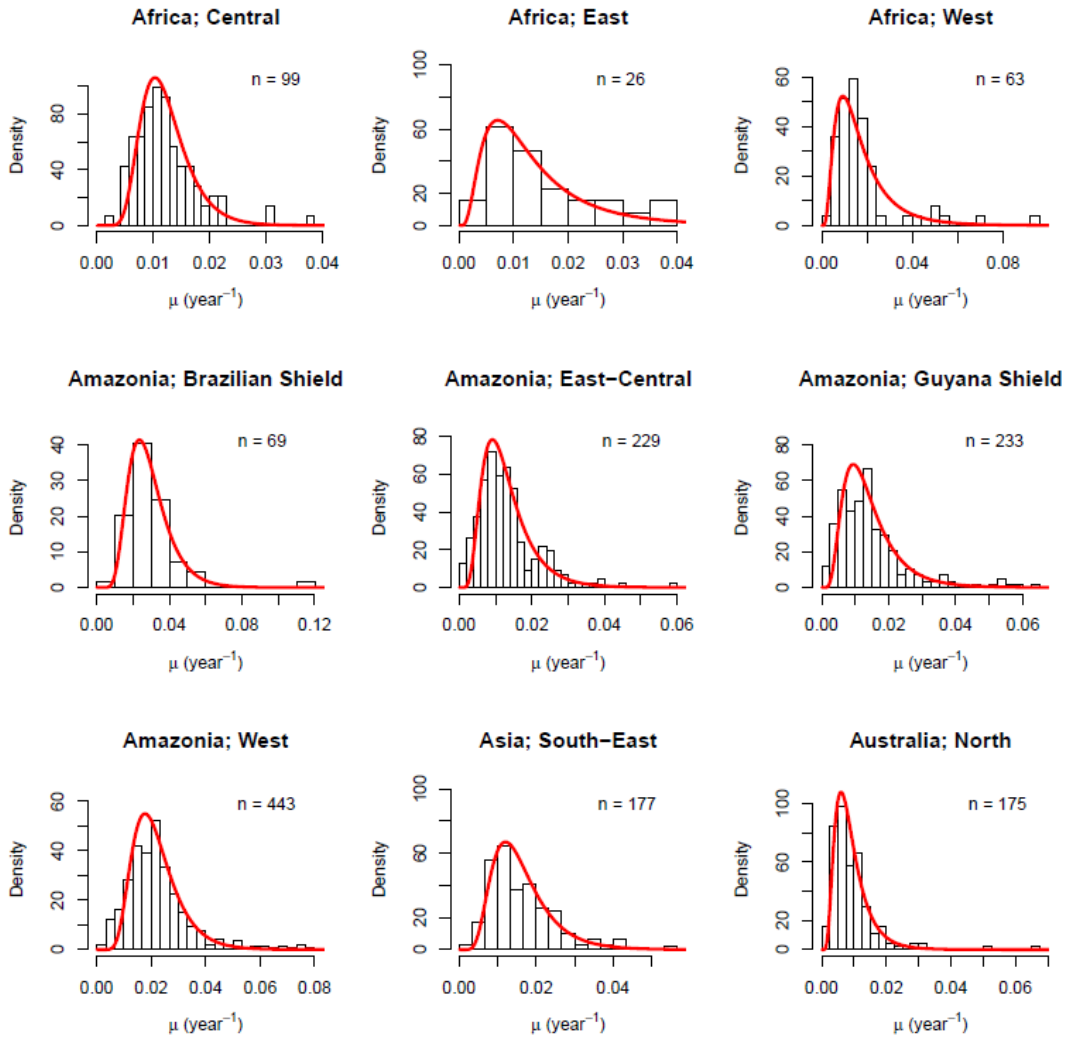

Figure 3.4. The fit of the estimated probability density distributions of each biogeographical region relative to their proportions of mortality rates observed for each plot census interval.
The number of observed plot censuses (n) is included for each region.

The pan-tropical hierarchical mortality model has a similar DIC score to the continental scale model ($3.25 \cdot 10^4$). The pan-tropical median estimate (1.43 %·yr^{-1}; mean 1.66 %·yr^{-1}) closely matches the rate observed in the actual plot census data of 1.42 %·yr^{-1}, and estimates from previous studies of a mean pan-tropical turnover rate of 1.74 %·yr^{-1} (SE 0.06; n=158; Stephenson and van Mantgem, 2005), and a median background tropical mortality rate of 1.6 %·yr^{-1} (n=68; Lugo and Scatena, 1996).

The final estimated distributions confirm that mortality rates vary at biogeographical regions within continents, indicating that variation in tropical tree mortality is likely to be driven by a combination of edaphic, climatic and compositional factors.

3.4 Discussion

Regional variation in pan-tropical annual tree mortality rates can be captured well by normal distributions in logit-space using random effect hierarchical Bayesian analyses at

biogeographical, continental and pan-tropical spatial scales. Furthermore, this study has shown that this method can be used to specify probability distributions at these different spatial scales, including credible intervals for the parameter estimates. Crucially, this approach therefore allows robust statistical comparisons of the distributions. Overall, variation in mortality rates was greater among, rather than within regions: there are distinctive mortality rate distributions for different biogeographical regions, reflecting not only regional differences in the median and mean mortality rates, but also the relative importance of the magnitude of mortality events in shaping overall forest dynamics.

Most estimated biogeographical region-specific mortality rate distribution parameters matched our expectations. The main inaccuracies in the predictions are in the variability of the mortality rates within a biogeographical region, with a third of them being the opposite of what was expected (high estimated variability in mortality rates, rather than the expected low variability, in East-Africa; low in West Amazonia; and high in Australia) and two being lower than expected (low in the Brazilian Shield (Amazonia) and average in South-East Asia). Of the median mortalities, only one estimate - for the Brazilian Shield - was higher than expected.

Overall, the consistency of the predictions with the results suggests that regional median mortality rates can be predicted based on an understanding of variation in climatic and edaphic conditions, and species composition. Although the approach does not provide definitive answers as to the specific drivers involved in each case, it is possible to speculate on the key attributes of each region that may determine the different patterns. The key patterns documented here are high levels of variation in mortality rates among different regions of African forests, low mortality rates but with high variability in forests in North Australia, and high mortality rates with low variability for forests both in West Amazonia and on the Brazilian Shield.

With regards to the influence of climatic and edaphic conditions on tree mortality rate distributions, we expected trees growing in arid, cooler, more seasonal and/or nutrient-poor conditions to grow more slowly, become denser-wooded, and thus more resilient to unexpected dry spells or snapping during multiple tree- fall or wind-throw events (e.g. Muller-Landau, 2004), corresponding to lower expected mean mortality rates and less variability (Hammond, 2005; **Error! Reference source not found.**). Cyclones are expected to not only increase average mortality rates, but also the intraregional spatiotemporal variability, since some patches can experience large-scale blow-downs, while others will be unaffected (Table 3.1). If trees have a shallow rooting system, for instance due to the presence of a physical barrier, or their soil becomes waterlogged, storm events increase the likelihood of these trees being uprooted (Gratkowski, 1956; Table 3.1). With increasing soil age, weathering tends to increase soil depth and increase tree stability (Table 3.1). Finally, the geological history of different continents has resulted in differences in forest

composition and diversity (Richards, 1996), which may also cause differences in mortality rate distributions among different biogeographical regions. For example, South-East Asian tropical forests tend to be dominated by Dipterocarpaceae, whereas African forests tend have a much lower diversity (Richards, 1996; Primack and Corlett, 2005), Australian rainforests have more sclerophyllic species (Bowman, 2000) and South American forests are highly diverse (Primack and Corlett, 2005; Richards, 2005). Through combining these hypothesised effects from climatic and edaphic conditions and species compositions and diversity for the different biogeographical regions, we formulated our expectations for their relative mortality rate distribution characteristics (Table 3.3).

Table 3.2. Hypothesised effect of climatic and edaphic variables on mean and variation in tree mortality rates
↑ = positive effect (increased mortality rates/greater variability), ↓ = negative effect (reduced)

	Hypothesised effect	
Climate	**Mean**	**Variability**
Mean annual precipitation	↑	↑
Seasonality	↓	↓
Mean annual temperature	↑	↑
Dry season (no. of months)	↓	↓
Cyclone events	↑	↑
Soils	**Mean**	**Variability**
Soil fertility (org. C content)	↓	↑
Soil rooting depth	↓	↓
Easily available moisture	↑	↑

The relatively low median mortality rates of Central African forests, with very few larger mortality events (Figure 3.4, Table 3.1), may be driven by a combination of deep, nutrient-poor, sandy, and acidic soils (Hart et al., 1989; Peh et al., 2011; Kearsley et al., 2013), a high abundance of shade-tolerant mono-dominant species (Lewis et al., 2013), and relatively low mean annual precipitation (Malhi and Wright, 2004). East African forests also had relatively low median mortality rates (Figure 3.2, Table 3.1), which may be due to relatively low mean annual precipitation and temperatures, with forests on deep soils with relatively little organic carbon content and little easily available moisture (Eggeling, 1947). While we expected there to be few larger mortality events, it actually appeared to be one of the mortality rate distributions with the heaviest tail (Figure 3.4), which could, amongst others, be caused by disturbances by elephants (Eggeling, 1947).

Table 3.3. Overall expected mean and variability in mortality rates for different biogeographic regions based on the hypothesized effects of predominant climatic and edaphic conditions (Table 3.1) and species composition.

↑ = higher rates/greater variability, - = average rates/variability, ↓ = lower rates/less variability, MAP = mean annual precipitation, Snl. = seasonality (inter- and intra-annual climatic variation), MAT = mean annual temperature, DSL = dry season length, CE = cyclone events, SF = soil fertility, SD = soil rooting depth, EAM = easily available moisture, FD = forest diversity

		MAP	Snl.	MAT	DSL	CE	SF	SD	EAM	FD	Overall	Motivation
Central Africa	*Mean*	↓	-	-	-	-	-	↓	-	↓	↓	Deep, nutrient-poor, sandy, acidic soils (Hart et al., 1989; Peh et al., 2011; Kearsley et al., 2013). El Niño temperature effect average, precipitation unaffected (Malhi and Wright, 2004), shade-tolerant *Gilbertiodendron* mono-dominance common (Primack & Corlett 2005), otherwise mixed forests on similar soils (Hart *et al.* 1989; Peh *et al.* 2011), thus slower growing.
	Var.	↓	-	-	-	-	-	↓	-	↓	↓	
East Africa	*Mean*	↓	-	↓	↓	-	↑	↑	↓	↓	↓	Relatively low mean annual precipitation and temperature, long dry season, on deep soils with relatively little organic carbon content and little easily available moisture (Eggeling, 1947). Slightly increased mortality and variability expected due to elevational, precipitation and edaphic gradients, combined with disturbances by elephants (Eggeling, 1947)
	Var.	↓	-	↓	↓	-	↓	↑	↓	↓	↓	
West Africa	*Mean*	-	↑	↑	↑	-	↑	-	↓	-	-	Overall higher mean annual temperatures, shorter dry seasons, little variation in precipitation throughout the year on comparably poor, slightly deeper soils, low mean wood density (Hammond, 2005), but strong gradient from forests on more fertile soils with less precipitation to less fertile, acidic soils with more precipitation (Swaine, 1996)
	Var.	-	↑	↑	↑	-	↓	-	↓	-	↑	
Brazilian Shield, Amazonia	*Mean*	↓	↓	-	↓	-	↓	-	-	↑	-	Relatively high abundance of disturbance-driven taxa like *Swietenia* and *Attalea*, with hyper-dominance by *Attalea speciosa* (Hammond, 2005), despite relatively low mean annual precipitation and average temperatures; long dry season length and nutrient poor soils (Malhi and Wright, 2004)
	Var.	↓	↓	-	↓	-	↑	-	-	↑	-	
East-Central Amazonia	*Mean*	-	-	↑	-	-	↑	-	↑	↓	-	Co-domination by dense-wooded Chysobalanaceae and Lacythidaceae (Hammond, 2005), average tropical climatic conditions, apart from a relatively high mean annual temperature, relatively young, clay-rich, but nutrient-poor soils (Quesada et al., 2011)
	Var.	-	-	↑	-	-	↓	-	↑	↓	-	
Guyana Shield, Amazonia	*Mean*	↑	↑	↑	↑	-	↓	↓	-	↓	-	Relatively high abundance of dense-wooded caesalpinoid legumes (Hammond, 2005), high mean annual precipitation and temperatures; old, nutrient poor soils, relatively strong intra- and inter-annual climatic variations
	Var.	↑	↑	↑	↑	-	↑	↓	-	↓	↑	
Western Amazonia	*Mean*	-	↑	↑	-	-	-	↑	↑	↑	↑	Relatively high abundance of more dense disturbance-associated taxa (e.g. *Iriartea* and *Swietenia*; (Baker et al., 2004b; Hammond, 2005), blow-down events (Espírito-Santo et al., 2010), relatively high mean annual temperature and little seasonality, nutrient rich, young soils. Have already been shown to have more rapid turnover rates than Eastern Amazonia (Phillips et al., 2004)
	Var.	-	↑	↑	-	-	-	↑	↑	↑	↑	
South-East Asia	*Mean*	↑	↑	↑	↑	↑	↓	↑	↑	↑	↑	No dry season, high mean annual temperatures and precipitation, relatively young and fertile soils, hurricane occurrences, mast-fruiting of Dipterocarps (creating disturbance-prone even-aged cohorts), higher temperatures and decreased precipitation during El Niño events relative to La Niña events (Malhi and Wright, 2004) causing high inter-annual climatic variation.
	Var.	↑	↑	↑	↑	↑	↑	↑	↑	↑	↑	
Australia	*Mean*	↓	↓	↓	↓	-	↓	-	-	↓	↓	Fertile basalt soils of an intermediate age (Bowman, 2000), but relatively low mean annual precipitation and temperatures; high seasonality with a long dry season, abundance of sclerophyllous species.
	Var.	↓	↓	↓	↓	-	↑	-	-	↓	↓	

Mortality rate distribution parameters for East Africa, and to a lesser extent West Africa, had relatively wide credible intervals on both estimates (Table 3.1). This pattern may be due to a combination of a relatively low number of observations, and a high proportion of larger mortality events, particularly for East Africa. When comparing this region's estimated distribution against the plot observations, the estimated distribution could be underestimating the likelihood of higher-mortality events (rates of circa 2-4 % ·year^{-1}; Figure 3.4), which suggests a relatively high occurrence of disturbances in this region during the measurement period. Adding an African continental hierarchical level on top of the biogeographical hierarchical level could help constrain the credible intervals, but would also pull their regional estimates towards an overall African distribution, which would most likely result in further underestimation of these moderate mortality events.

Unlike the other two African biogeographical regions, West African forests have mid-high median mortality rates, which may be primarily linked to the high soil fertility of the semi-deciduous forests in this region (Swaine, 1996), combined with relatively higher mean annual temperatures (Malhi and Wright, 2004). The West African mortality rate distribution has a relatively heavy tail (Figure 3.4), as was expected, which may be partially due to the presence of a strong gradient from forests on more fertile soils with less precipitation to less fertile, acidic soils with more precipitation (Swaine, 1996). Furthermore, Ghanaian forests have been experiencing a compositional shift towards more drought-tolerant vegetation during the past couple of decades (Fauset et al., 2012), following a prolonged (1968-97) non-ENSO type drought (Nicholson et al., 2000). This climatic shift may also be driving mortality events of increased magnitude of less drought-tolerant species (Fauset et al., 2012; Aguirre-Gutiérrez et al., 2019).

Unexpectedly, the Brazilian Shield region experienced the highest median mortality rates of the tropics during the study period (Figure 3.2, Table 3.1). Mid-low median mortality rates were expected, based on the relatively average mean annual precipitation and temperatures, relatively pronounced dry seasons in terms of experienced intensity (Malhi and Wright, 2004), and relatively old, deep soils (Hammond, 2005). However, Marimon et al., (2014) have shown that forest trees close to the transition zone with the Cerrado in the south of this region have experienced greatly elevated mortality rates following the 2005 non-ENSO drought (from ca. 1.5-1.6 %·yr^{-1} to ca. 4 %·yr^{-1}). The region experienced an even more severe non-ENSO drought during the dry season in 2010, and in general dry season length and severity have been increasing over the past decade (Marengo et al., 2011). Interestingly, the Brazilian Shield's mortality rate distribution also has the lightest tail, corresponding to a series of mortality events of largely similar magnitudes. Since nearly half of the plot census intervals in the Brazilian Shield span the period between these two drought events, the overall identified mortality rate distribution will have been largely influenced by these elevated mortality events.

The mid-low median mortality rates of East-Central Amazonian forests, with their average tail of slightly larger mortality events (Figure 3.2, Table 3.1), might results from their relatively young soils, which are rich in clay, but poor in available nutrients (Quesada et al., 2011) and co-domination by denser-wooded species (Hammond, 2005). Median mortality rates of the same order were identified for the forests of the Guyana Shield, though with a slightly heavier tail (Figure 3.2, Table 3.1).Here we find relatively high mean annual precipitation and temperatures, with potentially pronounced inter-annual variation in precipitation during, amongst others, El Niño Southern Oscillation or La Niña phases, tree species with relatively high mean wood densities on old, acidic soils, with poor nutrient availability (Hammond, 2005).

This in contrast to the forests in mostly aseasonal West Amazonia growing on soils enriched by erosion from the nearby mountain ranges (Hammond, 2005), which has been suggested as an important driver behind the relatively high observed median mortality rates (Figure 3.2, Table 3.1), especially relative to East-Central Amazonia (Phillips et al., 2004). Quesada *et al.* (2012) suggest that the higher mortality rates in West Amazonia could also be a consequence of adverse soil physical properties, which predispose trees to a higher mortality risk through unfavourable conditions like bad drainage, low water retention capacity or little easily available rooting space, rather than directly through enhanced dynamics due to an increased nutrient availability. However, the proportion of trees dying uprooted was not found to differ significantly between north-western and north-eastern Amazonia (Chao et al., 2009), suggesting there are not necessarily solely any soil structural drivers at play. As trees in western Amazonia tend to die in small-scale multiple treefall events (Espírito-Santo et al., 2014) and the main mode of death is by being broken (Chao et al., 2009), this suggests small gaps are created frequently, and are filled by disturbance-driven taxa that can utilize the abundant nutrients to grow quickly. However, the fast growth strategy of these species comes at the cost of having a lower wood density, which predisposes them in turn to future breakage-related mortality events (Quesada et al., 2012). This feedback reinforces the pattern of small-scale mortality events driving the overall forest dynamics in this region (Quesada et al. 2012), and is confirmed by the fact that, despite being a region with one of the highest median mortality rates, contrary to our expectations, the standard deviation of the logit-normal distribution was found to be one of the lowest (Figure 3.2, Table 3.1).

Forests in South-East Asia were found to have mid-high median mortality rates, with an average occurrence of larger-scale mortality events (Figure 3.2, Table 3.1). Here we find relatively high mean annual temperatures and precipitation, with little seasonality, relatively young and fertile soils, and a relatively high abundance of Dipterocarps, which have relatively lower wood densities (Hammond, 2005). El Niño Southern Oscillation

phases are accompanied by higher temperatures and decreased precipitation, relative to La Niña phases (Malhi and Wright, 2004) causing high inter-annual climatic variation.

Median annual tree mortality rates were found to be lowest in forests in Northern Australia, however standard deviations were found to be mid-high (Figure 3.2, Table 3.1). Australia has relatively low mean annual precipitation and temperatures, with the greatest seasonal variation in temperatures, and the most pronounced dry season (Malhi and Wright, 2004). These conditions were expected to favour overall lower mortality rates, however the relatively 'fat' tail suggests the forests in this region are occasionally disturbed by external forces, resulting in mortality events of moderate intensity. A forty-year study has indeed confirmed that Australian forests are regularly disturbed by soil pathogens, erosion, cyclones and droughts (Murphy et al., 2013).

The statistical approach developed here has a range of potential applications. Firstly, the mortality rate distributions identified here can be used to place the mortality rates identified in local studies in a regional, continental or pan-tropical context. Secondly, this approach could be used to provide an improved description of tree mortality within vegetation models. Since most dynamic vegetation models work with the fraction of biomass that is lost, a similar study on biomass-based mortality rate distributions would be recommended, ideally including potential drivers directly as factors (e.g. sensu Lines *et al.* (2010) for stem mortality rates for the eastern U.S.). This could be used as means to explore how changes in any drivers may influence these distributions of forest dynamics. Alternatively, the approach used here of defining mortality rate distributions, and quantifying the relative probabilities of the magnitudes of mortality events, could be used to create probability distributions for stochastic tropical individual-based models at any spatial scale. Finally, these distributions can also be used for assessing and informing sampling strategies, as shown in Chapter 2.

Overall, the inter-continental differences in median mortality rates identified in this study match those for woody biomass residence times from Galbraith *et al.* (2013), with mortality rates increasing, and thus residence times decreasing, from Australia, through Africa and Asia, to the Americas. However, here we also provide insight into the variability of the mortality rates within these regions, providing evidence of biological variation in their disturbance regimes at biogeographical scales.

4 4. Has drought stress caused the long-term increase in tree mortality rates in Amazonian forests?

4.1 Introduction

Tropical old-growth forests function as an important carbon sink, accounting for nearly two-thirds of the global biomass carbon sink in the period 1990-2007 (1.5 Pg C $year^{-1}$; Pan et al., 2011). However, during recent decades there have been strong increases in stem-based mortality rates in old growth South American tropical rain forests (Phillips *et al.*, 2008; Lewis et al., 2004b). Whilst increases in tree mortality rates are surpassed by recruitment, the tropical forests' carbon sink will likely be preserved, but increasing tree mortality rates might transform these forests into a carbon source in the near future. Indeed, spatially, stem-based tree mortality rates are an important predictor of AGB (Johnson et al., 2016; Vilanova et al., 2018), and recent evidence suggests the increase in recruitment rates in Amazonian tropical old growth forests is starting to level off, whilst mortality rates are still increasing (Brienen et al., 2015; Hubau et al., 2020). Understanding the mechanisms driving variation in tree mortality rates in South American forests is important for understanding what could happen to this important carbon sink in the future.

An increase in the prevalence and severity of droughts could be a crucial driver of the recent increase in tree mortality rates (Nepstad et al., 2007; Phillips et al., 2009; Allen et al., 2010; Marengo et al., 2011; Aubry-Kientz et al., 2015b). Studies of the impact of drought on Amazonian forests have mainly focussed on individual drought events (Bonal et al., 2016), and compared mortality rates of a pre-drought period, to those during or following these specific drought events (Phillips et al., 2009, 2010). For example, during the 2005 Amazon drought, biomass losses through individual tree mortality were found to increase linearly with drought intensity, expressed as a change in maximum cumulative water deficit (Phillips et al., 2009). A similar pattern was identified using stem-based mortality rates for various individual drought years observed across the tropics, with Amazonian forests occupying the lower end of this relationship (Phillips et al., 2010). In addition, there have also been studies of the effects of two consecutive droughts (e.g. Feldpausch et al., 2016). In this case, anomalous biomass losses observed for Amazonian plot censuses spanning the 2010 drought were unrelated to the severity of the MCWD anomaly, and unrelated to whether the plots had been droughted previously during either the 2005 or the 2007 drought, or both (Feldpausch et al., 2016). However, there has been no study of how long-term increases in stem mortality rates are linked to long-term changes in drought stress that incorporate both short term droughts, and longer term climatic trends. Here, I therefore analyse how drought stress over the past decades may

have contributed to the observed increased stem-based tree mortality rates in South American forests, based on a long-term monitoring effort of permanent sample plots.

This chapter thus aims to address the following questions:

- Is there evidence of temporal changes in stem-based tree mortality across or within tropical South American old growth forests?
- Is there evidence of temporal changes in the precipitation/transpiration-driven water balance in the climatologically differing biogeographical regions?
- Can variation in water deficits partially explain variation in mortality rates, independent of any long term linear trend over time?

4.2 Methods

Firstly, stem-based mortality rates were derived for each region Amazonian region from field data from a long-term permanent sampling plot network (see 4.2.1). Secondly, the precipitation/transpiration-driven water balance was derived for the corresponding plot censuses (see 4.2.2). Any potential temporal trends and relations between them were firstly investigated using correlation and linear analyses (see Section 4.2.3), followed by Bayesian parameter estimation (see 4.2.4).

4.2.1 Forest dynamics data from permanent sample plots

Mortality rates across South America were derived from the long-term forest dynamics permanent sample plots measurements of the RAINFOR network (Phillips *et al.* 2004), accessed through the Forest Plots Database (Lopez-Gonzalez et al., 2013), and census interval corrected for the linear analyses as per (Lewis et al., 2004c). These permanent sample plots are located in undisturbed old growth mixed forest, across a range of different edaphic, biogeographic and environmental conditions.

To determine whether variations in these conditions affect the dynamics of the forests in these regions differently, the 154 South American RAINFOR plots were split into 6 regions. A primary division was made based on biogeographic conditions following Feldpausch et al. (2011), distinguishing the Brazilian Shield, the Guyana Shield, and East-Central Amazonia. Feldpausch et al.'s West Amazonia was then further divided according to differing environmental conditions, resulting in separating the more aseasonal Northwest Amazonia, from the more seasonal Southwest Amazonia at -8° latitude as per Steege et al. (2013), and the drier Northwest Venezuelan plots north of 0° latitude (see Figure 4.1).

Mortality rates were derived for the 616 plot census intervals with an average length of 3.4 years (median 2.5) in a similar fashion as described in Chapter 3. On average the South American plots had been re-censused 4 times (range 1-20, median 3) between 1967-2008, with 16 plot census intervals in the Brazilian Shield, 64 in Northwest Amazonia, 119 in

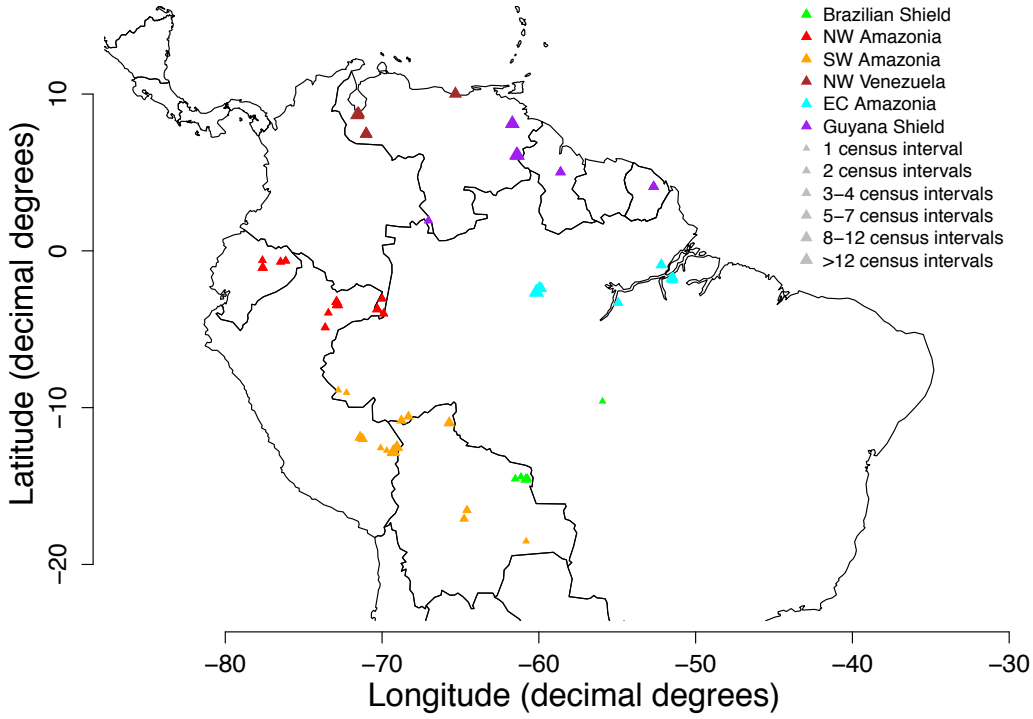

Figure 4.1. Permanent sample plot locations within the six South American regions.
Plot location indicators have been scaled for the number of census intervals.

Southwest Amazonia, 74 in Northwest Venezuela, 184 in East-Central Amazonia and 159 in the Guyana Shield.

The effect of the calculated maximum monthly cumulative water deficit (see Section 4.2.2) and the census interval mean and end date on these derived mortality rates for each plot census interval were estimated both using linear models (see Section 4.2.3) and using Hamiltonian MCMC parameter estimation techniques (see Section 4.2.4) in R using Stan as detailed below.

4.2.2 Maximum monthly cumulative water deficit

The maximum monthly cumulative water deficit (MCWD) was calculated using monthly precipitation data for the census interval period, including 2 years prior to the census date as per Aragão *et al.* (2007). The precipitation data was obtained from the high-resolution gridded time-series dataset CRU TS v. 3.10 (Harris et al., 2014), where the corresponding monthly data per 0.5° grid cell were selected using the 'RNetCDF' package (Michna and Woods, 2011) in R. In line with the procedure used by Aragão *et al.* (2007), transpiration from vegetation was assumed to be 100 mm/month. The cumulative water deficit calculations commenced at the wettest month of the year, when the soil is assumed to be fully saturated with water, corresponding to a deficit of 0 mm. If precipitation for the

following month(s) exceeded 100 mm, the soil was still assumed to be water-saturated and the MCWD calculation for the next month proceeded with no water deficit.

When monthly transpiration exceeded the monthly precipitation, a water deficit in the soil was noted for that month, which was carried over to the next month, requiring precipitation in the following month to exceed transpiration by the amount of the deficit in order to cancel it out. For the overall census period, the month with the highest obtained cumulative water deficit was denoted as the maximum monthly cumulative water deficit (MCWD) for that period. The MCWD thus provides an indication of the degree of water-stress the vegetation might have experienced during that census interval. However, during drought conditions, decreased precipitation may be accompanied by higher atmospheric temperatures and drier air, which increase evaporative demand, and might thus increase transpiration, unless stomatal conductance is adjusted accordingly(Bonal et al., 2016), resulting in a potential underestimation of soil water deficits by the MCWD (Malhi et al., 2009).

While some studies (e.g. Phillips et al., 2009) have used the mean annual MCWD for each census interval, here, we are interested in the effects of the highest overall MCWD observed during a census interval, similar to Feldpausch et al. (2016). The annual MCWD values (annMCWD) were calculated and evaluated as well, but mainly resulted in the same findings at the same level of significance. Additionally a tally was kept of the number of consecutive months during which a deficit was registered for each plot census interval.

4.2.3 Linear models

Firstly, for all South American regions, the Pearson product moment correlation coefficient between the tree mortality rates, MCWD and census mid and end date were examined using the 'cor.test' function from the 'stats' package available in base R. The pair-wise correlations included: (1) mortality rates versus census mid- and end-date, to test for an increase of mortality rates over time, using both the calculated observed mortality rates as they were (μ), and a normalised distribution of the mortality rates after a logit transformation (μ*); (2) MCWD versus census mid and end date, to test for an increase of maximum cumulative water deficits observed over time, using MCWD and a normalised distribution of the MCWD values (MCWD*). Since the MCWD values were negative, skewed towards smaller deficits, with only a few larger deficits, and also included zeroes in regions where precipitation exceeded 100 mm during each month of the year, the MCWD values were normalised as follows: $MCWD^{*} = -\ln(-(MCWD - 1))$, where 1 mm was subtracted from all deficits, to remove zeroes, and the deficits were transformed into positive numbers, both to enable a natural logarithm transformation, after which the values were returned to their original negative state, to facilitate comparison to the non-transformed MCWD values; (3) mortality rates versus MCWD, to see if increases in

mortality rates, irrespective of their overall timings or trends, correspond to any increases in water deficits, using the untransformed and the normalised values of both of these.

4.2.4 Hamiltonian parameter estimation

A variation of the non-hierarchical Bayesian inference model described in Chapter 3 was used, focussing on mortality and water deficit trends at a biogeographical scale, since the results from Chapter 3 showed this to be an important scale for describing variation in annual tree mortality rates. Specifically, we test whether census interval mid or end date or MCWD were found to be predictors of the annual mortality rates $m_{x,t}$ (year^{-1}; in logistic space) observed during census interval t in plot x of biogeographical region *r* as follows:

$$m_{x,t} = \frac{1}{1 + e^{-k_{x,t}}} \quad (4.1)$$

where $k_{x,t}$ is a linear function of either of the predictor variables:

$$k_{x,t} = \alpha_r + \beta_r f_{x,t} \quad (4.2)$$

with α_r being a region-specific constant parameter, β_r the region-specific scaling parameter, and $f_{x,t}$ the value of the predictor variable for that plot census interval. Both region-specific parameters are drawn from normal distributions:

$$\begin{aligned} \alpha_r &\sim N(\alpha_{r,0}, \sigma_{a_r}) \\ \beta_r &\sim N(\beta_{r,0}, \sigma_{\beta_r}) \end{aligned} \quad (4.3)$$

Since the MCWD values are negatively skewed, while also containing some zero values, their plot census specific normalised values were drawn from a regional normal distribution after transformation as per 4.2.3.

The parameter estimation was performed using the 'rstan' package (Stan Development Team, 2018), since it uses Hamiltonian Monte Carlo sampling and is compiled in C++ (Kruschke, 2015), and has proven more efficient in evaluating the models of interest presented here, as evaluated by the MCMC diagnostics adapted from those provided in the 'diagMCMC' function by Kruschke (2015), with regards to representative sampling of the posterior distribution by all chains, the autocorrelation observed, the effective sample size and the "shrink factor" (Gelman-Rubin) statistic being close to 1, which indicates that the chains have all converged.

All analyses described here were performed using R versions 3.2.1 and 3.4.4 (R Core Team, 2015; R Core Team, 2019) in RStudio (RStudio Team, 2016).

4.3 Results

4.3.1 Regional mortality trends

Both the linear and Stan models of mortality rates with census interval mid and end dates suggest there has indeed been a highly significant increase of mortality rates through time for South America as a whole, with the most significant increase observed in NW Venezuela (correlation 44 %, p<0.005; see Table 4.1, Figure 4.2), followed by the Guyana Shield when using the transformed mortality rates (μ^*; 34 %, p<0.005) and East-Central Amazonia for μ^* in Stan (18 %, p<0.005). Southwest Amazonia also seems to have experienced a similar increase in mortality rates (18 %, p<0.05). However, while the correlation and linear analyses suggest Northwest Amazonia actually might have been experiencing a substantial decrease in annual mortality rates over time, this result was not found to be significant in the Bayesian analyses in Stan (-32 %, p<0.05 for the linear analyses, p<0.1 for Stan). For the Brazilian Shield, which already has the highest mean annual mortality rates of all there regions, there are indications that a slight increase might have occurred, though no significant trend could be discerned, likely due to the smaller sample of plot censuses for this region (n=16).

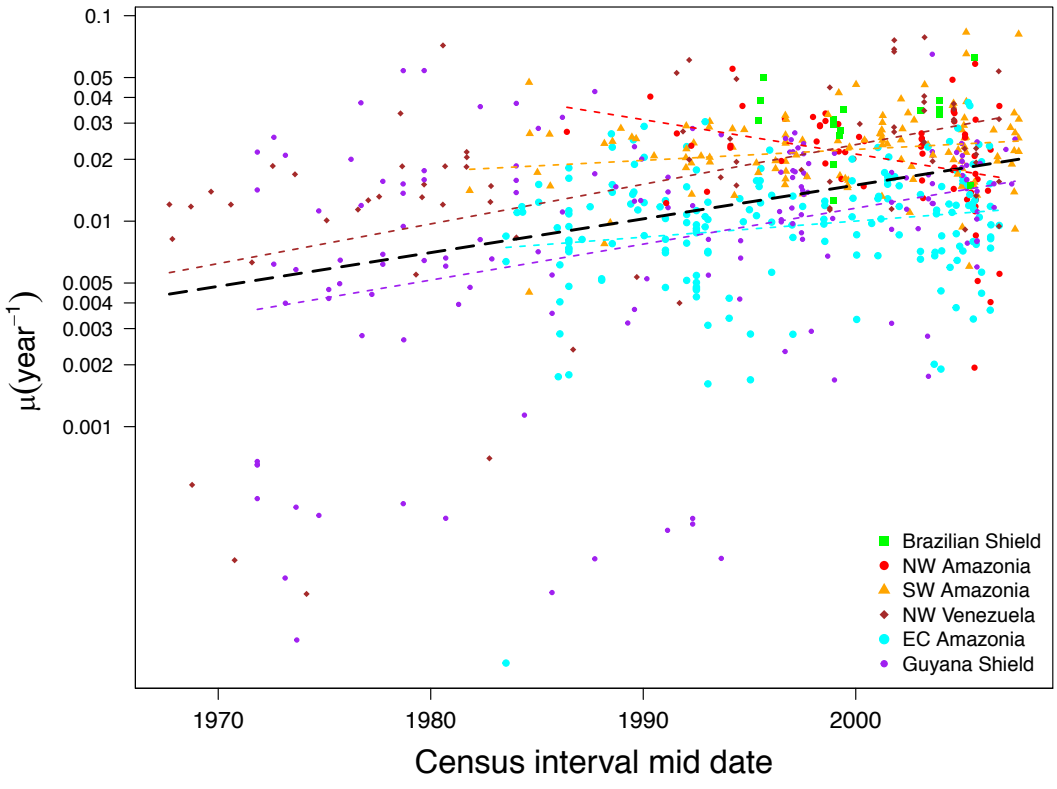

Figure 4.2. Regional South American annual mortality rates versus census interval mid date. Including significant trends (p<0.05; see Table 4.1) of increasing annual mortality rates with time as identified for Southwest Amazonia, East-Central Amazonia, the Guyana Shield and across all the South American regions (long-dashed trend line in black). A significant decrease was identified for Northwest Amazonia, but only in the linear models, not in the Bayesian analyses. No significant trend with census interval mid date was identified for the annual mortality rates observed in the Brazilian Shield (p>0.10).

Table 4.1. Parameter estimates for potential relationships between regional South American tree mortality rates, time, and maximum cumulative water deficit.
Analyses include correlation (Corr.; in %), linear (Glm) and Bayesian (Stan) pairwise comparisons (response variable ~ intercept + effect * predictor variable) for each of mortality rates, maximum cumulative water deficit (MCWD), and time per South American region and across all regions (*μ = census interval corrected annual mortality rate (%); μ* normalized mortality rates in logistic space; MCWD = maximum monthly cumulative water deficit (mm); MCWD* normalized MCWD rates; time = census interval mid date; p values: bold = ≤ 0.001, underlined = ≤ 0.01, regular = ≤ 0.05, dark grey = ≤ 0.10, light grey > 0.10*)

Estim. type	Response variable	Predictor variable	NW Venez. (n=74)	NW Amaz. (n=64)	EC Amaz. (n=184)	SW Amaz. (n=119)	Guyana Shield (n=159)	Brazil. Shield (n=16)	*All regions (n=616)*
Corr.	μ	Time	**44**	-27	16	19	18	10	***25***
Glm	μ	Time	**0.063**	-0.059	0.014	0.034	0.018	0.036	***0.033***
Stan	μ	Time	*NA*	*NA*	*NA*	*NA*	*NA*	*NA*	*NA*
Corr.	μ*	Time	**49**	-32	18	18	**34**	3	***36***
Glm	μ*	Time	**0.045**	-0.039	0.018	0.013	**0.040**	0.004	***0.038***
Stan	μ*	Time	**0.032**	-0.023	**0.022**	0.014	**0.017**	-0.009	***0.024***
Corr.	MCWD	Time	-20	-13	**36**	-20	10	**75**	*9*
Glm	MCWD	Time	-4.738	-1.401	**3.429**	-4.990	1.080	**9.370**	*1.714*
Stan	MCWD	Time	-4.727	-0.807	**2.813**	-4.793	1.129	**8.822**	*1.662*
Corr.	MCWD*	Time	**-38**	2	**26**	-21	10	**71**	***14***
Glm	MCWD*	Time	**-0.023**	0.006	**0.016**	-0.021	0.004	**0.025**	***0.017***
Stan	MCWD*	Time	**-0.023**	0.018	0.012	-0.019	0.005	0.025	***0.025***
Corr.	μ	MCWD	12	17	8	2	-13	-22	*3*
Glm	μ	MCWD	0.001	0.003	0.001	0.000	-0.001	-0.006	*0.000*
Stan	μ	MCWD	*NA*	*NA*	*NA*	*NA*	*NA*	*NA*	*NA*
Corr.	μ*	MCWD	8	15	4	13	-9	-30	*0*
Glm	μ*	MCWD	0.000	0.002	0.000	0.000	-0.001	-0.003	*0.000*
Stan	μ*	MCWD	0.000	0.001	0.001	0.000	-0.001	-0.003	*0.000*
Corr.	μ	MCWD*	-1	9	4	-9	-13	-25	*5*
Glm	μ	MCWD*	-0.029	0.055	0.060	-0.167	-0.266	-2.537	*0.053*
Stan	μ	MCWD*	*NA*	*NA*	*NA*	*NA*	*NA*	*NA*	*NA*
Corr.	μ*	MCWD*	6	12	1	-3	-9	-32	*9*
Glm	μ*	MCWD*	0.083	0.040	0.021	-0.021	-0.243	-1.127	*0.077*
Stan	μ*	MCWD*	0.034	0.022	0.108	-0.043	-0.192	-1.163	*0.057*

4.3.2 Regional changes in cumulative water deficits through time

Overall, a slight positive correlation (14 %, p<0.005; see Table 4.1, Figure 4.3) was identified between the maximum cumulative water deficit (MCWD*) observed during each census interval and the census date, which suggests that maximum drought intensity has been lessening over time across South American rainforests. There are only two regions for which this trend holds at the regional scale though, namely East-Central Amazonia (26 %, p<0.005) and the Brazilian Shield (71 %, p<0.005).

In East-Central Amazonia, the range of MCWD values observed ranged from -351 to -69 mm across all plot censuses in the 1980s, increasing to a range of -224 to -32 mm in the 2000s. As such, across the entire census range some plots only experienced two to three months where the cumulative water deficit exceeded precipitation, and the overall maximum duration of any consecutive dry period decreased from nine months in the 1980s, through eight in the 1990s, to seven in the 2000s.

While the Brazilian Shield does not have many plot censuses, the identified maximum water deficit has decreased for some plot census intervals, increasing from the narrow range of -428 to -424 mm observed during the 1990s to -398 to -275 mm in the 2000s. Of all the regions, this is the only region where all the plot census intervals had a cumulative water deficit for a minimum duration of 7 consecutive months, though it never exceeded a maximum of 11 months, despite longer census interval lengths. As such, for the plot census intervals observed, there has always been one month of the year where the water deficit was cancelled out, increasing to up to five months for some census intervals in the 2000s.

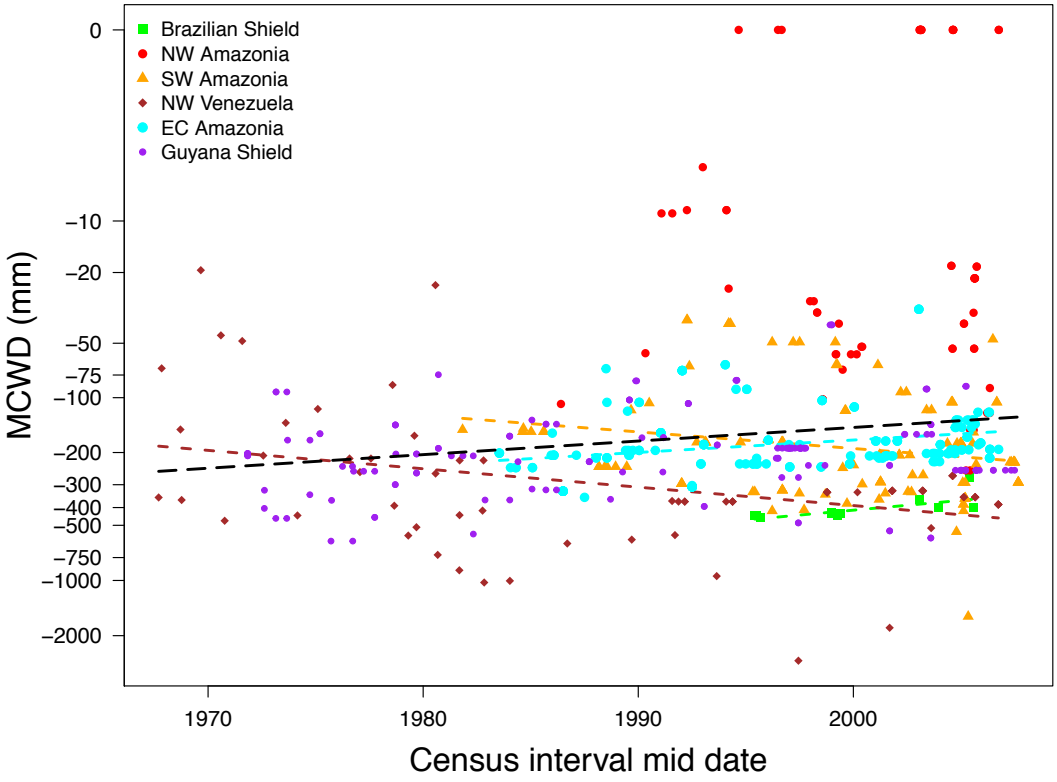

Figure 4.3. Regional South American maximum cumulative water deficits (MCWD) versus census interval mid dates.
Including significant trends ($p<0.05$; see Table 4.1) of increasing maximum cumulative water deficit with time as identified for Southwest Amazonia and Northwest Venezuela, and decreasing as identified for East-Central Amazonia, the Brazilian Shield and across all of the South American regions (long-dashed trend line in black). No significant trends were identified for Northwest Amazonia or the Guyana Shield.

Southwest Amazonia (-21 %, $p<0.05$; see Table 4.1, Figure 4.3) and to a greater extent also NW Venezuela (-38 %, $p<0.005$) have experienced droughts of increasing severity and duration. In Southwest Amazonia the maximum number of consecutive months with a water deficit across all plots census intervals increased from 7 in the 1980s, through 11 in the 1990s to 48 in the 2000s, and the cumulative water deficit increased from -239 mm, through -417 mm, to -1572mm. However, during this time period the median consecutive water deficit period stayed roughly the same at 6, 7, and 7 months respectively and the minimum actually decreased from -117 mm cumulative water deficit and 5 months duration, through -37 mm and 2 months, to -48 and 1 month. This result matches findings that since the mid 1970s the number of consecutive months with fewer than 100 mm precipitation has been gradually increasing in southern Amazonia (Marengo et al., 2011). The three census intervals with the greatest observed cumulative water deficit in terms of duration or magnitude covered the periods from March 1995-March 1997, July 2003-March 2007 and March 2003-May 2006. The latter two overlap with the 2005 drought, during which most of Southwest Amazonia experienced some of the largest observed maximum cumulative water deficits (Aragão et al., 2007; Marengo et al., 2008).

Despite the minimum consecutive period with a cumulative water deficit in Northwest Venezuela for the 1960s up until the 1990s having only been up to two months across all plot census intervals in Northwest Venezuela, this increased to 7 respectively 6 months in the 1990s and 2000s. Concurrently the deficit range increased from -364 to -19 mm in the 1960s to -1811 to -268 mm in the 2000s, with both the minimum and the maximum steadily increasing in magnitude through time. This indicates that there has been a strong increase in drought duration and magnitude over time across plot censuses in this region. The three plot census intervals with the greatest observed deficits were July 1984-October 1988, June 1994-June 2000, and June 2000-December 2002. The former two census interval each included a strong El Niño year: 1986-1987 (Yoon and Zeng, 2010) and 1997-1998 (Feely et al., 2006). Additionally, the first of these two census intervals contained one La Niña year (1984-1985; Feely et al., 2006; Tedeschi et al., 2013), while the second included the following La Niña years: 1995-1996 (Feely et al., 2006), 1998-1999 (Feely et al., 2006; Tedeschi et al., 2013) and 1999-2000 (Yoon and Zeng, 2010; Tedeschi et al., 2013). Typical La Niña years tend to decrease precipitation in northern South America (Tedeschi et al., 2013).

No significant trends in MCWD through time have been identified for Northwest Amazonia and the Guyana Shield. In Northwest Amazonia, the maximum cumulative water deficit increased from -102 mm in the 1990s to -250 mm in the 2000s, but this is the only region that never experienced a water deficit for any of the plot censuses during the wettest month of the year, and where some of the plot censuses never even had a single month of deficit throughout the year. The maximum consecutive deficit duration was only 4 months

in this region. The deficits of -250 mm were observed in two plot censuses, both covering the period of mid-2004 to late 2005, out of 40 total plot census intervals in the 2000s. Consistent with these patterns, in some parts of Northwest Amazonia, the 2005 Amazon drought resulted in reductions in monthly precipitation of over 100 mm per month for most months between November 2004 and July 2005 (Marengo et al., 2008).

The fact that no significant trend in cumulative water deficit was identified for the Guyana Shield, could partially be due to the fact that this region has relatively wide deficit ranges across the plot census intervals within each decade of the overall monitoring period. Furthermore, the region actually seemed to initially have been becoming wetter over time, gradually lessening its deficit range from -610 mm to -93 mm in the 1970s to -485 resp. -40 mm in the 1990s, before returning to a range of -587 to -87 mm in the 2000s. In the Guyana Shield there have been a number of plot census intervals in each decade which seem to have been experiencing substantial deficits.

These overall trends suggest that the south-eastern regions might be becoming moister on average and have been experiencing fewer intense droughts recently, whereas the droughts in the regions in the north- and south-western parts of South America may have been increasing in severity, with other areas remaining largely unaffected.

4.3.3 Water deficit and regional stem-based mortality

None of the individual regions in South America showed any correlation (see Table 4.1, Figure 4.4) between the maximum monthly cumulative water deficit (MCWD) and mortality rates, though a weak positive correlation was found between μ^* and MCWD* for all regions combined (9 %, $p<0.05$). An increase in MCWD (greater deficit), will correspond to larger negative numbers, and a greater water deficit could be expected to increase mortality rates. This result is therefore contrary to the negative correlation that would be expected, if an increased water deficit causes an increase in mortality rates. Since both individual variables exhibit a positive trend through time, this could even suggest that mortality rates have increased, despite an overall decrease in MCWD through time.

4.4 Discussion

This study confirms that old-growth tropical forests in most South American regions and across South America moist tropical forests have experienced increases in long-term stem-based tree mortality rates over time, as previously identified in other studies (Lewis et al., 2004b; Phillips et al., 2004). The increase in instantaneous mortality rates identified by Lewis et al. (2004b) across 50 South American plots over the period 1971-2002 from 1.50±0.19 % to 1.77±0.22 %·year^{-1}, resembles the increase in annual mortality rate estimates obtained here of 1.41±0.12 to 1.51±0.11 %·year^{-1} identified here for the same period, using 302 respectively 350 plot censuses. Phillips et al. (2004) also identified an

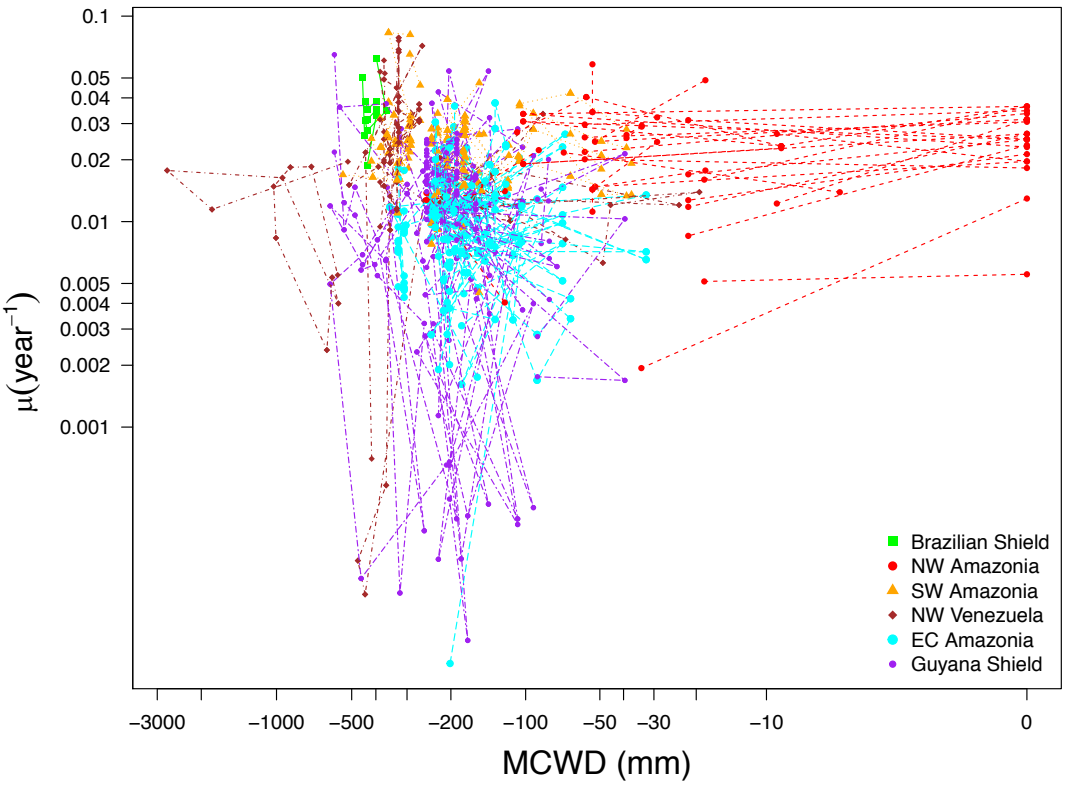

Figure 4.4. Regional South American mortality rates versus maximum monthly cumulative water deficit (MCWD) values per census interval.
Consecutive census intervals are connected with dashed lines.

increase in mortality rates for south and west Amazonia, as we did here. However, they did not find any significant increase for all of east and central Amazonia (1986-1996; n=28; p=0.23), yet a significant increase of 2.2 %·year^{-1} was detected here using 184 plot censuses (1984-2007). Additionally, this study identifies significant increases in mortality rates for the Guyana Shield and Northwest Venezuela. The only regions for which no significant increase in stem-based mortality rates over time was discerned here, were Northwest Amazonia and the Brazilian Shield. For the latter region, there are indications that it might be exhibiting the same trend, but the number of plot census intervals is not sufficient to detect a significant trends. For Northwest Amazonia, a significant decrease of mortality rates through time was identified in the correlation and linear analyses, but this was not found in the Stan parameter estimation analyses. Despite having corrected the observed annual mortality rates for any census interval effect (sensu Lewis et al., 2004c), this result identified in the non-Bayesian inference analyses is expected to be an artefact, caused by an increased re-census effort during the last decade, with the shorter census intervals more often having recorded zero or very few deaths. This was confirmed by selecting only those 30 plot censuses that had similar numbers of observations for the same census periods, which resulted in no significant trends being detected in the correlation or linear analyses. This finding demonstrates that the Bayesian inference analyses are more robust to this kind of artefact.

The increasing severity and duration of consecutive months with a cumulative water deficit identified in NW Venezuela and the Brazilian Shield, did not translate into a significant correlation between the maximum cumulative water deficit (MCWD) and the mortality rates in these regions. East-Central Amazonia and the Brazilian Shield showed evidence that the water deficits there might have actually been decreasing with time, and similarly no significant correlation with the increasing mortality rates could be identified in these regions. For neither the Guyana Shield nor for the aseasonal Northwest Amazonia regions could any trend in the MCWD be discerned, and consequently no correlation with mortality rates was established for these regions. As a result, no straightforward relationship could be identified between the MCWD and stem-based mortality rates across South American tropical forests.

This finding is in line with the results from a study by Feldpausch et al. (2016), which focussed on the impact of drought stress on biomass dynamics using precipitation data from the Tropical Rainfall Monitoring Mission (TRMM; available from 1998 onwards). Even when focussing only on those 97 plots that spanned the 2010 dry season with a census interval length of up to a maximum of 3.5 years, and using two additional alternative drought indices (the Standard Precipitation Index and the Standard Precipitation Evapotranspiration Index), Feldpausch et al. (2016) found that mortality biomass anomalies from the 2010 dry season water stress event varied independently of drought severity. Although Feldpausch et al. (2016) showed that a significantly greater number of trees died per year in the 46 plots that experienced relatively strong drought anomalies during the census intervals spanning the 2010 drought, relative to the number of dead trees per year identified in the pre-2010 census intervals, the lack of correlation between drought anomalies and mortality events demonstrates the difficulty of relating measures of drought stress to the magnitude of impact on forest structure.

While we did not detect an increase in maximum cumulative water deficits as expected, a recent study by Hubau et al. (2020) did identify an increase in MCWD values over time across a set of 321 old-growth Amazonian plots, for the period 1989-2013, and using CRU data up to 2015, but for a different set of plots, Esquivel-Muelbert et al. (2019) identified an overall pan-Amazonian increase in annual water deficits. Their results suggest dry season droughts have indeed been increasing in magnitude in South American tropical forests, unlike the decrease in magnitude identified here. In contrast to this analysis, Hubau et al. (2020) used precipitation data from the Global Precipitation Climatology Centre, augmented with TRMM, and downscaled to ~1 km resolution, rather than data from the CRU, due to the former being more spatially detailed for Africa. While generally their MCWD values matched those used here (74 % correlation, $p<0.001$), using their MCWD values for the 443 plot censuses of 114 plots shared between both studies, a significant increase in the magnitude of water deficits over time is identified across all sites

(p<0.001; see Table 4.2). It also suggests droughts in East-Central Amazonia have been increasing over time (MCWD p<0.001; MCWD* p<0.05; see Table 4.2), rather than lessening, and this dataset reports a significant increase for NW Amazonia too (MCWD; p<0.05), though for Northwest Venezuela it suggests the opposite trend (MCWD*; p<0.05).

Table 4.2. Re-evaluated parameter estimates for potential relationships between regional South American tree mortality rates, time, and maximum cumulative water deficit.
The mean annual maximum cumulative water deficit (MCWD) values as identified by Hubau et al. (2020) were used to re-evaluate the MCWD general linear models of Table 4.1 of pairwise comparisons (response variable ~ intercept + effect * predictor variable) with mortality rates, and time per South American region and across all regions (*μ = census interval corrected annual mortality rate (%); μ* normalized mortality rates in logistic space; MCWD = maximum monthly cumulative water deficit (mm); MCWD* normalized MCWD rates; time = census interval mid date; p values: bold = ≤ 0.001, regular = ≤ 0.05, dark grey = ≤ 0.10, light grey > 0.10*). Blue shading indicates significant relationships that changed sign. Underlined values indicate relationships that have changed significance.

Response variable	**Predictor variable**	**NW Venez.** *(n=34)*	**NW Amaz.** *(n=62)*	**EC Amaz.** *(n=167)*	**SW Amaz.** *(n=113)*	**Guyana Shield** *(n=51)*	**Brazil. Shield** *(n=16)*	***All regions*** *(n=443)*
MCWD	Time	-3.517	-2.137	**-4.535**	**-3.642**	0.215	-1.494	***-2.462***
MCWD*	Time	0.015	-0.047	-0.046	-0.045	-0.003	-0.005	*-0.017*
μ	MCWD	1.5E-05	3.0E-05	-2.1E-05	-5.9E-06	1.4E-09	1.4E-04	***-2.7E-05***
μ*	MCWD	-4.3E-04	2.5E-03	-2.2E-03	-1.9E-04	2.5E-03	4.5E-03	***-1.6E-03***
μ	MCWD*	3.1E-03	-7.0E-04	-1.3E-03	-9.9E-04	3.4E-04	5.0E-02	*-6.8E-04*
μ*	MCWD*	-0.125	-0.025	-0.147	-0.035	0.064	1.596	*-0.036*

Similar to this study, Hubau et al. (2020) also did not find a significant relationship between mortality losses (whether transformed to fit normality assumptions or not) and MCWD. Only after accounting for variation in mean annual surface temperature (MAT), atmospheric CO_2 concentrations, and the plot's carbon residence time (CRT), did a significant relationship between MCWD and mortality emerge (p=0.030; Hubau et al., 2020).

The difference between the findings of Hubau et al. (2020), and the results here, might be due to differences in the climatological datasets, not accounting for variation in other parameters such as temperature, or how they derived their metric of drought. The method of MCWD calculation used by Hubau et al. (2020) focused on the multi-year mean of the maximum annual deficit identified per plot census. As a result the extremes of any individual drought events will be smoothed out over the census interval (Feldpausch et al., 2016), in favour of identifying long-term trends and correlations. This thus resulted in identifying that plots with lower MCWD values (plots in wetter regions), tend to exhibit higher growth, and thus higher mortality, which resembles the overall trend identified across the regions here (Figure 4.4). Overall, while forest community responses to water deficits might be expected to vary at biogeographical scales, the variation in water deficits within regions happens at much smaller scales.

There are a number of additional reasons why even when observing a significant increase in mean water deficits through time, it is hard to translate this directly to increased

mortality rates. Firstly, while we tried to preserve the highest deficits encountered during a census interval, the same could not be done for the mortality rates. While some tropical studies (e.g. Phillips et al., 2010) have shown that droughts can have an impact on mortality rates for some years following the drought, other studies (e.g. Williamson et al., 2000) have shown that after an initial spike immediately following the drought event, mortality rates can return quite quickly to the pre-drought levels. Either of these will complicate relating mortality rate increases to greater water deficits. For instance, in the case of the former, especially if a re-census was timed shortly following the drought event, the lag could result in increased mortality rates during the following census interval. In the case of no lag, short-lived spikes in mortality rates will become more obscured by being averaged with multiple years at the non-droughted background mortality rate as the census interval length increases, regardless of the timing of the censuses relative to the drought event (see also Chapter 2). As the mean census interval length of these Amazonian long term forest plots used here is 3.4 years, this direct impact of droughts may thus be concealed. Ideally, only mortality rates derived from annual or biennial re-censuses should be used, though the increased biomass losses during the 2005 Amazon drought were detected using census intervals of up to five years (Phillips et al., 2009).

If increased drought stress is not the primary driver of the long-term increase in tree mortality rates in Amazonian forests, what other processes may be occurring? One candidate is increased resource availability, most notably an increase in carbon dioxide (Lewis et al., 2004a), which could lead to a decreased life expectancy of trees as a result of increased dynamics (Brienen et al., 2012; Körner, 2017). Other candidate drivers include an increase in liana abundance (Phillips et al., 1994; Phillips et al., 2002; Wright and Calderon, 2006), or rising temperatures. For example, the change in MAT was significant in the model of Hubau et al. (2020), suggesting that biomass losses from mortality may have increased along with increasing temperatures, due to the heat and water vapour deficit stresses (Hubau et al., 2020). Indeed, increased temperatures could also explain why increasing biomass losses were observed across Amazonia, regardless of whether plots were experiencing an anomalous maximum cumulative water deficit, in census intervals spanning the 2010 drought (Feldpausch et al., 2016). Similarly, a modelling study found the forest dynamics in the Guyana Shield to be more sensitive to increased temperatures than to precipitation anomalies and water stress (Aubry-Kientz et al., 2019).

Overall, this analysis suggests that the long-term rise in tree mortality rates in Amazonian forests cannot be simply understood as a result of increasing drought stress. Bayesian approaches, which can accommodate the spatial structure of the data, and are robust to census interval artefacts, are a promising avenue for probing the drivers of trends in this key ecosystem process.

5 Synthesis

In 2007 intact tropical forests accounted for ca. 63 % (228.2 GtC) of global C stored in living forest biomass (above- and belowground) and ca. 46 % (393.3±60.8 GtC) of total global C forest stocks (including deadwood, litter, and soil; Pan et al., 2011). While the terrestrial tropical net sink rates have been observed to have been increasing by 0.04±0.01 GtC year^{-1}, especially in Africa and Asia, during recent decades (1990-2009; Sitch et al., 2015), it is uncertain how long this trend might continue. For instance, in the Amazon, recent evidence suggests losses through mortality have been outpacing gains from recruitment and growth during the past decades, resulting in a steady decline of its carbon sink capacity since the early 1990s, and recent evidence suggests a similar trend has been occurring in African forests since 2010 (Brienen et al., 2015; Hubau et al., 2020). Droughts have been occurring more frequently, and increasing in severity, under warmer conditions, which could be one of the factors driving increasing tree mortality under climate change, and has been identified as one of the risk factors for tropical forests potentially becoming a carbon source in the future (e.g. Allen et al., 2010; Allen et al., 2015). Here, I have increased our understanding of stem-based tropical tree mortality rates by (1) deriving recommendations for sampling network sizes required to confidently detect long- and short-term changes in mortality rates, (2) identifying at which spatial scale variation in tropical mortality rates can best be described, and (3) investigating whether the observed recent increases in Amazonian tree mortality rates were driven by increasing water deficits.

5.1 Chapter 2: Criteria for designing optimal sampling strategies for detecting changes in tree mortality rates in tropical forests

Long-term trends in annual tree mortality rates have been observed across the tropics, with increases of 2 % per year observed across 20 plots in Australia (Murphy et al., 2013), and 3 % per year reported across 50 South American plots (Lewis et al., 2004b). Additionally, short-term increases in mortality rates can be observed in response to one-off catastrophic events. For example, the 1997 El Niño drought elevated mortality rates by 71 % in 12 central Amazonian plots (Williamson et al., 2000). In order to be able to relate these changes in mortality rates to variation in (environmental) drivers, it is important to be able to have a permanent plot sampling strategy that can confidently establish that the detected trend is not merely the result of natural variation in local or regional mortality rates. To this end, simulated forests were sampled at different intensities, using combinations of an increasing number of plots and increasing census interval lengths.

These simulated forests varied in their degree of background dynamics, and in the strength of their long- or short-term trends in mortality rates.

Overall, a minimum overall monitoring period of 20 years is recommended for detecting long-term changes in tree mortality rates, though increases of 2 % per year can be detected over the course of 10 years with two census intervals in a network of at least 90 plots. However, for detecting short-term increases in mortality rates, annual or biennial census intervals are recommended. The former will allow detecting an increase of 15 % in mortality rates with a network of 40 plots. Finally, more dynamic forests with higher base mortality rates were found to require fewer plots to detect an increase of the same relative magnitude, than forests which had lower base mortality rates. For example, a network of 40 plots will suffice to detect an annual mortality increase of 1 % with three censuses at intervals of 10 years in more dynamic regions like the Western Amazon (Johnson et al., 2016), whereas for less dynamic regions like the Guiana Shield (Johnson et al., 2016) this recommendation increases to 70 plots to detect a similar increase.

5.2 Chapter 3: Tree mortality rates vary among biogeographical regions across the tropics

In order to understand variation in tropical tree mortality rates, and relate this to any potential drivers, it is important to know at which scales spatial scales they vary. Annual mortality rates were derived from a permanent sample network spanning hundreds of plots, across all four tropical continents, which have been monitored for decades, as collated in the ForestPlots database (Lopez-Gonzalez et al., 2013). Repeated censuses of the same plot are expected to be more similar to each other, than censuses of different plots. As such, mortality rates observed during each census are assumed to be drawn from plot level mortality rate distributions in a hierarchical Bayesian model. These plots in turn were assumed to be more similar within an overarching spatial region. As such, this chapter tested whether mortality rate distributions are best characterised at the biogeographical, continental or pan-tropical scale. Nine biogeographical regions were distinguished (sensu Feldpausch et al., 2012), where variation among these regions is expected to be greater than variation within them: Central Africa, East Africa, West Africa, the Brazilian Shield (Amazonia), East-Central Amazonia, the Guyana Shield (Amazonia), West Amazonia, South-East Asia and North Australia.

Mortality rate distributions were found to be best described at the biogeographical level, indicating that variation in tropical tree mortality rates is likely the result of a combination of edaphic, climatic and compositional differences. The biogeographical regions cover a range of disturbance regimes, from Northwest Australia, which had the lowest median mortality rates (0.80 % yr^{-1}; mean 0.92 % yr^{-1}), but a relatively high coefficient of variation (0.57) – indicating a region with predominantly small-scale mortality events and occasional

larger disturbances (Murphy et al., 2013) – to West Amazonia, a region with relatively high median mortality rates (2.04 % yr^{-1}; mean 2.19 % yr^{-1}), but a relatively low coefficient of variation (0.39) – indicating a region in which most mortality events involve a small number of trees (Espírito-Santo et al., 2014).

5.3 Chapter 4: Has drought stress caused the long-term increase in tree mortality rates in Amazonian forests?

Mortality rates are reported to have increased since the mid 1970s in old-growth Amazonian forests (Phillips *et al.*, 2008; Lewis et al., 2004b), and have recently been outpacing gains from recruitment and growth since ca. 2000, resulting in a levelling off of its net carbon sink role (Brienen et al., 2015; Hubau et al., 2020). Concurrently, the severity and frequency of droughts has been increasing, and the duration of the dry season has become longer since the mid 1970s (Marengo et al., 2011). However, until recently no concerted attempt to relate any long-term trend in mortality rates to increasing deficits had been made (Hubau et al., 2020). As such, here I used Bayesian models to evaluate regional trends in mortality rates and cumulative water deficits, and any relationship between them.

In addition to Amazonia as a whole, forests in most biogeographical regions were found to have experienced increasing mortality rates, except the aseasonal Northwest Amazonia, and the Brazilian Shield. Cumulative water deficits were only found to have increased in magnitude in Northwest Venezuela and Southwest Amazonia, and actually lessened in East-Central Amazonia and the Brazilian Shield. However, changing water deficits were not found to be associated with increasing tree mortality rates in Amazonia.

5.4 Research implications and future research

With a changing climate, tropical tree mortality rates could be affected in a number of ways, ranging from increasing to even decreasing, with potentially different trends occurring at different locations and at different times across the tropics. Both increased atmospheric carbon dioxide concentrations, and increased catastrophic disturbances, might lead to an increased abundance of faster growing trees, with reduced longevity, and increased mortality rates, consequently resulting in reduced carbon storage in tropical forests (Bugmann and Bigler, 2011; Körner, 2017; McMahon et al., 2019; Büntgen et al., 2019). However, on the other end of the response spectrum, evidence also exists of compositional shifts towards more species with more drought-tolerant traits, as has been observed for example in the Neotropics and Africa, which might eventually result in a decrease of overall mortality rates (Fauset et al., 2012; van der Sande et al., 2016; Esquivel-Muelbert et al., 2019).

A recent review of 15 dynamic vegetation models (DVMs) found the mortality submodels to be the main predictor of the response of simulated long-term forest dynamics to different climate scenarios (Bugmann et al., 2019). The mortality models evaluated included a range of empirically, experimentally, and theoretically derived formulations, though the four global dynamic vegetation models evaluated all contained highly process-based mortality models. While most alternative mortality formulations did not affect the recreation of observed forest dynamics trends, they led to widely diverging basal area and number of stems trajectories for some of the DVMs, often representing a greater source of uncertainty than the climate change scenario used. This highlights the need for increased understanding and representation in mortality models of the underlying processes driving these changes (Adams et al., 2013). In addition to providing guidance for the expansion of monitoring networks, the methods applied here can also aid in further improving mortality models.

The individual-based Bayesian approach developed here could be readily used to calibrate patterns of tree mortality within emerging individual-based vegetation models. Historically, most large-scale vegetation models have represented carbon losses through average turnover rates for carbon pools of different vegetation compartments, generally using a single woody turnover value across one static tropical plant functional type (PFT) to represent losses from tree mortality (Galbraith et al., 2013). However, an appreciation of the importance of individual- and size-dependent processes for determining the dynamics of tropical forests (Fischer et al., 2016; Shugart et al., 2018), has led to the emergence of models that attempt to capture these stem-based processes (Fyllas et al., 2014; Aubry-Kientz et al., 2015a). Such models require stem-based estimation of mortality rates which could be supplied by further iterations of the analyses described here.

Secondly, the approaches used here could be developed to promote a better representation of biodiversity in vegetation models. A couple of the main limitations of previous iterations of dynamic vegetation models originate from the representation of vegetation by a limited set of static plant functional types represented by a few average trait values, with competition occurring at the PFT level, neither of which easily allows for compositional trait shifts under changing climatic conditions (Scheiter et al., 2013), thus potentially underestimating forest resilience (Sakschewski et al., 2016). Commonly used functional traits for representing the diversity of ecological responses of tropical rainforests in individual based forest models include wood density, maximum diameter, maximum height, leaf longevity, leaf nitrogen content, leaf phosphorus content, leaf dry mass per area (Fyllas et al., 2014; Sakschewski et al., 2015; Maréchaux and Chave, 2017; Aubry-Kientz et al., 2019). Estimates from the analytical approach here, through inclusion of functional traits in mortality models as predictor variables, could help identify distributions of and potential trends in mortality rates for different strategic groups, and

improve understanding of how tropical forests with different compositions might respond to changing environmental conditions.

Finally, a key strength of the hierarchical approach used here is that it can aid attempts to bridge the scale-gap for understanding how processes such as tree mortality vary at scales from individuals to regions (Allen et al., 2010). Being able to describe and verify forest processes at scales that are larger than individual plots is crucial for calibrating remote sensing and modelling products that have much larger pixel sizes (Fischer et al., 2016; Rödig et al., 2017; Rammig et al., 2018), and could allow for integration of flux measurements over large scales (Anderegg et al., 2016b).

Through expanded monitoring efforts, and further quantification and analyses of the underlying processes, utilising data from all available spatial scales, we can continue to improve our understanding of the mortality of tropical trees. Overall, the novel approaches and results described in this thesis could be used to address this challenge, and therefore contribute to a more robust understanding of the future of tropical carbon.

List of References

Adams, H.D., Guardiola-Claramonte, M., Barron-Gafford, G.A., Villegas, J.C., Breshears, D.D., Zou, C.B., Troch, P.A. and Huxman, T.E. 2009. Temperature sensitivity of drought-induced tree mortality portends increased regional die-off under global-change-type drought. *Proceedings of the National Academy of Sciences of the United States of America*. **106**(17), pp.7063–7066.

Adams, H.D., Williams, A.P., Xu, C., Rauscher, S.A., Jiang, X. and McDowell, N.G. 2013. Empirical and process-based approaches to climate-induced forest mortality models. *Frontiers in Plant Science*. **4**, Article 438, 1-5.

Adams, H.D., Zeppel, M.J.B.B., Anderegg, W.R.L., Hartmann, H., Landhäusser, S.M., Tissue, D.T., Huxman, T.E., Hudson, P.J., Franz, T.E., Allen, C.D., Anderegg, L.D.L.L., Barron-Gafford, G.A., Beerling, D.J., Breshears, D.D., Brodribb, T.J., Bugmann, H., Cobb, R.C., Collins, A.D., Dickman, L.T., Duan, H., Ewers, B.E., Galiano, L., Galvez, D.A., Garcia-Forner, N., Gaylord, M.L., Germino, M.J., Gessler, A., Hacke, U.G., Hakamada, R., Hector, A., Jenkins, M.W., Kane, J.M., Kolb, T.E., Law, D.J., Lewis, J.D., Limousin, J.-M., Love, D.M., Macalady, A.K., Martínez-Vilalta, J., Mencuccini, M., Mitchell, P.J., Muss, J.D., O'Brien, M.J., O'Grady, A.P., Pangle, R.E., Pinkard, E.A., Piper, F.I., Plaut, J.A., Pockman, W.T., Quirk, J., Reinhardt, K., Ripullone, F., Ryan, M.G., Sala, A., Sevanto, S., Sperry, J.S., Vargas, R., Vennetier, M., Way, D.A., Xu, C., Yepez, E.A. and McDowell, N.G. 2017. A multi-species synthesis of physiological mechanisms in drought-induced tree mortality. *Nature Ecology & Evolution*. **1**(9), pp.1285–1291.

Aguirre-Gutiérrez, J., Oliveras, I., Rifai, S., Fauset, S., Adu-Bredu, S., Affum-Baffoe, K., Baker, T.R., Feldpausch, T.R., Gvozdevaite, A., Hubau, W., Kraft, N.J.B., Lewis, S.L., Moore, S., Niinemets, Ü., Peprah, T., Phillips, O.L., Ziemińska, K., Enquist, B. and Malhi, Y. 2019. Drier tropical forests are susceptible to functional changes in response to a long-term drought J. Penuelas, ed. *Ecology Letters*. **22**(5), pp.855–865.

Aiba, S.I. and Kitayama, K. 2002. Effects of the 1997-98 El Niño drought on rain forests of Mount Kinabalu, Borneo. *Journal of Tropical Ecology*. **18**(2), pp.215–230.

Alder, D. and Synnott, T.J. 1992. *Permanent Sample Plot Techniques for Mixed Tropical Forest*. Oxford, UK: Oxford University Press.

Aleixo, I., Norris, D., Hemerik, L., Barbosa, A., Prata, E., Costa, F. and Poorter, L. 2019. Amazonian rainforest tree mortality driven by climate and functional traits. *Nature Climate Change*. **9**(5), pp.384–388.

Allen, C.D. 2009. Climate-induced forest dieback: an escalating global phenomenon? *Unasylva*. **60**(231–232), pp.43–49.

Allen, C.D., Breshears, D.D. and McDowell, N.G. 2015. On underestimation of global vulnerability to tree mortality and forest die-off from hotter drought in the Anthropocene. *Ecosphere*. **6**(8), pp.1–55.

Allen, C.D., Macalady, A.K., Chenchouni, H., Bachelet, D., McDowell, N., Vennetier, M., Kitzberger, T., Rigling, A., Breshears, D.D., Hogg, E.H. (Ted), Gonzalez, P., Fensham, R., Zhang, Z., Castro, J., Demidova, N., Lim, J.-H., Allard, G., Running, S.W., Semerci, A. and Cobb, N. 2010. A global overview of drought and heat-induced tree mortality reveals emerging climate change risks for forests. *Forest Ecology and Management*. **259**(4), pp.660–684.

Amigo, I. 2020. When will the Amazon hit a tipping point? *Nature*. **578**(7796), pp.505–507.

Anderegg, W.R.L. 2012. Complex aspen forest carbon and root dynamics during drought: A letter. *Climatic Change*. **111**(3), pp.983–991.

Anderegg, W.R.L., Berry, J.A. and Field, C.B. 2012a. Linking definitions, mechanisms, and modeling of drought-induced tree death. *Trends in Plant Science*. **17**(12), pp.693–700.

Anderegg, W.R.L., Berry, J.A., Smith, D.D., Sperry, J.S., Anderegg, L.D.L. and Field, C.B. 2012b. The roles of hydraulic and carbon stress in a widespread climate-induced forest die-off. *Proceedings of the National Academy of Sciences of the United States of America*. **109**(1), pp.233–237.

Anderegg, W.R.L., Klein, T., Bartlett, M., Sack, L., Pellegrini, A.F.A., Choat, B. and Jansen, S. 2016a. Meta-analysis reveals that hydraulic traits explain cross-species patterns of drought-induced tree mortality across the globe. *Proceedings of the National Academy of Sciences*. **113**(18), pp.5024–5029.

Anderegg, W.R.L., Martinez-Vilalta, J., Cailleret, M., Camarero, J.J., Ewers, B.E., Galbraith, D., Gessler, A., Grote, R., Huang, C., Levick, S.R., Powell, T.L., Rowland, L., Sánchez-Salguero, R. and Trotsiuk, V. 2016b. When a Tree Dies in the Forest: Scaling Climate-Driven Tree Mortality to Ecosystem Water and Carbon Fluxes. *Ecosystems*. **19**(6), pp.1133–1147.

Anderegg, W.R.L.L., Plavcová, L., Anderegg, L.D.L.L., Hacke, U.G., Berry, J.A. and Field, C.B. 2013. Drought's legacy: multiyear hydraulic deterioration underlies widespread aspen forest die-off and portends increased future risk. *Global Change Biology*. **19**(4), pp.1188–1196.

Anderson-Teixeira, K.J., Davies, S.J., Bennett, A.C., Gonzalez-Akre, E.B., Muller-Landau, H.C., Joseph Wright, S., Abu Salim, K., Almeyda Zambrano, A.M., Alonso, A., Baltzer, J.L., Basset, Y., Bourg, N.A., Broadbent, E.N., Brockelman, W.Y., Bunyavejchewin, S., Burslem, D.F.R.P., Butt, N., Cao, M., Cardenas, D., Chuyong, G.B., Clay, K., Cordell, S., Dattaraja, H.S., Deng, X., Detto, M., Du, X., Duque, A., Erikson, D.L., Ewango, C.E.N., Fischer, G.A., Fletcher, C., Foster, R.B., Giardina, C.P., Gilbert, G.S., Gunatilleke, N., Gunatilleke, S., Hao, Z., Hargrove, W.W., Hart, T.B., Hau, B.C.H., He, F., Hoffman, F.M., Howe, R.W., Hubbell, S.P., Inman-Narahari, F.M., Jansen, P.A., Jiang, M., Johnson, D.J., Kanzaki, M., Kassim, A.R., Kenfack, D., Kibet, S., Kinnaird, M.F., Korte, L., Kral, K., Kumar, J., Larson, A.J., Li, Y., Li, X., Liu, S., Lum, S.K.Y., Lutz, J.A., Ma, K., Maddalena, D.M., Makana, J.-R., Malhi, Y., Marthews, T., Mat Serudin, R., McMahon, S.M., McShea, W.J., Memiaghe, H.R., Mi, X., Mizuno, T., Morecroft, M., Myers, J.A., Novotny, V., de Oliveira, A.A., Ong, P.S., Orwig, D.A., Ostertag, R., den Ouden, J., Parker, G.G., Phillips, R.P., Sack, L., Sainge, M.N., Sang, W., Sri-ngernyuang, K., Sukumar, R., Sun, I.-F., Sungpalee, W., Suresh, H.S., Tan, S., Thomas, S.C., Thomas, D.W., Thompson, J., Turner, B.L., Uriarte, M., Valencia, R., Vallejo, M.I., Vicentini, A., Vrška, T., Wang, X., Wang, X., Weiblen, G., Wolf, A., Xu, H., Yap, S. and Zimmerman, J. 2015. CTFS-ForestGEO: a worldwide network monitoring forests in an era of global change. *Global Change Biology*. **21**(2), pp.528–549.

Anderson, L.O., Aragão, L.E.O.C., Gloor, M., Arai, E., Adami, M., Saatchi, S.S., Malhi, Y., Shimabukuro, Y.E., Barlow, J., Berenguer, E. and Duarte, V. 2015. Disentangling the contribution of multiple land covers to fire-mediated carbon emissions in Amazonia during the 2010 drought. *Global Biogeochemical Cycles*. **29**(10), pp.1739–1753.

de Andrade, D.F.C., Ruschel, A.R., Schwartz, G., de Carvalho, J.O.P., Humphries, S. and Gama, J.R.V. 2020. Forest resilience to fire in eastern Amazon depends on the intensity of pre-fire disturbance. *Forest Ecology and Management*. **472**, p.118258.

Aragão, L.E.O.C., Malhi, Y., Roman-Cuesta, R.M., Saatchi, S., Anderson, L.O. and

Shimabukuro, Y.E. 2007. Spatial patterns and fire response of recent Amazonian droughts. *Geophysical Research Letters*. **34**(7), p.L07701.

Archambeau, J., Ruiz-Benito, P., Ratcliffe, S., Fréjaville, T., Changenet, A., Muñoz Castañeda, J.M., Lehtonen, A., Dahlgren, J., Zavala, M.A. and Benito Garzón, M. 2020. Similar patterns of background mortality across Europe are mostly driven by drought in European beech and a combination of drought and competition in Scots pine. *Agricultural and Forest Meteorology*. **280**(March), p.107772.

Arriaga, L. 2000. Types and causes of tree mortality in a tropical montane cloud forest of Tamaulipas, Mexico. *Journal of Tropical Ecology*. **16**(5), pp.623–636.

Aubréville, A.M.A. 2013. The Disappearance of the Tropical Forests of Africa. *Fire Ecology*. **9**(2), pp.3–13.

Aubry-Kientz, M., Rossi, V., Boreux, J.-J. and Hérault, B. 2015a. A joint individual-based model coupling growth and mortality reveals that tree vigor is a key component of tropical forest dynamics. *Ecology and Evolution*. **5**(12), pp.2457–2465.

Aubry-Kientz, M., Rossi, V., Cornu, G., Wagner, F. and Hérault, B. 2019. Temperature rising would slow down tropical forest dynamic in the Guiana Shield. *Scientific Reports*. **9**(1), pp.1–8.

Aubry-Kientz, M., Rossi, V., Wagner, F. and Hérault, B. 2015b. Identifying climatic drivers of tropical forest dynamics. *Biogeosciences*. **12**(19), pp.5583–5596.

Baccini, A., Walker, W., Carvalho, L., Farina, M., Sulla-Menashe, D. and Houghton, R.A. 2017. Tropical forests are a net carbon source based on aboveground measurements of gain and loss. *Science*. **358**(6360), pp.230–234.

Bakayoko, A., Martin, P., Chatelain, C., Traore, D. and Gautier, L. 2011. Diversity, Family Dominance, Life Forms and Ecological Strategies of Forest Fragments Compared to Continuous Forest in Southwestern Côte d'Ivoire. *Candollea*. **66**(2), pp.255–262.

Baker, P.J., Bunyavejchewin, S. and Robinson, A.P. 2008. The impacts of large-scale, low-intensity fires on the forests of continental South-east Asia. *International Journal of Wildland Fire*. **17**(6), pp.782–792.

Baker, T.R., Phillips, O.L., Malhi, Y., Almeida, S., Arroyo, L., Di Fiore, A., Erwin, T., Higuchi, N., Killeen, T.J., Laurance, S.G., Laurance, W.F., Lewis, S.L., Monteagudo, A., Neill, D.A., Núñez Vargas, P., Pitman, N.C.A.A., Silva, J.N.M. and Vásquez Martínez, R. 2004a. Increasing biomass in Amazonian forest plots Y. Malhi & O. L. Phillips, eds. *Philosophical Transactions of the Royal Society of London. Series B: Biological Sciences*. **359**(1443), pp.353–365.

Baker, T.R., Phillips, O.L., Malhi, Y., Almeida, S., Arroyo, L., Di Fiore, A., Erwin, T., Killeen, T.J., Laurance, S.G., Laurance, W.F., Lewis, S.L., Lloyd, J., Monteagudo, A., Neill, D.A., Patiño, S., Pitman, N.C.A., Silva, J.N.M. and Martínez, R. V 2004b. Variation in wood density determines spatial patterns in Amazonian forest biomass. *Global Change Biology*. **10**(5), pp.545–562.

Balch, J.K., Nepstad, D.C., Curran, L.M., Brando, P.M., Portela, O., Guilherme, P., Reuning-Scherer, J.D. and de Carvalho, O.J. 2011. Size, species, and fire behavior predict tree and liana mortality from experimental burns in the Brazilian Amazon. *Forest Ecology and Management*. **261**(1), pp.68–77.

Barlow, J., Lagan, B.O. and Peres, C.A. 2003a. Morphological correlates of fire-induced tree mortality in a central Amazonian forest. *Journal of Tropical Ecology*. **19**(3), pp.291–299.

Barlow, J. and Peres, C.A. 2008. Fire-mediated dieback and compositional cascade in an Amazonian forest. *Philosophical Transactions of the Royal Society B: Biological Sciences*. **363**(1498), pp.1787–1794.

Barlow, J., Peres, C.A., Lagan, B.O. and Haugaasen, T. 2003b. Large tree mortality and the decline of forest biomass following Amazonian wildfires. *Ecology Letters*. **6**(1), pp.6–8.

Bellingham, P.J., Tanner, E.V.J. and Healey, J.R. 1995. Damage and responsiveness of Jamaican montane tree species after disturbance by a hurricane. *Ecology*. **76**(8), pp.2562–2580.

Bendix, J., Homeier, J., Cueva Ortiz, E., Emck, P., Breckle, S.-W., Richter, M. and Beck, E. 2006. Seasonality of weather and tree phenology in a tropical evergreen mountain rain forest. *International Journal of Biometeorology*. **50**(6), pp.370–384.

Bonal, D., Burban, B., Stahl, C., Wagner, F. and Hérault, B. 2016. The response of tropical rainforests to drought—lessons from recent research and future prospects. *Annals of Forest Science*. **73**(1), pp.27–44.

Bova, A.S. and Dickinson, M.B. 2005. Linking surface-fire behavior, stem heating, and tissue necrosis. *Canadian Journal of Forest Research*. **35**(4), pp.814–822.

Bowman, D.M.J.S. 2000. *Australian rainforests: islands of green in a land of fire*. Cambridge: Cambridge University Press.

Brando, P.M., Balch, J.K., Nepstad, D.C., Morton, D.C., Putz, F.E., Coe, M.T., Silvério, D., Macedo, M.N., Davidson, E.A., Nóbrega, C.C., Alencar, A. and Soares-Filho, B.S. 2014. Abrupt increases in Amazonian tree mortality due to drought-fire interactions. *Proceedings of the National Academy of Sciences of the United States of America*. **111**(17), pp.6347–6352.

Brando, P.M., Nepstad, D.C., Balch, J.K., Bolker, B., Christman, M.C., Coe, M. and Putz, F.E. 2012. Fire-induced tree mortality in a neotropical forest: The roles of bark traits, tree size, wood density and fire behavior. *Global Change Biology*. **18**(2), pp.630–641.

Brando, P.M., Paolucci, L., Ummenhofer, C.C., Ordway, E.M., Hartmann, H., Cattau, M.E., Rattis, L., Medjibe, V., Coe, M.T. and Balch, J. 2019. Droughts, Wildfires, and Forest Carbon Cycling: A Pantropical Synthesis. *Annual Review of Earth and Planetary Sciences*. **47**(1), pp.555–581.

Bréda, N., Huc, R., Granier, A. and Dreyer, E. 2006. Temperate forest trees and stands under severe drought: a review of ecophysiological responses, adaptation processes and long-term consequences. *Annals of Forest Science*. **63**(6), pp.625–644.

Breshears, D.D., Cobb, N.S., Rich, P.M., Price, K.P., Allen, C.D., Balice, R.G., Romme, W.H., Kastens, J.H., Floyd, M.L., Belnap, J., Anderson, J.J., Myers, O.B. and Meyer, C.W. 2005. Regional vegetation die-off in response to global-change-type drought. *Proceedings of the National Academy of Sciences of the United States of America*. **102**(42), pp.15144–15148.

Breshears, D.D., Myers, O.B., Meyer, C.W., Barnes, F.J., Zou, C.B., Allen, C.D., McDowell, N.G. and Pockman, W.T. 2009. Tree die-off in response to global change-type drought: mortality insights from a decade of plant water potential measurements. *Frontiers in Ecology and the Environment*. **7**(4), pp.185–189.

Brienen, R.J.W., Gloor, E. and Zuidema, P.A. 2012. Detecting evidence for CO2 fertilization from tree ring studies: The potential role of sampling biases. *Global Biogeochemical Cycles*. **26**(1), pp.1–13.

Brienen, R.J.W., Phillips, O.L., Feldpausch, T.R., Gloor, E., Baker, T.R., Lloyd, J., Lopez-

Gonzalez, G., Monteagudo-Mendoza, A., Malhi, Y., Lewis, S.L., Vásquez Martinez, R., Alexiades, M., Álvarez Dávila, E., Alvarez-Loayza, P., Andrade, A., Aragaõ, L.E.O.C., Araujo-Murakami, A., Arets, E.J.M.M., Arroyo, L., Aymard C., G.A., Bánki, O.S., Baraloto, C., Barroso, J., Bonal, D., Boot, R.G.A., Camargo, J.L.C., Castilho, C. V., Chama, V., Chao, K.J., Chave, J., Comiskey, J.A., Cornejo Valverde, F., Da Costa, L., De Oliveira, E.A., Di Fiore, A., Erwin, T.L., Fauset, S., Forsthofer, M., Galbraith, D.R., Grahame, E.S., Groot, N., Hérault, B., Higuchi, N., Honorio Coronado, E.N., Keeling, H., Killeen, T.J., Laurance, W.F., Laurance, S., Licona, J., Magnussen, W.E., Marimon, B.S., Marimon-Junior, B.H., Mendoza, C., Neill, D.A., Nogueira, E.M., Núñez, P., Pallqui Camacho, N.C., Parada, A., Pardo-Molina, G., Peacock, J., Penã-Claros, M., Pickavance, G.C., Pitman, N.C.A., Poorter, L., Prieto, A., Quesada, C.A., Ramírez, F., Ramírez-Angulo, H., Restrepo, Z., Roopsind, A., Rudas, A., Salomaõ, R.P., Schwarz, M., Silva, N., Silva-Espejo, J.E., Silveira, M., Stropp, J., Talbot, J., Ter Steege, H., Teran-Aguilar, J., Terborgh, J., Thomas-Caesar, R., Toledo, M., Torello-Raventos, M., Umetsu, R.K., Van Der Heijden, G.M.F., Van Der Hout, P., Guimarães Vieira, I.C., Vieira, S.A., Vilanova, E., Vos, V.A. and Zagt, R.J. 2015. Long-term decline of the Amazon carbon sink. *Nature*. **519**(7543), pp.344–348.

Bugmann, H. and Bigler, C. 2011. Will the CO_2 fertilization effect in forests be offset by reduced tree longevity? *Oecologia*. **165**(2), pp.533–544.

Bugmann, H., Seidl, R., Hartig, F., Bohn, F., Brůna, J., Cailleret, M., François, L., Heinke, J., Henrot, A.J., Hickler, T., Hülsmann, L., Huth, A., Jacquemin, I., Kollas, C., Lasch-Born, P., Lexer, M.J., Merganič, J., Merganičová, K., Mette, T., Miranda, B.R., Nadal-Sala, D., Rammer, W., Rammig, A., Reineking, B., Roedig, E., Sabaté, S., Steinkamp, J., Suckow, F., Vacchiano, G., Wild, J., Xu, C. and Reyer, C.P.O. 2019. Tree mortality submodels drive simulated long-term forest dynamics: assessing 15 models from the stand to global scale. *Ecosphere*. **10**(2).

Büntgen, U., Krusic, P.J., Piermattei, A., Coomes, D.A., Esper, J., Myglan, V.S., Kirdyanov, A. V., Camarero, J.J., Crivellaro, A. and Körner, C. 2019. Limited capacity of tree growth to mitigate the global greenhouse effect under predicted warming. *Nature Communications*. **10**(1), p.2171.

Caswell, H. and Salguero-Gómez, R. 2013. Age, stage and senescence in plants. *Journal of Ecology*. **101**(3), pp.585–595.

Chambers, J.Q., Higuchi, N. and Schimel, J.P. 1998. Ancient trees in Amazonia. *Nature*. **391**(6663), pp.135–136.

Chao, K.-J., Phillips, O.L., Monteagudo, A., Torres-Lezama, A. and Vásquez Martínez, R. 2009. How do trees die? Mode of death in northern Amazonia. *Journal of Vegetation Science*. **20**(2), pp.260–268.

Chao, K.J. and Phillips, O.L. 2005. *Field manual for mode of death census - Sixth Framework Programme (2002-2006)*. PAN-Amazonia - Project for the Advancement of Networked Science in Amazonia.

Chazdon, R.L., Redondo Brenes, A. and Vilchez Alvarado, B. 2005. Effects of climate and stand age on annual tree dynamics in tropical second-growth rain forests. *Ecology*. **86**(7), pp.1808–1815.

Cochrane, M.A. 2001. In the line of Fire Understanding the Impacts of Tropical Forest Fires. *Environment: Science and Policy for Sustainable Development*. **43**(8), pp.28–38.

Cochrane, M.A. 2003. Review Article: Fire science for rainforests. *Nature*. **421**(27), pp.913–919.

Cochrane, M.A., Alencar, A., Schulze, M.D., Souza Jr, C.M., Nepstad, D.C., Lefebvre, P. and Davidson, E.A. 1999. Positive feedbacks in the fire dynamic of closed canopy tropical forests. *Science*. **284**(5421), pp.1832–1835.

Condit, R. 1998. *Tropical Forest Census Plots*. Berlin, Heidelberg: Springer-Verlag Berlin Heidelberg.

Condit, R., Aguilar, S., Hernandez, A., Perez, R., Lao, S., Angehr, G., Hubbell, S.P. and Foster, R.B. 2004. Tropical forest dynamics across a rainfall gradient and the impact of an El Niño dry season. *Journal of Tropical Ecology*. **20**(1), pp.51–72.

Condit, R., Ashton, P.S., Manokaran, N., LaFrankie, J. V., Hubbell, S.P. and Foster, R.B. 1999. Dynamics of the forest communities at Pasoh and Barro Colorado: comparing two 50–ha plots D. M. Newbery, T. H. Clutton–Brock, & G. T. Prance, eds. *Philosophical Transactions of the Royal Society of London. Series B: Biological Sciences*. **354**(1391), pp.1739–1748.

Condit, R., Hubbell, S.P. and Foster, R.B. 1995. Mortality Rates of 205 Neotropical Tree and Shrub Species and the Impact of a Severe Drought. *Ecological Monographs*. **65**(4), pp.419–439.

Cramer, W., Bondeau, A., Woodward, F.I., Prentice, I.C., Betts, R.A., Brovkin, V., Cox, P.M., Fisher, V., Foley, J.A., Friend, A.D., Kucharik, C., Lomas, M.R., Ramankutty, N., Sitch, S., Smith, B., White, A. and Young-Molling, C. 2001. Global response of terrestrial ecosystem structure and function to CO_2 and climate change: results from six dynamic global vegetation models. *Global Change Biology*. **7**(4), pp.357–373.

Crouchet, S.E., Jensen, J., Schwartz, B.F. and Schwinning, S. 2019. Tree Mortality After a Hot Drought: Distinguishing Density-Dependent and -Independent Drivers and Why It Matters. *Frontiers in Forests and Global Change*. **2**, pp.1–14.

Dai, A. 2013. Increasing drought under global warming in observations and models. *Nature Climate Change*. **3**(1), pp.52–58.

Damasceno-Junior, G.A., Semir, J., Santos, F.A.M. dos and Leitão-Filho, H. de F. 2004. Tree mortality in a riparian forest at Rio Paraguai, Pantanal, Brazil, after an extreme flooding. *Acta Botanica Brasilica*. **18**(4), pp.839–846.

Das, A.J., Stephenson, N.L. and Davis, K.P. 2016. Why do trees die? Characterizing the drivers of background tree mortality. *Ecology*. **97**(10), pp.2616–2627.

Davies, S.J. 2001. Tree mortality and growth in 11 sympatric Macaranga species in Borneo. *Ecology*. **82**(4), pp.920–932.

Drobyshev, I., Linderson, H. and Sonesson, K. 2007. Temporal mortality pattern of pedunculate oaks in southern Sweden. *Dendrochronologia*. **24**(2–3), pp.97–108.

Duffy, P.B., Brando, P., Asner, G.P. and Field, C.B. 2015. Projections of future meteorological drought and wet periods in the Amazon . *Proceedings of the National Academy of Sciences* . **112**(43), pp.13172–13177.

Dwomoh, F.K. and Wimberly, M.C. 2017. Fire regimes and forest resilience: alternative vegetation states in the West African tropics. *Landscape Ecology*. **32**(9), pp.1849–1865.

Ediriweera, S., Bandara, C., Woodbury, D.J., Mi, X., Gunatilleke, I.A.U.N., Gunatilleke, C.V.S. and Ashton, M.S. 2020. Changes in tree structure, composition, and diversity of a mixed-dipterocarp rainforest over a 40-year period. *Forest Ecology and Management*. **458**, p.117764.

Eggeling, W.J. 1947. Observations on the ecology of the Budongo rain forest, Uganda.

Journal of Ecology. **34**(1), pp.20–87.

Elmqvist, T., Rainey, W.E., Pierson, E.D. and Cox, P.A. 1994. Effects of tropical cyclones Ofa and Val on the structure of a Samoan lowland rain forest. *Biotropica*. **26**(4), pp.384–391.

Eppinga, M.B. and Pucko, C.A. 2018. The impact of hurricanes Irma and Maria on the forest ecosystems of Saba and St. Eustatius, northern Caribbean. *Biotropica*. **50**(5), pp.723–728.

Espírito-Santo, F.D.B., Gloor, M., Keller, M., Malhi, Y., Saatchi, S., Nelson, B., Junior, R.C.O., Pereira, C., Lloyd, J., Frolking, S., Palace, M., Shimabukuro, Y.E., Duarte, V., Mendoza, A.M., López-González, G., Baker, T.R., Feldpausch, T.R., Brienen, R.J.W., Asner, G.P., Boyd, D.S. and Phillips, O.L. 2014. Size and frequency of natural forest disturbances and the Amazon forest carbon balance. *Nature Communications*. **5**(3434), pp.1–27.

Espírito-Santo, F.D.B., Keller, M., Braswell, B., Nelson, B.W., Frolking, S. and Vicente, G. 2010. Storm intensity and old-growth forest disturbances in the Amazon region. *Geophysical Research Letters*. **37**(11), p.L11403.

Esquivel-Muelbert, A., Baker, T.R., Dexter, K.G., Lewis, S.L., Brienen, R.J.W., Feldpausch, T.R., Lloyd, J., Monteagudo-Mendoza, A., Arroyo, L., Álvarez-Dávila, E., Higuchi, N., Marimon, B.S., Marimon-Junior, B.H., Silveira, M., Vilanova, E., Gloor, E., Malhi, Y., Chave, J., Barlow, J., Bonal, D., Davila Cardozo, N., Erwin, T., Fauset, S., Hérault, B., Laurance, S., Poorter, L., Qie, L., Stahl, C., Sullivan, M.J.P., ter Steege, H., Vos, V.A., Zuidema, P.A., Almeida, E., Almeida de Oliveira, E., Andrade, A., Vieira, S.A., Aragão, L., Araujo-Murakami, A., Arets, E., Aymard C, G.A., Baraloto, C., Camargo, P.B., Barroso, J.G., Bongers, F., Boot, R., Camargo, J.L., Castro, W., Chama Moscoso, V., Comiskey, J., Cornejo Valverde, F., Lola da Costa, A.C., del Aguila Pasquel, J., Di Fiore, A., Fernanda Duque, L., Elias, F., Engel, J., Flores Llampazo, G., Galbraith, D., Herrera Fernández, R., Honorio Coronado, E., Hubau, W., Jimenez-Rojas, E., Lima, A.J.N., Umetsu, R.K., Laurance, W., Lopez-Gonzalez, G., Lovejoy, T., Aurelio Melo Cruz, O., Morandi, P.S., Neill, D., Núñez Vargas, P., Pallqui Camacho, N.C., Parada Gutierrez, A., Pardo, G., Peacock, J., Peña-Claros, M., Peñuela-Mora, M.C., Petronelli, P., Pickavance, G.C., Pitman, N., Prieto, A., Quesada, C., Ramírez-Angulo, H., Réjou-Méchain, M., Restrepo Correa, Z., Roopsind, A., Rudas, A., Salomão, R., Silva, N., Silva Espejo, J., Singh, J., Stropp, J., Terborgh, J., Thomas, R., Toledo, M., Torres-Lezama, A., Valenzuela Gamarra, L., van de Meer, P.J., van der Heijden, G., van der Hout, P., Vasquez Martinez, R., Vela, C., Vieira, I.C.G. and Phillips, O.L. 2019. Compositional response of Amazon forests to climate change. *Global Change Biology*. **25**(1), pp.39–56.

European Commission. Joint Research Center 2003. Global Land Cover 2000 database. Available from: http://bioval.jrc.ec.europa.eu/products/glc2000/glc2000.php.

Farquhar, G.D., von Caemmerer, S. and Berry, J.A. 1980. A biochemical model of photosynthetic CO_2 assimilation in leaves of C_3 species. *Planta*. **149**(1), pp.78–90.

Fauset, S., Baker, T.R., Lewis, S.L., Feldpausch, T.R., Affum-Baffoe, K., Foli, E.G., Hamer, K.C. and Swaine, M.D. 2012. Drought-induced shifts in the floristic and functional composition of tropical forests in Ghana. *Ecology Letters*. **15**(10), pp.1120–1129.

Feely, R.A., Takahashi, T., Wanninkhof, R., McPhaden, M.J., Cosca, C.E., Sutherland, S.C. and Carr, M.E. 2006. Decadal variability of the air-sea CO_2 fluxes in the equatorial Pacific Ocean. *Journal of Geophysical Research: Oceans*. **111**(8), pp.1–16.

Feldpausch, T.R., Banin, L., Phillips, O.L., Baker, T.R., Lewis, S.L., Quesada, C.A., Affum-Baffoe, K., Arets, E.J.M.M., Berry, N.J., Bird, M., Brondizio, E.S., Camargo, P. de,

Chave, J., Djagbletey, G., Domingues, T.F., Drescher, M., Fearnside, P.M., França, M.B., Fyllas, N.M., Lopez-Gonzalez, G., Hladik, A., Higuchi, N., Hunter, M.O., Iida, Y., Salim, K.A., Kassim, A.R., Keller, M., Kemp, J., King, D.A., Lovett, J.C., Marimon, B.S., Marimon-Junior, B.H., Lenza, E., Marshall, A.R., Metcalfe, D.J., Mitchard, E.T.A., Moran, E.F., Nelson, B.W., Nilus, R., Nogueira, E.M., Palace, M., Patiño, S., Peh, K.S.-H., Raventos, M.T., Reitsma, J.M., Saiz, G., Schrodt, F., Sonké, B., Taedoumg, H.E., Tan, S., White, L., Wöll, H. and Lloyd, J. 2011. Height-diameter allometry of tropical forest trees. *Biogeosciences*. **8**(5), pp.1081–1106.

Feldpausch, T.R., Lloyd, J., Lewis, S.L., Brienen, R.J.W., Gloor, M., Monteagudo Mendoza, A., Lopez-Gonzalez, G., Banin, L., Abu Salim, K., Affum-Baffoe, K., Alexiades, M., Almeida, S., Amaral, I., Andrade, A., Aragão, L.E.O.C., Araujo Murakami, A., Arets, E.J.M.M., Arroyo, L., Aymard C., G. a., Baker, T.R., Bánki, O.S., Berry, N.J., Cardozo, N., Chave, J., Comiskey, J.A., Alvarez, E., de Oliveira, A., Di Fiore, A., Djagbletey, G., Domingues, T.F., Erwin, T.L., Fearnside, P.M., França, M.B., Freitas, M.A., Higuchi, N., Iida, Y., Jiménez, E., Kassim, A.R., Killeen, T.J., Laurance, W.F., Lovett, J.C., Malhi, Y., Marimon, B.S., Marimon-Junior, B.H., Lenza, E., Marshall, A.R., Mendoza, C., Metcalfe, D.J., Mitchard, E.T.A., Neill, D.A., Nelson, B.W., Nilus, R., Nogueira, E.M., Parada, A., Peh, K.S.-H., Pena Cruz, A., Peñuela, M.C., Pitman, N.C.A., Prieto, A., Quesada, C.A., Ramírez, F., Ramírez-Angulo, H., Reitsma, J.M., Rudas, A., Saiz, G., Salomão, R.P., Schwarz, M., Silva, N., Silva-Espejo, J.E., Silveira, M., Sonké, B., Stropp, J., Taedoumg, H.E., Tan, S., ter Steege, H., Terborgh, J., Torello-Raventos, M., van der Heijden, G.M.F., Vásquez, R., Vilanova, E., Vos, V.A., White, L., Willcock, S., Woell, H. and Phillips, O.L. 2012. Tree height integrated into pantropical forest biomass estimates. *Biogeosciences*. **9**(8), pp.3381–3403.

Feldpausch, T.R., Phillips, O.L., Brienen, R.J.W., Gloor, E., Lloyd, J., Lopez-Gonzalez, G., Monteagudo-Mendoza, A., Malhi, Y., Alarcón, A., Álvarez Dávila, E., Alvarez-Loayza, P., Andrade, A., Aragao, L.E.O.C., Arroyo, L., Aymard C., G.A., Baker, T.R., Baraloto, C., Barroso, J., Bonal, D., Castro, W., Chama, V., Chave, J., Domingues, T.F., Fauset, S., Groot, N., Honorio Coronado, E., Laurance, S., Laurance, W.F., Lewis, S.L., Licona, J.C., Marimon, B.S., Marimon-Junior, B.H., Mendoza Bautista, C., Neill, D.A., Oliveira, E.A., Oliveira dos Santos, C., Pallqui Camacho, N.C., Pardo-Molina, G., Prieto, A., Quesada, C.A., Ramírez, F., Ramírez-Angulo, H., Réjou-Méchain, M., Rudas, A., Saiz, G., Salomão, R.P., Silva-Espejo, J.E., Silveira, M., ter Steege, H., Stropp, J., Terborgh, J., Thomas-Caesar, R., van der Heijden, G.M.F., Vásquez Martinez, R., Vilanova, E. and Vos, V.A. 2016. Amazon forest response to repeated droughts. *Global Biogeochemical Cycles*. **30**(7), pp.964–982.

Fischer, R., Bohn, F., Dantas de Paula, M., Dislich, C., Groeneveld, J., Gutiérrez, A.G., Kazmierczak, M., Knapp, N., Lehmann, S., Paulick, S., Pütz, S., Rödig, E., Taubert, F., Köhler, P. and Huth, A. 2016. Lessons learned from applying a forest gap model to understand ecosystem and carbon dynamics of complex tropical forests. *Ecological Modelling*. **326**, pp.124–133.

Fontes, C.G., Chambers, J.Q. and Higuchi, N. 2018. Revealing the causes and temporal distribution of tree mortality in Central Amazonia. *Forest Ecology and Management*. **424**(May), pp.177–183.

Franklin, J., Drake, D.R., McConkey, K.R., Tonga, F. and Smith, L.B. 2004. The effects of Cyclone Waka on the structure of lowland tropical rain forest in Vava'u, Tonga. *Journal of Tropical Ecology*. **20**(4), pp.409–420.

Franklin, J.F., Shugart, H.H. and Harmon, M.E. 1987. Tree death as an ecological process: The causes, consequences, and variability of tree mortality. *BioScience*. **37**(8), pp.550–556.

Friedlingstein, P., Jones, M.W., O'Sullivan, M., Andrew, R.M., Hauck, J., Peters, G.P., Peters, W., Pongratz, J., Sitch, S., Le Quéré, C., DBakker, O.C.E., Canadell1, J.G., Ciais1, P., Jackson, R.B., Anthoni1, P., Barbero, L., Bastos, A., Bastrikov, V., Becker, M., Bopp, L., Buitenhuis, E., Chandra, N., Chevallier, F., Chini, L.P., Currie, K.I., Feely, R.A., Gehlen, M., Gilfillan, D., Gkritzalis, T., Goll, D.S., Gruber, N., Gutekunst, S., Harris, I., Haverd, V., Houghton, R.A., Hurtt, G., Ilyina, T., Jain, A.K., Joetzjer, E., Kaplan, J.O., Kato, E., Goldewijk, K.K., Korsbakken, J.I., Landschützer, P., Lauvset, S.K., Lefèvre, N., Lenton, A., Lienert, S., Lombardozzi, D., Marland, G., McGuire, P.C., Melton, J.R., Metzl, N., Munro, D.R., Nabel, J.E.M.S., Nakaoka, S.I., Neill, C., Omar, A.M., Ono, T., Peregon, A., Pierrot, D., Poulter, B., Rehder, G., Resplandy, L., Robertson, E., Rödenbeck, C., Séférian, R., Schwinger, J., Smith, N., Tans, P.P., Tian, H., Tilbrook, B., Tubiello, F.N., Van Der Werf, G.R., Wiltshire, A.J. and Zaehle, S. 2019. Global carbon budget 2019. *Earth System Science Data*. **11**(4), pp.1783–1838.

Friend, A.D., Lucht, W., Rademacher, T.T., Keribin, R., Betts, R., Cadule, P., Ciais, P., Clark, D.B., Dankers, R., Falloon, P.D., Ito, A., Kahana, R., Kleidon, A., Lomas, M.R., Nishina, K., Ostberg, S., Pavlick, R., Peylin, P., Schaphoff, S., Vuichard, N., Warszawski, L., Wiltshire, A. and Woodward, F.I. 2014. Carbon residence time dominates uncertainty in terrestrial vegetation responses to future climate and atmospheric CO_2. *Proceedings of the National Academy of Sciences of the United States of America*. **111**(9), pp.3280–3285.

Fyllas, N.M., Gloor, E., Mercado, L.M., Sitch, S., Quesada, C.A., Domingues, T.F., Galbraith, D.R., Torre-Lezama, A., Vilanova, E., Ramírez-Angulo, H., Higuchi, N., Neill, D.A., Silveira, M., Ferreira, L., Aymard C., G.A., Malhi, Y., Phillips, O.L. and Lloyd, J. 2014. Analysing Amazonian forest productivity using a new individual and trait-based model (TFS v.1). *Geoscientific Model Development*. **7**(4), pp.1251–1269.

Galbraith, D., Levy, P.E., Sitch, S., Huntingford, C., Cox, P., Williams, M. and Meir, P. 2010. Multiple mechanisms of Amazonian forest biomass losses in three dynamic global vegetation models under climate change. *New Phytologist*. **187**(3), pp.647–665.

Galbraith, D., Malhi, Y., Affum-Baffoe, K., Castanho, A.D.A., Doughty, C.E., Fisher, R.A., Lewis, S.L., Peh, K.S.-H., Phillips, O.L., Quesada, C.A., Sonké, B. and Lloyd, J. 2013. Residence times of woody biomass in tropical forests. *Plant Ecology & Diversity*. **6**(1), pp.139–157.

Gale, N. and Barfod, A.S. 1999. Canopy tree mode of death in a western Ecuadorian rain forest. *Journal of Tropical Ecology*. **15**(4), pp.415–436.

Gale, N. and Hall, P. 2001. Factors determining the modes of tree death in three Bornean rain forests. *Journal of Vegetation Science*. **12**(3), pp.337–346.

Gallagher, R. V. and Leishman, M.R. 2012. A global analysis of trait variation and evolution in climbing plants. *Journal of Biogeography*. **39**(10), pp.1757–1771.

Garcia-Forner, N., Biel, C., Savé, R. and Martínez-Vilalta, J. 2017. Isohydric species are not necessarily more carbon limited than anisohydric species during drought. *Tree Physiology*. **37**(4), pp.441–455.

Gatti, L. V., Gloor, M., Miller, J.B., Doughty, C.E., Malhi, Y., Domingues, L.G., Basso, L.S., Martinewski, A., Correia, C.S.C., Borges, V.F., Freitas, S., Braz, R., Anderson, L.O., Rocha, H., Grace, J., Phillips, O.L. and Lloyd, J. 2014. Drought sensitivity of Amazonian carbon balance revealed by atmospheric measurements. *Nature*. **506**(7486), pp.76–80.

Goldammer, J.G. and Seibert, B. 1989. Natural rain forest fires in Eastern Borneo during the Pleistocene and Holocene. *The Science of Nature*. **76**(11), pp.518–520.

Goldammer, J.G. and Seibert, B. 1990. The impact of droughts and forest fires on tropical lowland rain forest of East Kalimantan *In*: W. D. Billings, F. Golley, O. L. Lange, J. S. Olson and H. Remmert, eds. *Fire in the tropical biota*. Heidelberg: Springer Verlag Berlin, pp.11–31.

Gora, E.M., Bitzer, P.M., Burchfield, J.C., Schnitzer, S.A. and Yanoviak, S.P. 2017. Effects of lightning on trees: A predictive model based on in situ electrical resistivity. *Ecology and Evolution*. **7**(20), pp.8523–8534.

Gora, E.M., Burchfield, J.C., Muller-Landau, H.C., Bitzer, P.M. and Yanoviak, S.P. 2020. Pantropical geography of lightning-caused disturbance and its implications for tropical forests. *Global Change Biology*. **26**(9), pp.5017–5026.

Granzow-de la Cerda, Í., Lloret, F., Ruiz, J.E. and Vandermeer, J.H. 2012. Tree mortality following ENSO-associated fires and drought in lowland rain forests of Eastern Nicaragua. *Forest Ecology and Management*. **265**, pp.248–257.

Gratkowski, H.J. 1956. Windthrow around staggered settings in old-growth Douglas-fir. *Forest Science*. **2**(1), pp.60–74.

Grégoire, J.M., Eva, H.D., Belward, A.S., Palumbo, I., Simonetti, D. and Brink, A. 2013. Effect of land-cover change on Africa's burnt area. *International Journal of Wildland Fire*. **22**(2), pp.107–120.

Grussu, G., Testolin, R., Saulei, S., Farcomeni, A., Yosi, C.K., De Sanctis, M. and Attorre, F. 2016. Optimum plot and sample sizes for carbon stock and biodiversity estimation in the lowland tropical forests of Papua New Guinea. *Forestry*. **89**(2), pp.150–158.

Gu, L., Pallardy, S.G., Hosman, K.P. and Sun, Y. 2015. Drought-influenced mortality of tree species with different predawn leaf water dynamics in a decade-long study of a central US forest. *Biogeosciences*. **12**(10), pp.2831–2845.

Hamilton Jr., D.A. and Edwards, B.M. 1976. *Modeling the probability of individual tree mortality*. Ogden, Utah: Intermountain Forest and Range Experiment Station, Forest Service, U.S. Dept. of Agriculture.

Hammond, D. 2005. *Tropical forests of the Guiana Shield: ancient forests in a modern world*. Wallingford: CABI Pub.

Harris, I., Jones, P.D., Osborn, T.J. and Lister, D.H. 2014. Updated high-resolution grids of monthly climatic observations - the CRU TS3.10 Dataset. *International Journal of Climatology*. **34**(3), pp.623–642.

Hart, T.B., Hart, J.A. and Murphy, P.G. 1989. Monodominant and species-rich forests of the humid tropics: causes for their co-occurrence. *The American Naturalist*. **133**(5), pp.613–633.

Hartmann, H., Moura, C.F., Anderegg, W.R.L., Ruehr, N.K., Salmon, Y., Allen, C.D., Arndt, S.K., Breshears, D.D., Davi, H., Galbraith, D., Ruthrof, K.X., Wunder, J., Adams, H.D., Bloemen, J., Cailleret, M., Cobb, R., Gessler, A., Grams, T.E.E., Jansen, S., Kautz, M., Lloret, F. and O'Brien, M. 2018. Research frontiers for improving our understanding of drought-induced tree and forest mortality. *New Phytologist*. **218**(1), pp.15–28.

Hartmann, H., Ziegler, W., Kolle, O. and Trumbore, S. 2013a. Thirst beats hunger - declining hydration during drought prevents carbon starvation in Norway spruce saplings. *New Phytologist*. **200**(2), pp.340–349.

Hartmann, H., Ziegler, W. and Trumbore, S. 2013b. Lethal drought leads to reduction in nonstructural carbohydrates in Norway spruce tree roots but not in the canopy. *Functional Ecology*. **27**(2), pp.413–427.

van der Heijden, G.M.F., Powers, J.S. and Schnitzer, S.A. 2015. Lianas reduce carbon accumulation and storage in tropical forests. *Proceedings of the National Academy of Sciences*. **112**(43), pp.13267–13271.

Hennon, P.E. and McClellan, M.H. 2003. Tree mortality and forest structure in the temperate rain forests of southeast Alaska. *Canadian Journal of Forest Research*. **33**(9), pp.1621–1634.

Hiernaux, P., Diarra, L., Trichon, V., Mougin, E., Soumaguel, N. and Baup, F. 2009. Woody plant population dynamics in response to climate changes from 1984 to 2006 in Sahel (Gourma, Mali). *Journal of Hydrology*. **375**(1–2), pp.103–113.

Hisano, M., Chen, H.Y.H., Searle, E.B. and Reich, P.B. 2019. Species-rich boreal forests grew more and suffered less mortality than species-poor forests under the environmental change of the past half-century. *Ecology Letters*. **22**(6), pp.999–1008.

Hochberg, U., Rockwell, F.E., Holbrook, N.M. and Cochard, H. 2018. Iso/Anisohydry: A Plant–Environment Interaction Rather Than a Simple Hydraulic Trait. *Trends in Plant Science*. **23**(2), pp.112–120.

Hoffmann, W.A., Geiger, E.L., Gotsch, S.G., Rossatto, D.R., Silva, L.C.R., Lau, O.L., Haridasan, M. and Franco, A.C. 2012a. Ecological thresholds at the savanna-forest boundary: how plant traits, resources and fire govern the distribution of tropical biomes F. Lloret, ed. *Ecology Letters*. **15**(7), pp.759–768.

Hoffmann, W.A., Jaconis, S.Y., Mckinley, K.L., Geiger, E.L., Gotsch, S.G. and Franco, A.C. 2012b. Fuels or microclimate? Understanding the drivers of fire feedbacks at savanna-forest boundaries. *Austral Ecology*. **37**(6), pp.634–643.

Hood, S.M., Varner, J.M., Van Mantgem, P. and Cansler, C.A. 2018. Fire and tree death: Understanding and improving modeling of fire-induced tree mortality. *Environmental Research Letters*. **13**(11).

Hubau, W., Lewis, S.L., Phillips, O.L., Affum-Baffoe, K., Beeckman, H., Cuní-Sanchez, A., Daniels, A.K., Ewango, C.E.N., Fauset, S., Mukinzi, J.M., Sheil, D., Sonké, B., Sullivan, M.J.P., Sunderland, T.C.H., Taedoumg, H., Thomas, S.C., White, L.J.T., Abernethy, K.A., Adu-Bredu, S., Amani, C.A., Baker, T.R., Banin, L.F., Baya, F., Begne, S.K., Bennett, A.C., Benedet, F., Bitariho, R., Bocko, Y.E., Boeckx, P., Boundja, P., Brienen, R.J.W., Brncic, T., Chezeaux, E., Chuyong, G.B., Clark, C.J., Collins, M., Comiskey, J.A., Coomes, D.A., Dargie, G.C., de Haulleville, T., Kamdem, M.N.D., Doucet, J.-L., Esquivel-Muelbert, A., Feldpausch, T.R., Fofanah, A., Foli, E.G., Gilpin, M., Gloor, E., Gonmadje, C., Gourlet-Fleury, S., Hall, J.S., Hamilton, A.C., Harris, D.J., Hart, T.B., Hockemba, M.B.N., Hladik, A., Ifo, S.A., Jeffery, K.J., Jucker, T., Yakusu, E.K., Kearsley, E., Kenfack, D., Koch, A., Leal, M.E., Levesley, A., Lindsell, J.A., Lisingo, J., Lopez-Gonzalez, G., Lovett, J.C., Makana, J.-R., Malhi, Y., Marshall, A.R., Martin, J., Martin, E.H., Mbayu, F.M., Medjibe, V.P., Mihindou, V., Mitchard, E.T.A., Moore, S., Munishi, P.K.T., Bengone, N.N., Ojo, L., Ondo, F.E., Peh, K.S.-H., Pickavance, G.C., Poulsen, A.D., Poulsen, J.R., Qie, L., Reitsma, J., Rovero, F., Swaine, M.D., Talbot, J., Taplin, J., Taylor, D.M., Thomas, D.W., Toirambe, B., Mukendi, J.T., Tuagben, D., Umunay, P.M., van der Heijden, G.M.F., Verbeeck, H., Vleminckx, J., Willcock, S., Wöll, H., Woods, J.T. and Zemagho, L. 2020. Asynchronous carbon sink saturation in African and Amazonian tropical forests. *Nature*. **579**(7797), pp.80–87.

Ingwell, L.L., Wright, S.J., Becklund, K.K., Hubbell, S.P. and Schnitzer, S.A. 2010. The impact of lianas on 10 years of tree growth and mortality on Barro Colorado Island, Panama. *Journal of Ecology*. **98**(4), pp.879–887.

Itoh, A., Nanami, S., Harata, T., Ohkubo, T., Tan, S., Chong, L., Davies, S.J. and Yamakura, T.

2012. The Effect of Habitat Association and Edaphic Conditions on Tree Mortality during El Niño-induced Drought in a Bornean Dipterocarp Forest. *Biotropica*. **44**(5), pp.606–617.

Jackson, W.D. 1968. Fire, air, water and earth - an elemental ecology of Tasmania. *The Proceedings of the Ecological Society of Australia*. **3**, pp.9–16.

Johnson, D.M., Domec, J.-C., Woodruff, D.R., McCulloh, K.A. and Meinzer, F.C. 2013. Contrasting hydraulic strategies in two tropical lianas and their host trees. *American Journal of Botany*. **100**(2), pp.374–383.

Johnson, M.O., Galbraith, D., Gloor, M., De Deurwaerder, H., Guimberteau, M., Rammig, A., Thonicke, K., Verbeeck, H., von Randow, C., Monteagudo, A., Phillips, O.L., Brienen, R.J.W., Feldpausch, T.R., Lopez Gonzalez, G., Fauset, S., Quesada, C.A., Christoffersen, B., Ciais, P., Sampaio, G., Kruijt, B., Meir, P., Moorcroft, P., Zhang, K., Alvarez-Davila, E., Alves de Oliveira, A., Amaral, I., Andrade, A., Aragao, L.E.O.C., Araujo-Murakami, A., Arets, E.J.M.M., Arroyo, L., Aymard, G.A., Baraloto, C., Barroso, J., Bonal, D., Boot, R., Camargo, J., Chave, J., Cogollo, A., Cornejo Valverde, F., Lola da Costa, A.C., Di Fiore, A., Ferreira, L., Higuchi, N., Honorio, E.N., Killeen, T.J., Laurance, S.G., Laurance, W.F., Licona, J., Lovejoy, T., Malhi, Y., Marimon, B., Marimon, B.H., Matos, D.C.L., Mendoza, C., Neill, D.A., Pardo, G., Peña-Claros, M., Pitman, N.C.A., Poorter, L., Prieto, A., Ramirez-Angulo, H., Roopsind, A., Rudas, A., Salomao, R.P., Silveira, M., Stropp, J., ter Steege, H., Terborgh, J., Thomas, R., Toledo, M., Torres-Lezama, A., van der Heijden, G.M.F., Vasquez, R., Guimarães Vieira, I.C., Vilanova, E., Vos, V.A. and Baker, T.R. 2016. Variation in stem mortality rates determines patterns of above-ground biomass in Amazonian forests: implications for dynamic global vegetation models. *Global Change Biology*. **22**(12), pp.3996–4013.

Jones, J.L., Webb, B.W., Butler, B.W., Dickinson, M.B., Jimenez, D., Reardon, J. and Bova, A.S. 2006. Prediction and measurement of thermally induced cambial tissue necrosis in tree stems. *International Journal of Wildland Fire*. **15**(1), p.3.

Kannenberg, S.A., Novick, K.A. and Phillips, R.P. 2018. Coarse roots prevent declines in whole-tree non-structural carbohydrate pools during drought in an isohydric and an anisohydric species. *Tree Physiology*. **38**(4), pp.582–590.

Kearsley, E., de Haulleville, T., Hufkens, K., Kidimbu, A., Toirambe, B., Baert, G., Huygens, D., Kebede, Y., Defourny, P., Bogaert, J., Beeckman, H., Steppe, K., Boeckx, P. and Verbeeck, H. 2013. Conventional tree height–diameter relationships significantly overestimate aboveground carbon stocks in the Central Congo Basin. *Nature Communications*. **4**(2269), pp.1–8.

King, D.A., Davies, S.J. and Nur Supardi, M.N. 2006. Growth and mortality are related to adult tree size in a Malaysian mixed dipterocarp forest. *Forest Ecology and Management*. **223**(1–3), pp.152–158.

Klockow, P.A., Vogel, J.G., Edgar, C.B. and Moore, G.W. 2018. Lagged mortality among tree species four years after an exceptional drought in east Texas. *Ecosphere*. **9**(10).

Köhl, M., Lister, A., Scott, C.T., Baldauf, T. and Plugge, D. 2011. Implications of sampling design and sample size for national carbon accounting systems. *Carbon Balance and Management*. **6**, pp.1–20.

Körner, C. 2017. A matter of tree longevity. *Science*. **355**(6321), pp.130–131.

Kruschke, J.K. 2015. *Doing Bayesian Data Analysis* 2nd ed. Oxford, UK: Elsevier.

Kubo, T., Kohyama, T., Potts, M.D. and Ashton, P.S. 2000. Mortality rate estimation when inter-census intervals vary. *Journal of Tropical Ecology*. **16**(5), pp.753–756.

Laurance, S.G.W., Laurance, W.F., Nascimento, H.E.M., Andrade, A., Fearnside, P.M., Rebello, E.G.R. and Condit, R. 2009. Long-term variation in Amazon forest dynamics. *Journal of Vegetation Science*. **20**(2), pp.323–333.

Laurance, W.F., Andrade, A.S., Magrach, A., Camargo, J.L.C., Valsko, J.J., Campbell, M., Fearnside, P.M., Edwards, W., Lovejoy, T.E. and Laurance, S.G. 2014. Long-term changes in liana abundance and forest dynamics in undisturbed Amazonian forests. *Ecology*. **95**(6), pp.1604–1611.

Laurance, W.F., Laurance, S.G., Ferreira, L. V, Rankin-de Merona, J.M., Gascon, C. and Lovejoy, T.E. 1997. Biomass collapse in Amazonian forest fragments. *Science*. **278**(5340), pp.1117–1118.

Laurance, W.F., Nascimento, H.E.M., Laurance, S.G., Condit, R., D'Angelo, S. and Andrade, A. 2004. Inferred longevity of Amazonian rainforest trees based on a long-term demographic study. *Forest Ecology and Management*. **190**(2–3), pp.131–143.

Laurance, W.F., Perez-Salicrup, D., Delamonica, P., Fearnside, P.M., D'Angelo, S., Jerozolinski, A., Pohl, L. and Lovejoy, T.E. 2001. Rain Forest Fragmentation and the Structure of Amazonian Liana Communities. *Ecology*. **82**(1), p.105.

Laurance, W.F. and Williamson, G.B. 2001. Positive feedbacks among forest fragmentation, drought, and climate change in the Amazon. *Conservation Biology*. **15**(6), pp.1529–1535.

Lawes, M.J., Adie, H., Russell-Smith, J., Murphy, B. and Midgley, J.J. 2011. How do small savanna trees avoid stem mortality by fire? the roles of stem diameter, height and bark thickness. *Ecosphere*. **2**(4), pp.1–13.

Lewis, S.L., Lopez-Gonzalez, G., Sonké, B., Affum-Baffoe, K., Baker, T.R., Ojo, L.O., Phillips, O.L., Reitsma, J.M., White, L., Comiskey, J. a, Djuikouo K, M.-N., Ewango, C.E.N., Feldpausch, T.R., Hamilton, A.C., Gloor, M., Hart, T., Hladik, A., Lloyd, J., Lovett, J.C., Makana, J.-R., Malhi, Y., Mbago, F.M., Ndangalasi, H.J., Peacock, J., Peh, K.S.-H., Sheil, D., Sunderland, T., Swaine, M.D., Taplin, J., Taylor, D., Thomas, S.C., Votere, R. and Wöll, H. 2009. Increasing carbon storage in intact African tropical forests. *Nature*. **457**(7232), pp.1003–1006.

Lewis, S.L., Malhi, Y. and Phillips, O.L. 2004a. Fingerprinting the impacts of global change on tropical forests. *Philosophical Transactions of the Royal Society B: Biological Sciences*. **359**(1443), pp.437–462.

Lewis, S.L., Phillips, O.L., Baker, T.R., Lloyd, J., Malhi, Y., Almeida, S., Higuchi, N., Laurance, W.F., Neill, D.A., Silva, J.N.M.M., Terborgh, J., Torres Lezama, A., Vásquez Martinez, R., Brown, S., Chave, J., Kuebler, C., Núñez Vargas, P. and Vinceti, B. 2004b. Concerted changes in tropical forest structure and dynamics: evidence from 50 South American long-term plots Y. Malhi & O. L. Phillips, eds. *Philosophical Transactions of the Royal Society of London. Series B: Biological Sciences*. **359**(1443), pp.421–436.

Lewis, S.L., Phillips, O.L., Sheil, D., Vinceti, B., Baker, T.R., Brown, S., Graham, A.W., Higuchi, N., Hilbert, D.W., Laurance, W.F., Lejoly, J., Malhi, Y., Monteagudo, A., Nuñéz Vargas, P., Sonké, B., Nur Supardi, M.N., Terborgh, J.W. and Vásquez Martínez, R. 2004c. Tropical forest tree mortality, recruitment and turnover rates: calculation, interpretation and comparison when census intervals vary. *Journal of Ecology*. **92**(6), pp.929–944.

Lewis, S.L., Sonké, B., Sunderland, T., Begne, S.K., Lopez-Gonzalez, G., van der Heijden, G.M.F., Phillips, O.L., Affum-Baffoe, K., Baker, T.R., Banin, L., Bastin, J.-F., Beeckman, H., Boeckx, P., Bogaert, J., De Cannière, C., Chezeaux, E., Clark, C.J., Collins, M.,

Djagbletey, G., Djuikouo, M.N.K., Droissart, V., Doucet, J.-L., Ewango, C.E.N., Fauset, S., Feldpausch, T.R., Foli, E.G., Gillet, J.-F., Hamilton, A.C., Harris, D.J., Hart, T.B., de Haulleville, T., Hladik, A., Hufkens, K., Huygens, D., Jeanmart, P., Jeffery, K.J., Kearsley, E., Leal, M.E., Lloyd, J., Lovett, J.C., Makana, J.-R., Malhi, Y., Marshall, A.R., Ojo, L., Peh, K.S.-H., Pickavance, G., Poulsen, J.R., Reitsma, J.M., Sheil, D., Simo, M., Steppe, K., Taedoumg, H.E., Talbot, J., Taplin, J.R.D., Taylor, D., Thomas, S.C., Toirambe, B., Verbeeck, H., Vleminckx, J., White, L.J.T., Willcock, S., Woell, H. and Zemagho, L. 2013. Above-ground biomass and structure of 260 African tropical forests. *Philosophical Transactions of the Royal Society B: Biological Sciences*. **368**(1625), p.20120295.

Lines, E.R., Coomes, D.A. and Purves, D.W. 2010. Influences of forest structure, climate and species composition on tree mortality across the eastern US. *PLoS ONE*. **5**(10), p.e13212.

Lloyd, J. and Farquhar, G.D. 2008. Effects of rising temperatures and [CO_2] on the physiology of tropical forest trees. *Philosophical Transactions of the Royal Society B: Biological Sciences*. **363**(1498), pp.1811–1817.

Lloyd, J., Gloor, E.U. and Lewis, S.L. 2009. Are the dynamics of tropical forests dominated by large and rare disturbance events? *Ecology Letters*. **12**(12), pp.E19–E21.

Lopez-Gonzalez, G., Lewis, S.L., Phillips, O.L. and Burkitt, M. 2013. ForestPlots.net Database. Available from: www.forestplots.net.

Lugo, A.E. and Scatena, F.N. 1996. Background and catastrophic tree mortality in tropical moist, wet and rain forests. *Biotropica*. **28**(4a), pp.585–599.

Lyons, W.A., Nelson, T.E., Williams, E.R., Cramer, J.A. and Turner, T.R. 1998. Enhanced Positive Cloud-to-Ground Lightning in Thunderstorms Ingesting Smoke from Fires. *Science*. **282**(5386), pp.77–80.

Ma, Z., Peng, C., Zhu, Q., Chen, H., Yu, G., Li, W., Zhou, X., Wang, W. and Zhang, W. 2012. Regional drought-induced reduction in the biomass carbon sink of Canada's boreal forests. *Proceedings of the National Academy of Sciences of the United States of America*. **109**(7), pp.2423–2427.

MacAllister, S., Mencuccini, M., Sommer, U., Engel, J., Hudson, A., Salmon, Y. and Dexter, K.G. 2019. Drought-induced mortality in Scots pine: opening the metabolic black box. *Tree physiology*. **39**(8), pp.1358–1370.

Mackay, D.S., Roberts, D.E., Ewers, B.E., Sperry, J.S., McDowell, N.G. and Pockman, W.T. 2015. Interdependence of chronic hydraulic dysfunction and canopy processes can improve integrated models of tree response to drought. *Water Resources Research*. **51**(8), pp.6156–6176.

Magnabosco Marra, D., Trumbore, S.E., Higuchi, N., Ribeiro, G.H.P.M., Negrón-Juárez, R.I., Holzwarth, F., Rifai, S.W., dos Santos, J., Lima, A.J.N., Kinupp, V.F., Chambers, J.Q. and Wirth, C. 2018. Windthrows control biomass patterns and functional composition of Amazon forests. *Global Change Biology*. **24**(12), pp.5867–5881.

Magnusson, W.E., Lima, A.P. and De Lima, O. 1996. Group lightning mortality of trees in a Neotropical forest. *Journal of Tropical Ecology*. **12**(06), pp.899–903.

Malhi, Y., Aragão, L.E.O.C., Galbraith, D., Huntingford, C., Fisher, R., Zelazowski, P., Sitch, S., McSweeney, C. and Meir, P. 2009. Exploring the likelihood and mechanism of a climate-change-induced dieback of the Amazon rainforest. *Proceedings of the National Academy of Sciences of the United States of America*. **106**(49), pp.20610–20615.

Malhi, Y., Phillips, O.L., Lloyd, J., Baker, T., Wright, J., Almeida, S., Arroyo, L., Frederiksen, T., Grace, J., Higuchi, N., Killeen, T., Laurance, W.F., Leaño, C., Lewis, S., Meir, P., Monteagudo, A., Neill, D., Núñez Vargas, P., Panfil, S.N., Patiño, S., Pitman, N., Quesada, C.A., Rudas-Ll., A., Salomão, R., Saleska, S., Silva, N., Silveira, M., Sombroek, W.G., Valencia, R., Vásquez Martínez, R., Vieira, I.C.G. and Vinceti, B. 2002. An international network to monitor the structure, composition and dynamics of Amazonian forests (RAINFOR). *Journal of Vegetation Science*. **13**(3), pp.439–450.

Malhi, Y. and Wright, J. 2004. Spatial patterns and recent trends in the climate of tropical rainforest regions. *Philosophical Transactions of the Royal Society B: Biological Sciences*. **359**(1443), pp.311–329.

van Mantgem, P.J. and Stephenson, N.L. 2007. Apparent climatically induced increase of tree mortality rates in a temperate forest. *Ecology Letters*. **10**(10), pp.909–916.

Maréchaux, I. and Chave, J. 2017. An individual-based forest model to jointly simulate carbon and tree diversity in Amazonia: description and applications. *Ecological Monographs*. **87**(4), pp.632–664.

Marengo, J.A., Chou, S.C., Kay, G., Alves, L.M., Pesquero, J.F., Soares, W.R., Santos, D.C., Lyra, A.A., Sueiro, G., Betts, R., Chagas, D.J., Gomes, J.L., Bustamante, J.F. and Tavares, P. 2012. Development of regional future climate change scenarios in South America using the Eta CPTEC/HadCM3 climate change projections: Climatology and regional analyses for the Amazon, São Francisco and the Paraná River basins. *Climate Dynamics*. **38**(9–10), pp.1829–1848.

Marengo, J.A., Nobre, C.A., Tomasella, J., Oyama, M.D., de Oliveira, G.S., de Oliveira, R., Camargo, H., Alves, L.M. and Brown, I.F. 2008. The drought of Amazonia in 2005. *Journal of Climate*. **21**(3), pp.495–516.

Marengo, J.A., Tomasella, J., Alves, L.M., Soares, W.R. and Rodriguez, D.A. 2011. The drought of 2010 in the context of historical droughts in the Amazon region. *Geophysical Research Letters*. **38**(L12703), pp.1–5.

Marimon, B.S., Marimon-Junior, B.H., Feldpausch, T.R., Oliveira-Santos, C., Mews, H.A., Lopez-Gonzalez, G., Lloyd, J., Franczak, D.D., de Oliveira, E.A., Maracahipes, L., Miguel, A., Lenza, E. and Phillips, O.L. 2014. Disequilibrium and hyperdynamic tree turnover at the forest-cerrado transition zone in southern Amazonia. *Plant Ecology and Diversity*. **7**(1–2), pp.281–292.

Marshall, A.R., Coates, M.A., Archer, J., Kivambe, E., Mnendendo, H., Mtoka, S., Mwakisoma, R., de Figueiredo, R.J.R.L.R.L. and Njilima, F.M. 2017. Liana cutting for restoring tropical forests: a rare palaeotropical trial. *African Journal of Ecology*. **55**(3), pp.282–297.

Martinez-Vilalta, J., Anderegg, W.R.L., Sapes, G. and Sala, A. 2019. Greater focus on water pools may improve our ability to understand and anticipate drought-induced mortality in plants. *New Phytologist*. **223**(1), pp.22–32.

Martini, A.M.Z., Lima, R.A.F., Franco, G.A.D.C. and Rodrigues, R.R. 2008. The need for full inventories of tree modes of disturbance to improve forest dynamics comprehension: An example from a semideciduous forest in Brazil. *Forest Ecology and Management*. **255**(5–6), pp.1479–1488.

McDowell, N., Pockman, W.T., Allen, C.D., Breshears, D.D., Cobb, N., Kolb, T., Plaut, J., Sperry, J., West, A., Williams, D.G. and Yepez, E.A. 2008. Mechanisms of plant survival and mortality during drought: why do some plants survive while others succumb to drought? *New Phytologist*. **178**(4), pp.719–739.

McDowell, N.G. 2011. Mechanisms linking drought, hydraulics, carbon metabolism, and vegetation mortality. *Plant Physiology*. **155**(3), pp.1051–1059.

McDowell, N.G., Beerling, D.J., Breshears, D.D., Fisher, R.A., Raffa, K.F. and Stitt, M. 2011. The interdependence of mechanisms underlying climate-driven vegetation mortality. *Trends in Ecology and Evolution*. **26**(10), pp.523–532.

McElreath, R. 2016. *Statistical Rethinking: A Bayesian Course with Examples in R and Stan Richard McElreath CRC Press, 2015, 469 pages, £67.99, hardcover ISBN: 978-1-482-25344-3*. Boca Raton, FL: Taylor & Francis.

McMahon, S.M., Arellano, G. and Davies, S.J. 2019. The importance and challenges of detecting changes in forest mortality rates. *Ecosphere*. **10**(2).

Meir, P., Mencuccini, M. and Dewar, R.C. 2015. Drought-related tree mortality: addressing the gaps in understanding and prediction. *New Phytologist*. **207**(1), pp.28–33.

Meir, P. and Woodward, F.I. 2010. Amazonian rain forests and drought: response and vulnerability. *New Phytologist*. **187**(3), pp.553–557.

Mencuccini, M., Martínez-Vilalta, J., Vanderklein, D., Hamid, H.A., Korakaki, E., Lee, S. and Michiels, B. 2005. Size-mediated ageing reduces vigour in trees. *Ecology Letters*. **8**(11), pp.1183–1190.

Mencuccini, M., Minunno, F., Salmon, Y., Martínez-Vilalta, J. and Hölttä, T. 2015. Coordination of physiological traits involved in drought-induced mortality of woody plants. *New Phytologist*. **208**(2), pp.396–409.

Michaletz, S.T. and Johnson, E.A. 2007. How forest fires kill trees: A review of the fundamental biophysical processes. *Scandinavian Journal of Forest Research*. **22**(6), pp.500–515.

Michaletz, S.T., Johnson, E.A. and Tyree, M.T. 2012. Moving beyond the cambium necrosis hypothesis of post-fire tree mortality: Cavitation and deformation of xylem in forest fires. *New Phytologist*. **194**(1), pp.254–263.

Michna, P. and Woods, M. 2011. RNetCDF: Interface to 'NetCDF' Datasets.

Misson, L., Rocheteau, A., Rambal, S., Ourcival, J.M., Limousin, J.M. and Rodriguez, R. 2010. Functional changes in the control of carbon fluxes after 3 years of increased drought in a Mediterranean evergreen forest? *Global Change Biology*. **16**(9), pp.2461–2475.

Mitchard, E.T.A. 2018. The tropical forest carbon cycle and climate change. *Nature*. **559**(7715), pp.527–534.

Mitchell, P.J., O'Grady, A.P., Tissue, D.T., White, D.A., Ottenschlaeger, M.L. and Pinkard, E.A. 2013. Drought response strategies define the relative contributions of hydraulic dysfunction and carbohydrate depletion during tree mortality. *New Phytologist*. **197**(3), pp.862–872.

Mitton, J.B. and Grant, M.C. 1996. Genetic variation and the natural history of quaking aspen. *BioScience*. **46**(1), pp.25–31.

Moore, G.W., Edgar, C.B., Vogel, J.G., Washington-Allen, R.A., March, R.G. and Zehnder, R. 2016. Tree mortality from an exceptional drought spanning mesic to semiarid ecoregions. *Ecological Applications*. **26**(2), pp.602–611.

Moser, G., Schuldt, B., Hertel, D., Horna, V., Coners, H., Barus, H. and Leuschner, C. 2014. Replicated throughfall exclusion experiment in an Indonesian perhumid rainforest: Wood production, litter fall and fine root growth under simulated drought. *Global Change Biology*. **20**(5), pp.1481–1497.

Moser, P., Simon, M.F., Medeiros, M.B., Gontijo, A.B. and Costa, F.R.C. 2019. Interaction between extreme weather events and mega-dams increases tree mortality and alters functional status of Amazonian forests C. Macinnis-Ng, ed. *Journal of Applied Ecology*. **56**, pp.2641–2651.

Mueller-Dombois, D. 1986. Perspectives for an etiology of stand-level dieback. *Annual Review of Ecology and Systematics*. **17**, pp.221–243.

Mueller, R.C., Scudder, C.M., Porter, M.E., Talbot Trotter, R.I., Gehring, C.A. and Whitham, T.G. 2005. Differential tree mortality in response to severe drought: evidence for long-term vegetation shifts. *Journal of Ecology*. **93**(6), pp.1085–1093.

Muller-Landau, H.C. 2004. Interspecific and inter-site variation in wood specific gravity of tropical trees. *Biotropica*. **36**(1), pp.20–32.

Munné-Bosch, S. 2014. Perennial roots to immortality. *Plant Physiology*. **166**(2), pp.720–725.

Murphy, H.T., Bradford, M.G., Dalongeville, A., Ford, A.J. and Metcalfe, D.J. 2013. No evidence for long-term increases in biomass and stem density in the tropical rain forests of Australia F. Gilliam, ed. *Journal of Ecology*. **101**(6), pp.1589–1597.

Nakagawa, M., Tanaka, K., Nakashizuka, T., Ohkubo, T., Kato, T., Maeda, T., Sato, K., Miguchi, H., Nagamasu, H., Ogino, K., Teo, S., Hamid, A.A. and Seng, L.H. 2000. Impact of severe drought associated with the 1997–1998 El Niño in a tropical forest in Sarawak. *Journal of Tropical Ecology*. **16**(3), pp.355–367.

Naumann, G., Alfieri, L., Wyser, K., Mentaschi, L., Betts, R.A., Carrao, H., Spinoni, J., Vogt, J. and Feyen, L. 2018. Global Changes in Drought Conditions Under Different Levels of Warming. *Geophysical Research Letters*. **45**(7), pp.3285–3296.

Negrón-Juárez, R.I., Chambers, J.Q., Guimaraes, G., Zeng, H., Raupp, C.F.M., Marra, D.M., Ribeiro, G.H.P.M., Saatchi, S.S., Nelson, B.W. and Higuchi, N. 2010. Widespread Amazon forest tree mortality from a single cross-basin squall line event. *Geophysical Research Letters*. **37**(16), p.L16701.

Negrón-Juárez, R.I., Holm, J.A., Marra, D.M., Rifai, S.W., Riley, W.J., Chambers, J.Q., Koven, C.D., Knox, R.G., McGroddy, M.E., Di Vittorio, A. V., Urquiza-Muñoz, J., Tello-Espinoza, R., Muñoz, W.A., Ribeiro, G.H.P.M. and Higuchi, N. 2018. Vulnerability of Amazon forests to storm-driven tree mortality. *Environmental Research Letters*. **13**(5).

Nelson, B.W., Kapos, V., Adams, J.B., Oliveira, W.J. and Braun, O.P.G. 1994. Forest disturbance by large blowdowns in the Brazilian Amazon. *Ecology*. **75**(3), pp.853–858.

Nepstad, D.C., Tohver, I.M., Ray, D., Moutinho, P. and Cardinot, G. 2007. Mortality of large trees and lianas following experimental drought in an Amazon forest. *Ecology*. **88**(9), pp.2259–2269.

Newbery, D.M., Kennedy, D.N., Petol, G.H., Madani, L. and Ridsdale, C.E. 1999. Primary forest dynamics in lowland dipterocarp forest at Danum Valley, Sabah, Malaysia, and the role of the understorey. *Philosophical Transactions of the Royal Society B: Biological Sciences*. **354**(1391), pp.1763–1782.

Nicholson, S.E., Some, B. and Kone, B. 2000. An analysis of recent rainfall conditions in West Africa, including the rainy seasons of the 1997 El Niño and the 1998 La Niña years. *Journal of Climate*. **13**(14), pp.2628–2640.

van Nieuwstadt, M.G.L. and Sheil, D. 2005. Drought, fire and tree survival in a Borneo rain forest, East Kalimantan, Indonesia. *Journal of Ecology*. **93**(1), pp.191–201.

Nolan, R.H., Tarin, T., Santini, N.S., McAdam, S.A.M., Ruman, R. and Eamus, D. 2017.

Differences in osmotic adjustment, foliar abscisic acid dynamics, and stomatal regulation between an isohydric and anisohydric woody angiosperm during drought. *Plant Cell and Environment*. **40**(12), pp.3122–3134.

O'Brien, S.T., Hayden, B.P. and Shugart, H.H. 1992. Global climatic change, hurricanes, and a tropical forest. *Climatic Change*. **22**(3), pp.175–190.

O'Grady, A.P., Mitchell, P.J.M., Pinkard, E.A. and Tissue, D.T. 2013. Thirsty roots and hungry leaves: Unravelling the roles of carbon and water dynamics in tree mortality. *New Phytologist*. **200**(2), pp.294–297.

Oliveira, A.P. de and Felfili, J.M. 2008. Dinâmica da comunidade arbórea de uma mata de galeria do Brasil Central em um período de 19 anos (1985-2004). *Revista Brasileira de Botânica*. **31**(4), pp.597–610.

Pan, Y., Birdsey, R.A., Fang, J., Houghton, R., Kauppi, P.E., Kurz, W.A., Phillips, O.L., Shvidenko, A., Lewis, S.L., Canadell, J.G., Ciais, P., Jackson, R.B., Pacala, S.W., McGuire, Ad.D., Piao, S., Rautiainen, A., Sitch, S. and Hayes, D. 2011. A Large and Persistent Carbon Sink in the World's Forests. *Science*. **333**, pp.988–993.

Papaik, M.J. and Canham, C.D. 2006. Species resistance and community response to wind disturbance regimes in northern temperate forests. *Journal of Ecology*. **94**(5), pp.1011–1026.

Papaik, M.J., Canham, C.D., Latty, E.F. and Woods, K.D. 2005. Effects of an introduced pathogen on resistance to natural disturbance: Beech bark disease and windthrow. *Canadian Journal of Forest Research*. **35**(8), pp.1832–1843.

Parolari, A.J., Katul, G.G. and Porporato, A. 2014. An ecohydrological perspective on drought-induced forest mortality. *Journal of Geophysical Research: Biogeosciences*. **119**(5), pp.965–981.

Paul, G.S. and Yavitt, J.B. 2011. Tropical Vine Growth and the Effects on Forest Succession: A Review of the Ecology and Management of Tropical Climbing Plants. *The Botanical Review*. **77**(1), pp.11–30.

Peh, K.S.-H., Sonké, B., Lloyd, J., Quesada, C.A. and Lewis, S.L. 2011. Soil does not explain monodominance in a Central African tropical forest. *PLoS ONE*. **6**(2), p.e16996.

Pellegrini, A.F.A., Anderegg, W.R.L., Paine, C.E.T., Hoffmann, W.A., Kartzinel, T., Rabin, S.S., Sheil, D., Franco, A.C. and Pacala, S.W. 2017. Convergence of bark investment according to fire and climate structures ecosystem vulnerability to future change. *Ecology Letters*. **20**(3), pp.307–316.

Peng, C., Ma, Z., Lei, X., Zhu, Q., Chen, H., Wang, W., Liu, S., Li, W., Fang, X. and Zhou, X. 2011. A drought-induced pervasive increase in tree mortality across Canada's boreal forests. *Nature Climate Change*. **1**(9), pp.467–471.

Phillips, O.L., Aragão, L.E.O.C., Lewis, S.L., Fisher, J.B., Lloyd, J., López-González, G., Malhi, Y., Monteagudo, A., Peacock, J., Quesada, C.A., van der Heijden, G., Almeida, S., Amaral, I., Arroyo, L., Aymard, G., Baker, T.R., Bánki, O., Blanc, L., Bonal, D., Brando, P., Chave, J., de Oliveira, A.C.A., Cardozo, N.D., Czimczik, C.I., Feldpausch, T.R., Freitas, M.A., Gloor, E., Higuchi, N., Jiménez, E., Lloyd, G., Meir, P., Mendoza, C., Morel, A., Neill, D.A., Nepstad, D., Patino, S., Peñuela, M.C., Prieto, A., Ramírez, F., Schwarz, M., Silva, J., Silveira, M., Thomas, A.S., Steege, H. ter, Stropp, J., Vasquez, R., Zelazowski, P., Dávila, E.A., Andelman, S., Andrade, A., Chao, K.-J., Erwin, T., Di Fiore, A., Honorio C., E., Keeling, H., Killeen, T.J., Laurance, W.F., Cruz, A.P., Pitman, N.C.A., Vargas, P.N., Ramírez-Angulo, H., Rudas, A., Salamão, R., Silva, N., Terborgh, J. and Torres-Lezama, A. 2009. Drought Sensitivity of the Amazon Rainforest. *Science*. **323**(5919), pp.1344–

1347.

Phillips, O.L., Baker, T.R., Arroyo, L., Higuchi, N., Killeen, T.J., Laurance, W.F., Lewis, S.L., Lloyd, J., Malhi, Y., Monteagudo, A., Neill, D.A., Núñez Vargas, P., Silva, J.N.M., Terborgh, J., Vásquez Martínez, R., Alexiades, M., Almeida, S., Brown, S., Chave, J., Comiskey, J.A., Czimczik, C.I., Di Fiore, A., Erwin, T., Kuebler, C., Laurance, S.G., Nascimento, H.E.M., Olivier, J., Palacios, W., Patiño, S., Pitman, N.C.Q., Quesada, C.A., Saldias, M., Lezama, A.T. and Vinceti, B. 2004. Pattern and process in Amazon tree turnover, 1976-2001. *Philosophical Transactions of the Royal Society B: Biological Sciences*. **359**(1443), pp.381–407.

Phillips, O.L. and Gentry, A.H. 1994. Increasing turnover through time in tropical forests. *Science*. **263**(5149), pp.954–958.

Phillips, O.L., Hall, P., Gentry, A.H., Sawyer, S.A. and Vásquez, R. 1994. Dynamics and species richness of tropical rain forests. *Proceedings of the National Academy of Sciences of the United States of America*. **91**(7), pp.2805–2809.

Phillips, O.L., van der Heijden, G., Lewis, S.L., López-González, G., Aragão, L.E.O.C., Lloyd, J., Malhi, Y., Monteagudo, A., Almeida, S., Dávila, E.A., Amaral, I., Andelman, S., Andrade, A., Arroyo, L., Aymard, G., Baker, T.R., Blanc, L., Bonal, D., de Oliveira, Á.C.A., Chao, K.-J., Cardozo, N.D., da Costa, L., Feldpausch, T.R., Fisher, J.B., Fyllas, N.M., Freitas, M.A., Galbraith, D., Gloor, E., Higuchi, N., Honorio, E., Jiménez, E., Keeling, H., Killeen, T.J., Lovett, J.C., Meir, P., Mendoza, C., Morel, A., Vargas, P.N., Patiño, S., Peh, K.S., Cruz, A.P., Prieto, A., Quesada, C.A., Ramírez, F., Ramírez, H., Rudas, A., Salamão, R., Schwarz, M., Silva, J., Silveira, M., Ferry Slik, J.W., Sonké, B., Thomas, A.S., Stropp, J., Taplin, J.R.D., Vásquez, R. and Vilanova, E. 2010. Drought-mortality relationships for tropical forests. *New Phytologist*. **187**(3), pp.631–646.

Phillips, O.L., Lewis, S.L., Baker, T.R., Chao, K.J. and Higuchi, N. 2008. The changing Amazon forest. *Philosophical Transactions of the Royal Society B: Biological Sciences*. **363**(1498), pp.1819–1827.

Phillips, O.L., Malhi, Y., Higuchi, N., Laurance, W.F., Núñez, P. V., Vásquez, R.M., Laurance, S.G., Ferreira, L. V., Stern, M., Brown, S. and Grace, J. 1998. Changes in the Carbon Balance of Tropical Forests: Evidence from Long-Term Plots. *Science*. **282**(5388), pp.439–442.

Phillips, O.L., Martínez, R.V., Vargas, P.N., Monteagudo, A.L., Zans, M.E.C., Sánchez, W.G., Cruz, A.P., Timaná, M., Yli-Halla, M. and Rose, S. 2003. Efficient plot-based floristic assessment of tropical forests. *Journal of Tropical Ecology*. **19**(6), pp.629–645.

Phillips, O.L., Vásquez Martínez, R., Arroyo, L., Baker, T.R., Killeen, T., Lewis, S.L., Malhi, Y., Monteagudo Mendoza, A., Neill, D., Núñez Vargas, P., Alexiades, M., Cerón, C., Di Fiore, A., Erwin, T., Jardim, A., Palacios, W., Saldias, M. and Vinceti, B. 2002. Increasing dominance of large lianas in Amazonian forests. *Nature*. **418**(6899), pp.770–774.

Phillips, O.L., Vásquez Martínez, R., Monteagudo Mendoza, A., Baker, T.R. and Núñez Vargas, P. 2005. Large lianas as hyperdynamic elements of the tropical forest canopy. *Ecology*. **86**(5), pp.1250–1258.

Plaut, J.A., Yepez, E.A., Hill, J., Pangle, R., Sperry, J.S., Pockman, W.T. and Mcdowell, N.G. 2012. Hydraulic limits preceding mortality in a piñon-juniper woodland under experimental drought. *Plant, Cell and Environment*. **35**(9), pp.1601–1617.

Poorter, L., McNeil, A., Hurtado, V.-H., Prins, H.H.T. and Putz, F.E. 2014. Bark traits and life-history strategies of tropical dry- and moist forest trees K. Kitajima, ed. *Functional*

Ecology. **28**(1), pp.232–242.

Poulsen, J.R., Koerner, S.E., Miao, Z., Medjibe, V.P., Banak, L.N. and White, L.J.T. 2017. Forest structure determines the abundance and distribution of large lianas in Gabon. *Global Ecology and Biogeography*. **26**(4), pp.472–485.

Price, C. and Rind, D. 1994. Possible implications of global climate change on global lightning distributions and frequencies. *Journal of Geophysical Research*. **99**(D5), pp.10823–10831.

Price, M. 2017. Tallying the tropical toll on trees from lightning. *Science*. **356**(6344), p.1222.

Primack, R.B. and Corlett, R. 2005. *Tropical rain forests: an ecological and biogeographical comparison*. Oxford: Blackwell.

Purves, D. and Lyutsarev, V. 2011. Filzbach.

Putz, F.E. 1984. How trees avoid and shed lianas. *Biotropica*. **16**(1), pp.19–23.

Putz, F.E., Coley, P.D., Lu, K., Montalvo, A. and Aiello, A. 1983. Uprooting and snapping of trees: structural determinants and ecological consequences. *Canadian Journal of Forest Research*. **13**(5), pp.1011–1020.

Quesada, C. a., Lloyd, J., Anderson, L.O., Fyllas, N.M., Schwarz, M. and Czimczik, C.I. 2011. Soils of Amazonia with particular reference to the RAINFOR sites. *Biogeosciences*. **8**(6), pp.1415–1440.

Quesada, C.A., Phillips, O.L., Schwarz, M., Czimczik, C.I., Baker, T.R., Patiño, S., Fyllas, N.M., Hodnett, M.G., Herrera, R., Almeida, S., Alvarez Dávila, E., Arneth, A., Arroyo, L., Chao, K.J., Dezzeo, N., Erwin, T., di Fiore, A., Higuchi, N., Honorio Coronado, E., Jimenez, E.M., Killeen, T., Lezama, A.T., Lloyd, G., López-González, G., Luizão, F.J., Malhi, Y., Monteagudo, A., Neill, D.A., Núñez Vargas, P., Paiva, R., Peacock, J., Peñuela, M.C., Peña Cruz, A., Pitman, N., Priante Filho, N., Prieto, A., Ramírez, H., Rudas, A., Salomão, R., Santos, A.J.B., Schmerler, J., Silva, N., Silveira, M., Vásquez, R., Vieira, I., Terborgh, J. and Lloyd, J. 2012. Basin-wide variations in Amazon forest structure and function are mediated by both soils and climate. *Biogeosciences*. **9**(6), pp.2203–2246.

R Core Team 2019. R: A language and environment for statistical computing.

R Core Team 2015. R: A language and environment for statistical computing.

Rammig, A., Heinke, J., Hofhansl, F., Verbeeck, H., Baker, T.R., Christoffersen, B., Ciais, P., De Deurwaerder, H., Fleischer, K., Galbraith, D., Guimberteau, M., Huth, A., Johnson, M., Krujit, B., Langerwisch, F., Meir, P., Papastefanou, P., Sampaio, G., Thonicke, K., Von Randow, C., Zang, C. and Rödig, E. 2018. A generic pixel-to-point comparison for simulated large-scale ecosystem properties and ground-based observations: An example from the Amazon region. *Geoscientific Model Development*. **11**(12), pp.5203–5215.

Ratzmann, G., Meinzer, F.C. and Tietjen, B. 2019. Iso/Anisohydry: Still a Useful Concept. *Trends in Plant Science*. **24**(3), pp.191–194.

Resco de Dios, V., Arteaga, C., Hedo, J., Gil-Pelegrín, E. and Voltas, J. 2018. A trade-off between embolism resistance and bark thickness in conifers: are drought and fire adaptations antagonistic? *Plant Ecology and Diversity*. **11**(3), pp.253–258.

Richards, P.W. 1996. *The tropical rain forest: an ecological study* (P. W. Richards, ed.). Cambridge, UK: Cambridge University Press.

Richards, S.A. 2005. Testing ecological theory using the information-theoretic approach: examples and cautionary results. *Ecology*. **86**(10), pp.2805–2814.

Rödig, E., Cuntz, M., Heinke, J., Rammig, A. and Huth, A. 2017. Spatial heterogeneity of biomass and forest structure of the Amazon rain forest: Linking remote sensing, forest modelling and field inventory. *Global Ecology and Biogeography*. **26**(11), pp.1292–1302.

Rolim, S.G., Jesus, R.M., Nascimento, H.E.M., do Couto, H.T.Z. and Chambers, J.Q. 2005. Biomass change in an Atlantic tropical moist forest: the ENSO effect in permanent sample plots over a 22-year period. *Oecologia*. **142**(2), pp.238–246.

Roman, D.T., Novick, K.A., Brzostek, E.R., Dragoni, D., Rahman, F. and Phillips, R.P. 2015. The role of isohydric and anisohydric species in determining ecosystem-scale response to severe drought. *Oecologia*. **179**(3), pp.641–654.

Rowland, L., Da Costa, A.C.L., Galbraith, D.R., Oliveira, R.S., Binks, O.J., Oliveira, A.A.R., Pullen, A.M., Doughty, C.E., Metcalfe, D.B., Vasconcelos, S.S., Ferreira, L. V., Malhi, Y., Grace, J., Mencuccini, M. and Meir, P. 2015. Death from drought in tropical forests is triggered by hydraulics not carbon starvation. *Nature*. **528**(7580), pp.119–122.

RStudio Team 2016. RStudio: Integrated Development for R.

Sakschewski, B., Von Bloh, W., Boit, A., Poorter, L., Peña-Claros, M., Heinke, J., Joshi, J. and Thonicke, K. 2016. Resilience of Amazon forests emerges from plant trait diversity. *Nature Climate Change*. **6**(11), pp.1032–1036.

Sakschewski, B., von Bloh, W., Boit, A., Rammig, A., Kattge, J., Poorter, L., Peñuelas, J. and Thonicke, K. 2015. Leaf and stem economics spectra drive diversity of functional plant traits in a dynamic global vegetation model. *Global Change Biology*. **21**(7), pp.2711–2725.

Sala, A. 2009. Lack of direct evidence for the carbon-starvation hypothesis to explain drought-induced mortality in trees. *Proceedings of the National Academy of Sciences*. **106**(26), pp.E68–E68.

Sala, A., Piper, F. and Hoch, G. 2010. Physiological mechanisms of drought-induced tree mortality are far from being resolved. *New Phytologist*. **186**(2), pp.274–281.

Sala, A., Woodruff, D.R. and Meinzer, F.C. 2012. Carbon dynamics in trees: Feast or famine? *Tree Physiology*. **32**(6), pp.764–775.

van der Sande, M.T., Arets, E.J.M.M., Peña-Claros, M., de Avila, A.L., Roopsind, A., Mazzei, L., Ascarrunz, N., Finegan, B., Alarcón, A., Cáceres-Siani, Y., Licona, J.C., Ruschel, A., Toledo, M. and Poorter, L. 2016. Old-growth Neotropical forests are shifting in species and trait composition. *Ecological Monographs*. **86**(2), pp.228–243.

van der Sande, M.T., Peña-Claros, M., Ascarrunz, N., Arets, E.J.M.M., Licona, J.C., Toledo, M. and Poorter, L. 2017. Abiotic and biotic drivers of biomass change in a Neotropical forest A. Hector, ed. *Journal of Ecology*. **105**(5), pp.1223–1234.

Sanford, R.L., Saldarriaga, J., Clark, K.E., Uhl, C. and Herrera, R. 1985. Amazon Rain-Forest Fires. *Science*. **227**(4682), pp.53–55.

Sarmiento, J.L., Gloor, M., Gruber, N., Beaulieu, C., Jacobson, A.R., Mikaloff Fletcher, S.E., Pacala, S. and Rodgers, K. 2010. Trends and regional distributions of land and ocean carbon sinks. *Biogeosciences*. **7**(8), pp.2351–2367.

Scheiter, S., Langan, L. and Higgins, S.I. 2013. Next-generation dynamic global vegetation models: Learning from community ecology. *New Phytologist*. **198**(3), pp.957–969.

Schnitzer, S.A. and Bongers, F. 2011. Increasing liana abundance and biomass in tropical forests: Emerging patterns and putative mechanisms. *Ecology Letters*. **14**(4), pp.397–406.

Searle, E.B. and Chen, H.Y.H. 2017. Climate change-associated trends in biomass dynamics are consistent across soil drainage classes in western boreal forests of Canada. *Forest Ecosystems*. **4**(1), pp.1–11.

Sevanto, S., Mcdowell, N.G., Dickman, L.T., Pangle, R. and Pockman, W.T. 2014. How do trees die? A test of the hydraulic failure and carbon starvation hypotheses. *Plant, Cell and Environment*. **37**(1), pp.153–161.

Sheil, D., Burslem, D.F.R.P. and Alder, D. 1995. The interpretation and misinterpretation of mortality rate measures. *Journal of Ecology*. **83**(2), pp.331–333.

Sheil, D., Jennings, S. and Savill, P. 2000. Long-term permanent plot observations of vegetation dynamics in Budongo, a Ugandan rain forest. *Journal of Tropical Ecology*. **16**(6), pp.765–800.

Sheil, D. and May, R.M. 1996. Mortality and recruitment rate evaluations in heterogeneous tropical forests. *Journal of Ecology*. **84**(1), pp.91–100.

Shugart, H.H., Wang, B., Fischer, R., Ma, J., Fang, J., Yan, X., Huth, A. and Armstrong, A.H. 2018. Gap models and their individual-based relatives in the assessment of the consequences of global change. *Environmental Research Letters*. **13**(3).

Silva, C.V.J., Aragão, L.E.O.C., Barlow, J., Espirito-Santo, F., Young, P.J., Anderson, L.O., Berenguer, E., Brasil, I., Brown, I.F., Castro, B., Farias, R., Ferreira, J., França, F., Graça, P.M.L.A., Kirsten, L., Lopes, A.P., Salimon, C., Scaranello, M.A., Seixas, M., Souza, F.C. and Xaud, H.A.M. 2018. Drought-induced Amazonian wildfires instigate a decadal-scale disruption of forest carbon dynamics. *Philosophical Transactions of the Royal Society B: Biological Sciences*. **373**(1760), pp.1–25.

Silva Junior, C.H.L., Anderson, L.O., Silva, A.L., Almeida, C.T., Dalagnol, R., Pletsch, M.A.J.S., Penha, T. V., Paloschi, R.A. and Aragão, L.E.O.C. 2019. Fire responses to the 2010 and 2015/2016 Amazonian droughts. *Frontiers in Earth Science*. **7**(May), pp.1–16.

Silvério, D. V., Brando, P.M., Bustamante, M.M.C., Putz, F.E., Marra, D.M., Levick, S.R. and Trumbore, S.E. 2019. Fire, fragmentation, and windstorms: A recipe for tropical forest degradation. *Journal of Ecology*. **107**(2), pp.656–667.

Sitch, S., Friedlingstein, P., Gruber, N., Jones, S.D., Murray-Tortarolo, G., Ahlström, A., Doney, S.C., Graven, H., Heinze, C., Huntingford, C., Levis, S., Levy, P.E., Lomas, M., Poulter, B., Viovy, N., Zaehle, S., Zeng, N., Arneth, A., Bonan, G., Bopp, L., Canadell, J.G., Chevallier, F., Ciais, P., Ellis, R., Gloor, M., Peylin, P., Piao, S., Le Quéré, C., Smith, B., Zhu, Z. and Myneni, R. 2015. Recent trends and drivers of regional sources and sinks of carbon dioxide. *Biogeosciences Discussions*. **12**, pp.653–679.

Skelton, R.P., West, A.G. and Dawson, T.E. 2015. Predicting plant vulnerability to drought in biodiverse regions using functional traits. *Proceedings of the National Academy of Sciences of the United States of America*. **112**(18), pp.5744–5749.

Sperry, J.S. and Love, D.M. 2015. What plant hydraulics can tell us about responses to climate-change droughts. *New Phytologist*. **207**(1), pp.14–27.

Spiegelhalter, D.J., Best, N.G., Carlin, B.P. and Van Der Linde, A. 2002. Bayesian measures of model complexity and fit. *Journal of the Royal Statistical Society. Series B: Statistical Methodology*. **64**(4), pp.583–616.

Stan Development Team 2018. RStan: the R interface to Stan.

Steege, H. ter, Pitman, N.C.A., Sabatier, D., Baraloto, C., Salomao, R.P., Guevara, J.E., Phillips, O.L., Castilho, C. V, Magnusson, W.E., Molino, J.-F., Monteagudo, A., Nunez Vargas, P., Montero, J.C., Feldpausch, T.R., Coronado, E.N.H., Killeen, T.J., Mostacedo,

B., Vasquez, R., Assis, R.L., Terborgh, J., Wittmann, F., Andrade, A., Laurance, W.F., Laurance, S.G.W., Marimon, B.S., Marimon, B.-H., Guimaraes Vieira, I.C., Amaral, I.L., Brienen, R., Castellanos, H., Cardenas Lopez, D., Duivenvoorden, J.F., Mogollon, H.F., Matos, F.D. d. A., Davila, N., Garcia-Villacorta, R., Stevenson Diaz, P.R., Costa, F., Emilio, T., Levis, C., Schietti, J., Souza, P., Alonso, A., Dallmeier, F., Montoya, A.J.D., Fernandez Piedade, M.T., Araujo-Murakami, A., Arroyo, L., Gribel, R., Fine, P.V.A., Peres, C.A., Toledo, M., Aymard C., G.A., Baker, T.R., Ceron, C., Engel, J., Henkel, T.W., Maas, P., Petronelli, P., Stropp, J., Zartman, C.E., Daly, D., Neill, D., Silveira, M., Paredes, M.R., Chave, J., Lima Filho, D. de A., Jorgensen, P.M., Fuentes, A., Schongart, J., Cornejo Valverde, F., Di Fiore, A., Jimenez, E.M., Penuela Mora, M.C., Phillips, J.F., Rivas, G., van Andel, T.R., von Hildebrand, P., Hoffman, B., Zent, E.L., Malhi, Y., Prieto, A., Rudas, A., Ruschell, A.R., Silva, N., Vos, V., Zent, S., Oliveira, A.A., Schutz, A.C., Gonzales, T., Trindade Nascimento, M., Ramirez-Angulo, H., Sierra, R., Tirado, M., Umana Medina, M.N., Heijden, G. van der, Vela, C.I.A., Vilanova Torre, E., Vriesendorp, C., Wang, O., Young, K.R., Baider, C., Balslev, H., Ferreira, C., Mesones, I., Torres-Lezama, A., Urrego Giraldo, L.E., Zagt, R., Alexiades, M.N., Hernandez, L., Huamantupa-Chuquimaco, I., Milliken, W., Palacios Cuenca, W., Pauletto, D., Valderrama Sandoval, E., Valenzuela Gamarra, L., Dexter, K.G., Feeley, K., Lopez-Gonzalez, G. and Silman, M.R. 2013. Hyperdominance in the Amazonian Tree Flora. *Science*. **342**(6156), pp.1243092–1243092.

Stephens, S.L. and Finney, M.A. 2002. Prescribed fire mortality of Sierra Nevada mixed conifer tree species: effects of crown damage and forest floor combustion. *Forest Ecology and Management*. **162**(2–3), pp.261–271.

Stephenson, N.L. and van Mantgem, P.J. 2005. Forest turnover rates follow global and regional patterns of productivity. *Ecology Letters*. **8**(5), pp.524–531.

Stott, P. 2000. Combustion in tropical biomass fires: A critical review. *Progress in Physical Geography*. **24**(3), pp.355–377.

Sturrock, R.N., Frankel, S.J., Brown, A. V., Hennon, P.E., Kliejunas, J.T., Lewis, K.J., Worrall, J.J. and Woods, A.J. 2011. Climate change and forest diseases. *Plant Pathology*. **60**(1), pp.133–149.

Suresh, H.S., Dattaraja, H.S. and Sukumar, R. 2010. Relationship between annual rainfall and tree mortality in a tropical dry forest: Results of a 19-year study at Mudumalai, southern India. *Forest Ecology and Management*. **259**(4), pp.762–769.

Swaine, M.D. 1992. Characteristics of dry forest in West Africa and the influence of fire. *Journal of Vegetation Science*. **3**(3), pp.365–374.

Swaine, M.D. 1996. Rainfall and soil fertility as factors limiting forest species distributions in Ghana. *Journal of Ecology*. **84**(3), pp.419–428.

Tagesson, T., Schurgers, G., Horion, S., Ciais, P., Tian, F., Brandt, M., Ahlström, A., Wigneron, J.P., Ardö, J., Olin, S., Fan, L., Wu, Z. and Fensholt, R. 2020. Recent divergence in the contributions of tropical and boreal forests to the terrestrial carbon sink. *Nature Ecology and Evolution*.

Taylor, D., Hamilton, A.C., Lewis, S.L. and Nantale, G. 2008. Thirty-eight years of change in a tropical forest: plot data from Mpanga Forest Reserve, Uganda. *African Journal of Ecology*. **46**(4), pp.655–667.

Tedeschi, R.G., Cavalcanti, I.F.A. and Grimm, A.M. 2013. Influences of two types of ENSO on South American precipitation. *International Journal of Climatology*. **33**(6), pp.1382–1400.

Teskey, R., Wertin, T., Bauweraerts, I., Ameye, M., McGuire, M.A. and Steppe, K. 2015. Responses of tree species to heat waves and extreme heat events. *Plant Cell and Environment*. **38**(9), pp.1699–1712.

de Toledo, J.J., Magnusson, W.E., Castilho, C. V. and Nascimento, H.E.M. 2011. How much variation in tree mortality is predicted by soil and topography in Central Amazonia? *Forest Ecology and Management*. **262**(3), pp.331–338.

Toledo, J.J., Magnusson, W.E. and Castilho, C. V. 2013. Competition, exogenous disturbances and senescence shape tree size distribution in tropical forest: Evidence from tree mode of death in Central Amazonia. *Journal of Vegetation Science*. **24**(4), pp.651–663.

Trenberth, K.E., Dai, A., Van Der Schrier, G., Jones, P.D., Barichivich, J., Briffa, K.R. and Sheffield, J. 2014. Global warming and changes in drought. *Nature Climate Change*. **4**(1), pp.17–22.

Trifilò, P., Kiorapostolou, N., Petruzzellis, F., Vitti, S., Petit, G., Lo Gullo, M.A., Nardini, A. and Casolo, V. 2019. Hydraulic recovery from xylem embolism in excised branches of twelve woody species: Relationships with parenchyma cells and non-structural carbohydrates. *Plant Physiology and Biochemistry*. **139**(April), pp.513–520.

Tutin, C.E.G., White, L.J.T. and Mackanga-Missandzou, A. 1996. Lightning Strike Burns Large Forest Tree in the Lope Reserve, Gabon. *Global Ecology and Biogeography Letters*. **5**(1), pp.36–41.

Tymen, B., Réjou-Méchain, M., Dalling, J.W., Fauset, S., Feldpausch, T.R., Norden, N., Phillips, O.L., Turner, B.L., Viers, J. and Chave, J. 2016. Evidence for arrested succession in a liana-infested Amazonian forest P. Zuidema, ed. *Journal of Ecology*. **104**(1), pp.149–159.

Uhl, C. 1998. Perspectives on Wildfire in the Humid Tropics. *Conservation Biology*. **12**(5), pp.942–943.

Uriarte, M., Thompson, J. and Zimmerman, J.K. 2019. Hurricane María tripled stem breaks and doubled tree mortality relative to other major storms. *Nature Communications*. **10**(1), pp.1–7.

Vanderwel, M.C., Coomes, D.A. and Purves, D.W. 2013. Quantifying variation in forest disturbance, and its effects on aboveground biomass dynamics, across the eastern United States. *Global Change Biology*. **19**(5), pp.1504–1517.

Veldman, J.W. and Putz, F.E. 2011. Grass-dominated vegetation, not species-diverse natural savanna, replaces degraded tropical forests on the southern edge of the Amazon Basin. *Biological Conservation*. **144**(5), pp.1419–1429.

Vicuña Miñano, E., Baker, T.R., Banda-R., K., Honorio Coronado, E., Monteagudo, A., Phillips, O.L., Del Castillo Torres, D., Farfan Rios, W., Flores, G., Huaman, D., Huaman Tantte, K., Hidalgo Pizango, G., Lojas Aleman, E., Melo, J.B., Pickavance, G.C., Rios, M., Rojas, M., Salinas, N. and Vasquez Martinez, R. 2019. El sumidero de carbono en los bosques primarios Amazónicos es una oportunidad para lograr la sostenibilidad de su convercacíon. *Folia Amazónica*. **27**(1), pp.101–109.

Vilanova, E., Ramírez-Angulo, H., Torres-Lezama, A., Aymard, G., Gámez, L., Durán, C., Hernández, L., Herrera, R., van der Heijden, G., Phillips, O.L. and Ettl, G.J. 2018. Environmental drivers of forest structure and stem turnover across Venezuelan tropical forests R. Zang, ed. *PLOS ONE*. **13**(6), p.e0198489.

Villalba, R. and Veblen, T.T. 1998. Influences of large-scale climatic variability on episodic tree mortality in northern Patagonia. *Ecology*. **79**(8), pp.2624–2640.

Vozmishcheva, A.S., Bondarchuk, S.N., Gromyko, M.N., Kislov, D.E., Pimenova, E.A., Salo, M.A. and Korznikov, K.A. 2019. Strong Disturbance Impact of Tropical Cyclone Lionrock (2016) on Korean Pine-Broadleaved Forest in the Middle Sikhote-Alin Mountain Range, Russian Far East. *Forests*. **10**(1017), pp.1–14.

Webb, E.L., Bult, M. van de, Fa'aumu, S., Webb, R.C., Tualaulelei, A. and Carrasco, L.R. 2014. Factors affecting tropical tree damage and survival after catastrophic wind disturbance. *Biotropica*. **46**(1), pp.32–41.

West, A.G., Nel, J.A., Bond, W.J. and Midgley, J.J. 2016. Experimental evidence for heat plume-induced cavitation and xylem deformation as a mechanism of rapid post-fire tree mortality. *New Phytologist*. **211**(3), pp.828–838.

Westing, A.H. 1964. The longevity and aging of trees. *Gerontologist*. **4**(1), pp.10–15.

Whittaker, R.J., Schmitt, S.F., Jones, S.H., Partomihardijo, T. and Bush, M.B. 1998. Stand biomass and tree mortality from permanent forest plots on Krakatau, Indonesia, 1989-1995. *Biotropica*. **30**(4), pp.519–529.

Williams, A.P., Allen, C.D., Millar, C.I., Swetnam, T.W., Michaelsen, J., Still, C.J. and Leavitt, S.W. 2010. Forest responses to increasing aridity and warmth in the southwestern United States. *Proceedings of the National Academy of Sciences of the United States of America*. **107**(50), pp.21289–94.

Williamson, G.B., Laurance, W.F., Oliveira, A.A., Delamônica, P., Gascon, C., Lovejoy, T.E. and Pohl, L. 2000. Amazonian tree mortality during the 1997 El Niño drought. *Conservation Biology*. **14**(5), pp.1538–1542.

Wright, S.J. and Calderon, O. 2006. Seasonal, El Niño and longer term changes in flower and seed production in a moist tropical forest. *Ecology Letters*. **9**, pp.35–44.

Yanoviak, S.P., Gora, E.M., Bitzer, P.M., Burchfield, J.C., Muller-Landau, H.C., Detto, M., Paton, S. and Hubbell, S.P. 2020. Lightning is a major cause of large tree mortality in a lowland neotropical forest. *New Phytologist*. **225**(5), pp.1936–1944.

Yanoviak, S.P., Gora, E.M., Burchfield, J.M., Bitzer, P.M. and Detto, M. 2017. Quantification and identification of lightning damage in tropical forests. *Ecology and Evolution*. **7**(14), pp.5111–5122.

Yoon, J.H. and Zeng, N. 2010. An Atlantic influence on Amazon rainfall. *Climate Dynamics*. **34**(2), pp.249–264.

Zhang, X., Lei, Y., Pang, Y., Liu, X. and Wang, J. 2014. Tree mortality in response to climate change induced drought across Beijing, China. *Climatic Change*. **124**(1–2), pp.179–190.

Zimmerman, J.K., Everham III, E.M., Waide, R.B., Lodge, D.J., Taylor, C.M. and Brokaw, N.V.L. 1994. Responses of tree species to hurricane winds in subtropical wet forest in Puerto Rico: implications for tropical tree life-histories. *Journal of Ecology*. **82**(4), pp.911–922.

Zimmerman, J.K., Hogan, J.A., Shiels, A.B., Bithorn, J.E., Carmona, S.M. and Brokaw, N. 2014. Seven-year responses of trees to experimental hurricane effects in a tropical rainforest, Puerto Rico. *Forest Ecology and Management*. **332**, pp.64–74.

List of Abbreviations

CRU	Climatic Research Unit
dbh	diameter at breast height
DVM	dynamic vegetation model
ENSO	El Niño-Southern Oscillation
HL0	Bayesian model with no hierarchical levels
HL1	Bayesian model with one hierarchical level
HL2	Bayesian model with two hierarchical levels
m0r0	forest dynamics scenario, where neither mortality nor recruitment rates increase over time
m0r1	forest dynamics scenario, where recruitment rates increase by 1 % per year, mortality rates stay the same
m1r1	forest dynamics scenario, where both mortality and recruitment rates increase by 1% per year
m1r2	forest dynamics scenario, where mortality rates increase by 1% per year, and recruitment rates by 2% per year
m2r2	forest dynamics scenario, where both mortality and recruitment rates increase by 2% per year
m3r4	forest dynamics scenario, where mortality rates increase by 3% per year, and recruitment rates by 4% per year
PFT	plant functional type
TRMM	Tropical Rainfall Monitoring Mission

Appendix A. Long-term mortality rate trend simulation and analysis process overview

Figure A.1. Overview of the first step of the long-term trend simulation process, including descriptions and snippets of output.

Step 1

Input

Mort. incr.	Recr. incr.
0*	0*
1	1
2	2
0*	1*
1	2
3	4

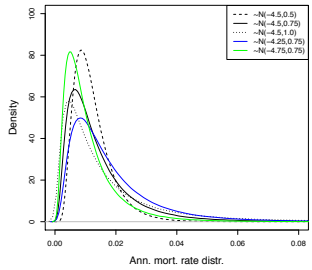

nPlots = 100, nCensInts= 50

Output

Row nr.	Distr. mean	Distr. s.d.	Mort. incr.	Recr. incr.	Plot id.	Cens. year	Cens. id	Tree id	Mort. prob.(%)	Alive status	Recruit status	Cens. died
1	-4.25	0.75	0	0	1	1970	0	1	3.52	1	0	*NA*
2	-4.25	0.75	0	0	1	1970	0	2	1.08	1	0	*NA*
3	-4.25	0.75	0	0	1	1970	0	3	5.52	1	0	*NA*
4	-4.25	0.75	0	0	1	1970	0	4	0.61	1	0	*NA*
5	-4.25	0.75	0	0	1	1970	0	5	0.45	1	0	*NA*
…	…	…	…	…	…	…	…	…	…	…	…	…
2049029	-4.25	0.75	0	0	66	2010	40	265	1.86	0	0	40
2049030	-4.25	0.75	0	0	66	2010	40	270	1.07	1	0	*NA*
…	…	…	…	…	…	…	…	…	…	…	…	…
3079485	-4.25	0.75	0	0	100	2020	50	1133	9.99	1	1	*NA*

Result: 28 plot census tables, containing ca. 3-3.5 million rows each for all trees in 100 plots, each with 50 re-censuses from 1970-2020; 1 plot census table for every unique combination of dynamics scenario and mortality rate distribution (see “Input”: five distributions for each of the four non-baseline dynamics variations and four distributions for the two “baseline” variations, denoted by asterisks).

Row nr.	Distr. mean	Distr. s.d.	Mort. incr.	Recr. incr.	Plot id.	Cens. year	Cens. id	Cens.int. ln. (yr)	N_0	N_t	N_d	N_r	Ann.mort. rate (%)
1	-4.25	0.75	0	0	1	1971	1	1	581	582	5	6	0.86
2	-4.25	0.75	0	0	1	1972	2	1	582	597	10	25	1.72
3	-4.25	0.75	0	0	1	1973	3	1	597	597	14	14	2.35
4	-4.25	0.75	0	0	1	1974	4	1	597	595	8	8	1.34
5	-4.25	0.75	0	0	1	1975	5	1	595	594	5	5	0.84
…	…	…	…	…	…	…	…	…	…	…	…	…	…
3390	-4.25	0.75	0	0	66	2010	40	1	581	584	6	9	1.03
3391	-4.25	0.75	0	0	66	2011	41	1	584	578	9	3	1.54
…	…	…	…	…	…	…	…	…	…	…	…	…	…
5000	-4.25	0.75	0	0	100	2020	50	1	609	602	13	6	2.13

The 28 individual tree-level plot census dynamics tables from above are summarized per plot census interval in 28 tables, containing 5000 rows each (100 plots, all with 50 census intervals).

Figure A.2. Overview of the second step of the long-term trend simulation process, including descriptions and snippets of output.

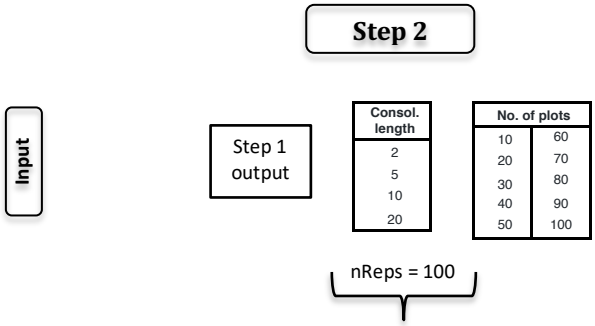

Output

Plot id.	Cens. year 1	Cens. year2	Cens. id 1	Cens id. 2	C.ln. (yr)	Mort. r.1 (%)	Mort. r.2 (%)	Abs.dif (pp)	Rel.dif (%)
26	1976	1981	6	11	5	1.96	2.20	0.24	2.29
31	2013	2018	43	48	5	1.84	1.44	-0.41	-5.02
33	1991	1996	21	26	5	2.25	1.80	-0.45	-4.42
39	2006	2011	36	41	5	1.87	1.44	-0.43	-5.21
41	1982	1987	12	17	5	1.53	2.27	0.74	7.95
55	1981	1986	11	16	5	1.77	1.93	0.16	1.72
65	2000	2005	30	35	5	1.87	1.91	0.04	0.38
93	1989	1994	19	24	5	1.81	1.41	-0.40	-4.98
95	1988	1993	18	23	5	1.68	1.74	0.05	0.62
99	2005	2010	35	40	5	1.60	1.52	-0.08	-1.03

Result: 112,000 consolidated plot census tables (28 plot census dynamics tables, resampled for 4 different interval lengths, each for 10 different numbers of plots in total; repeated 100 times per unique combination of the preceding) with the number of table rows corresponding to that of the number of consolidated plots of that resampling run. The above illustrates the $\sim N(-4.25, 0.75^2)$, no increase, consolidation interval length 5 years, number of plots 10, repetition ID 12 run.

No. plot	C.ln (yr)	Rep. id.	Mean m1(%)	Med. m1(%)	L95 m1	U95 m1	Mean m2(%)	Med. m2(%)	L95 m2	U95 m2	Ovl. 95%	(...)
10	2	1	1.88	1.78	1.62	2.14	1.54	1.50	1.35	1.73	1	...
10	2	2	1.60	1.67	1.20	2.00	1.85	1.85	1.57	2.14	1	...
10	2	3	1.73	1.77	1.41	2.04	1.66	1.75	1.41	1.91	1	...
10	2	4	1.72	1.66	1.32	2.12	1.84	1.84	1.52	2.16	1	...
10	2	5	1.96	1.86	1.67	2.26	2.02	1.91	1.72	2.32	1	...
...	...	...	...	...	...	...	...	...	...	...	...	...
20	20	40	1.83	1.84	1.78	1.89	1.82	1.80	1.76	1.88	1	...
20	20	41	1.82	1.82	1.77	1.86	1.84	1.84	1.77	1.91	1	...
...	...	...	...	...	...	...	...	...	...	...	...	...
100	20	100	1.84	1.83	1.81	1.87	1.81	1.79	1.78	1.83	1	...

The first nine trend result summary statistics of the "no increase" scenario of the $\sim N(-4.25, 0.75^2)$ distribution. In total 28 trend result metrics tables are created with 4000 rows each (4 consolidation interval lengths for 10 different numbers of plots, repeated 100 times).

Figure A.3. Overview of the third step of the long-term trend simulation process, including descriptions and snippets of output.

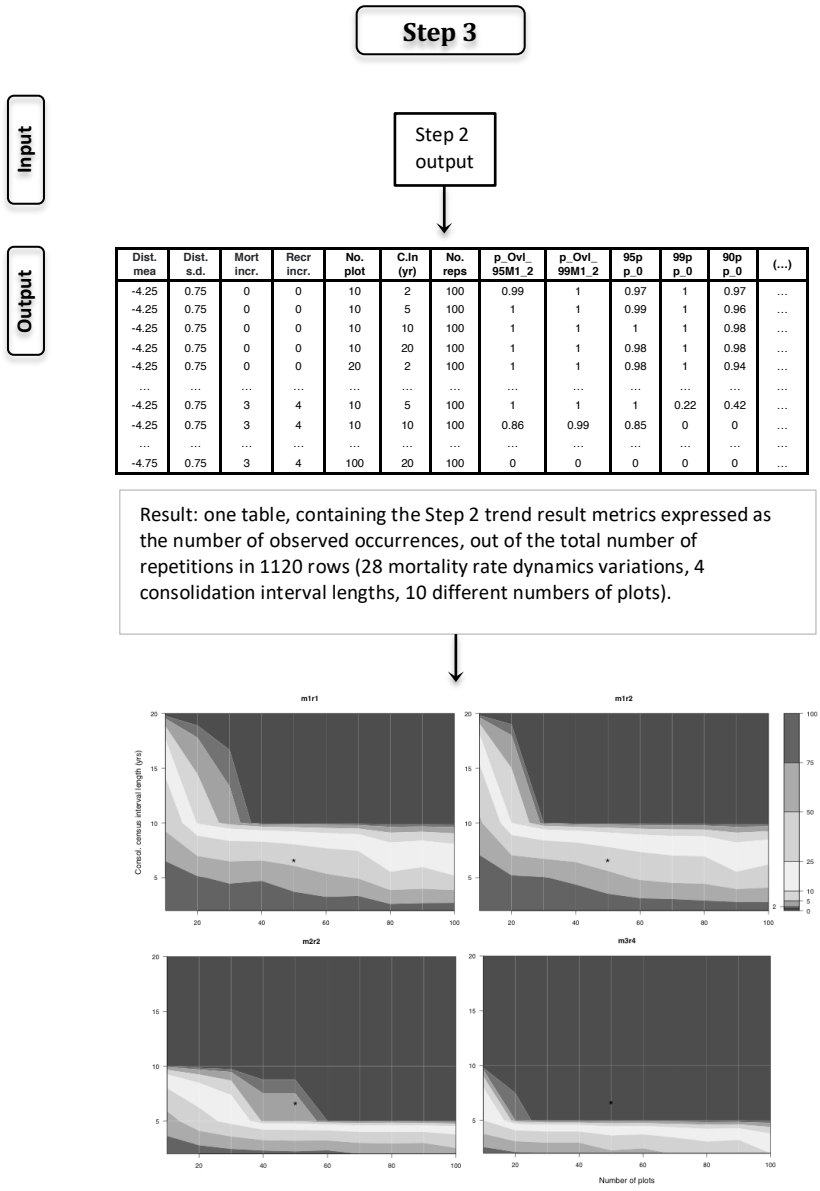

Appendix B. Plot numbers for long-term increase detection for all metrics and levels of confidence

Table B.1. The number of plots needed to achieve no overlap for any of the repetitions.
As determined using the 2-tailed 95 or 99 % confidence intervals of the annual mortality rates of the first and second consolidated sets (M1M2_95, M1M2_99), or no overlap with zero of the two-tailed and one-tailed 95 or 99 % confidence intervals of the absolute (in percentage points) and relative difference between the annual mortality rates of the second and the first consolidated sets (ppD_95(2), ppD_95(1), ppD_9592), ppD_99(1), relD_95(2), relD_95(1), relD_99(2), relD_99(1)), for the different consolidated interval lengths (consolLn), population dynamics variations (dynVar), and mortality rate distributions (mortDistr). Darker shading indicates more plots are needed, up to a simulated maximum of 100.

consolLn	dynVar	mortDistr	M1M2_95	M1M2_99	ppD_95(2)	ppD_95(1)	ppD_99(2)	ppDiff_99(1)	relD_95(2)	relD_95(1)	relD_99(2)	relD_99(1)
5	m3r4	$N(-4.25, 0.75^2)$	>100	>100	20	20	40	40	20	20	40	30
		$N(-4.5, 0.5^2)$	>100	>100	30	30	40	30	40	30	50	40
		$N(-4.5, 0.75^2)$	>100	>100	30	30	40	40	40	40	40	40
		$N(-4.5, 1.0^2)$	>100	>100	20	20	40	40	20	20	40	40
		$N(-4.75, 0.75^2)$	>100	>100	30	30	30	30	30	30	40	40
	m2r2	$N(-4.25, 0.75^2)$	>100	>100	60	60	90	80	60	60	>100	80
		$N(-4.5, 0.5^2)$	>100	>100	70	60	>100	80	80	70	>100	>100
		$N(-4.5, 0.75^2)$	>100	>100	90	60	90	90	90	60	90	90
		$N(-4.5, 1.0^2)$	>100	>100	70	70	100	70	70	50	80	70
		$N(-4.75, 0.75^2)$	>100	>100	>100	>100	>100	>100	>100	>100	>100	>100
10	m3r4	$N(-4.25, 0.75^2)$	30	40	10	10	10	10	10	10	10	10
		$N(-4.5, 0.5^2)$	30	50	10	10	10	10	10	10	10	10
		$N(-4.5, 0.75^2)$	30	50	10	10	10	10	10	10	10	10
		$N(-4.5, 1.0^2)$	30	50	10	10	10	10	10	10	10	10
		$N(-4.75, 0.75^2)$	30	50	10	10	10	10	10	10	10	10
	m2r2	$N(-4.25, 0.75^2)$	30	50	10	10	20	20	10	10	20	20
		$N(-4.5, 0.5^2)$	40	60	20	10	20	20	20	20	20	20
		$N(-4.5, 0.75^2)$	40	60	20	20	20	20	20	20	20	20
		$N(-4.5, 1.0^2)$	40	60	10	10	20	20	10	10	20	20
		$N(-4.75, 0.75^2)$	40	60	20	20	20	20	20	20	20	20

Table B.1. (Continued) The number of plots needed to achieve no overlap for any of the repetitions.

consolLn	dynVar	mortDistr	M1M2_95	M1M2_99	ppD_95(2)	ppD_95(1)	ppD_99(2)	ppDiff_99(1)	relD_95(2)	relD_95(1)	relD_99(2)	relD_99(1)
10	m1r2	$N(-4.25, 0.75^2)$	70	>100	30	30	50	50	40	30	50	40
		$N(-4.5, 0.5^2)$	90	>100	60	40	60	60	60	40	60	60
		$N(-4.5, 0.75^2)$	100	>100	40	30	70	70	30	30	70	70
		$N(-4.5, 1.0^2)$	80	100	40	40	50	50	40	40	50	50
		$N(-4.75, 0.75^2)$	>100	>100	60	60	90	70	60	60	90	70
	m1r1	$N(-4.25, 0.75^2)$	70	100	50	40	50	50	40	40	50	50
		$N(-4.5, 0.5^2)$	>100	>100	70	70	80	70	70	70	80	70
		$N(-4.5, 0.75^2)$	80	100	40	40	60	40	40	40	60	50
		$N(-4.5, 1.0^2)$	80	100	30	30	60	60	40	30	60	60
		$N(-4.75, 0.75^2)$	100	>100	50	50	70	60	50	50	70	60
20	m3r4	$N(-4.25, 0.75^2)$	10	10	10	10	10	10	10	10	10	10
		$N(-4.5, 0.5^2)$	10	10	10	10	10	10	10	10	10	10
		$N(-4.5, 0.75^2)$	10	10	10	10	10	10	10	10	10	10
		$N(-4.5, 1.0^2)$	10	10	10	10	10	10	10	10	10	10
		$N(-4.75, 0.75^2)$	10	10	10	10	10	10	10	10	10	10
	m2r2	$N(-4.25, 0.75^2)$	10	10	10	10	10	10	10	10	10	10
		$N(-4.5, 0.5^2)$	10	10	10	10	10	10	10	10	10	10
		$N(-4.5, 0.75^2)$	10	10	10	10	10	10	10	10	10	10
		$N(-4.5, 1.0^2)$	10	10	10	10	10	10	10	10	10	10
		$N(-4.75, 0.75^2)$	10	10	10	10	10	10	10	10	10	10
	m1r2	$N(-4.25, 0.75^2)$	10	20	10	10	20	10	10	10	20	10
		$N(-4.5, 0.5^2)$	20	20	10	10	20	20	10	10	20	20
		$N(-4.5, 0.75^2)$	20	20	10	10	10	10	10	10	10	10
		$N(-4.5, 1.0^2)$	20	20	10	10	20	10	10	10	20	10
		$N(-4.75, 0.75^2)$	20	20	10	10	20	20	10	10	20	20
	m1r1	$N(-4.25, 0.75^2)$	10	20	10	10	10	10	10	10	10	10
		$N(-4.5, 0.5^2)$	20	20	10	10	20	20	10	10	20	20
		$N(-4.5, 0.75^2)$	20	20	10	10	20	10	10	10	20	10
		$N(-4.5, 1.0^2)$	20	20	10	10	20	10	10	10	20	10
		$N(-4.75, 0.75^2)$	20	20	10	10	20	10	10	10	20	20

Table B.2. The number of plots needed to achieve overlap for a maximum of just one of the repetitions.
As determined using the 2-tailed 95 or 99 % confidence intervals of the annual mortality rates of the first and second consolidated sets (M1M2_95, M1M2_99), or a maximum of one repetition where zero was contained within the two-tailed and one-tailed 95 or 99 % confidence intervals of the absolute (in percentage points) and relative difference between the annual mortality rates of the second and the first consolidated sets (ppD_95(2), ppD_95(1), ppD_9592), ppD_99(1), relD_95(2), relD_95(1), relD_99(2), relD_99(1)), for the different consolidated interval lengths (consolLn), population dynamics variations (dynVar), and mortality rate distributions (mortDistr). Darker shading indicates more plots are needed, up to a simulated maximum of 100.

consolLn	dynVar	mortDistr	M1M2_95	M1M2_99	ppD_95(2)	ppD_95(1)	ppD_99(2)	ppDiff_99(1)	relD_95(2)	relD_95(1)	relD_99(2)	relD_99(1)
5	m3r4	$N(-4.25, 0.75^2)$	>100	>100	20	20	40	20	20	20	40	20
		$N(-4.5, 0.5^2)$	>100	>100	30	30	40	30	30	30	30	30
		$N(-4.5, 0.75^2)$	>100	>100	30	20	30	30	30	20	40	40
		$N(-4.5, 1.0^2)$	>100	>100	20	20	30	30	20	20	30	20
		$N(-4.75, 0.75^2)$	>100	>100	30	30	30	30	30	30	40	30
	m2r2	$N(-4.25, 0.75^2)$	>100	>100	50	50	80	70	60	50	80	80
		$N(-4.5, 0.5^2)$	>100	>100	60	60	80	80	80	60	>100	80
		$N(-4.5, 0.75^2)$	>100	>100	60	60	80	60	60	60	70	70
		$N(-4.5, 1.0^2)$	>100	>100	50	50	70	80	60	50	70	70
		$N(-4.75, 0.75^2)$	>100	>100	60	60	>100	>100	>100	60	>100	>100
10	m3r4	$N(-4.25, 0.75^2)$	30	40	10	10	10	10	10	10	10	10
		$N(-4.5, 0.5^2)$	30	40	10	10	10	10	10	10	10	10
		$N(-4.5, 0.75^2)$	30	50	10	10	10	10	10	10	10	10
		$N(-4.5, 1.0^2)$	30	40	10	10	10	10	10	10	10	10
		$N(-4.75, 0.75^2)$	30	40	10	10	10	10	10	10	10	10
	m2r2	$N(-4.25, 0.75^2)$	30	50	10	10	20	20	10	10	20	20
		$N(-4.5, 0.5^2)$	40	60	20	10	20	20	20	10	20	20
		$N(-4.5, 0.75^2)$	40	50	10	10	20	20	10	10	20	20
		$N(-4.5, 1.0^2)$	40	50	10	10	20	20	10	10	20	20
		$N(-4.75, 0.75^2)$	40	60	20	10	20	20	20	10	20	20
	m1r2	$N(-4.25, 0.75^2)$	70	90	30	30	50	40	30	30	50	40
		$N(-4.5, 0.5^2)$	90	>100	40	40	60	50	40	40	60	60
		$N(-4.5, 0.75^2)$	80	>100	30	30	50	40	30	30	70	40
		$N(-4.5, 1.0^2)$	60	90	40	20	50	40	40	20	50	40
		$N(-4.75, 0.75^2)$	>100	>100	60	50	70	70	60	50	70	70

Table B.2. (Continued) The number of plots needed to achieve overlap for a maximum of just one of the repetitions.

consolLn	dynVar	mortDistr	M1M2_95	M1M2_99	ppD_95(2)	ppD_95(1)	ppD_99(2)	ppDiff_99(1)	relD_95(2)	relD_95(1)	relD_99(2)	relD_99(1)
10	m1r1	$N(-4.25, 0.75^2)$	70	100	40	40	40	40	40	40	40	40
		$N(-4.5, 0.5^2)$	>100	>100	50	50	70	70	50	50	70	70
		$N(-4.5, 0.75^2)$	80	90	40	30	50	40	40	30	50	40
		$N(-4.5, 1.0^2)$	80	100	30	30	60	40	30	30	60	50
		$N(-4.75, 0.75^2)$	100	>100	50	40	50	50	50	40	50	50
20	m3r4	$N(-4.25, 0.75^2)$	10	10	10	10	10	10	10	10	10	10
		$N(-4.5, 0.5^2)$	10	10	10	10	10	10	10	10	10	10
		$N(-4.5, 0.75^2)$	10	10	10	10	10	10	10	10	10	10
		$N(-4.5, 1.0^2)$	10	10	10	10	10	10	10	10	10	10
		$N(-4.75, 0.75^2)$	10	10	10	10	10	10	10	10	10	10
	m2r2	$N(-4.25, 0.75^2)$	10	10	10	10	10	10	10	10	10	10
		$N(-4.5, 0.5^2)$	10	10	10	10	10	10	10	10	10	10
		$N(-4.5, 0.75^2)$	10	10	10	10	10	10	10	10	10	10
		$N(-4.5, 1.0^2)$	10	10	10	10	10	10	10	10	10	10
		$N(-4.75, 0.75^2)$	10	10	10	10	10	10	10	10	10	10
	m1r2	$N(-4.25, 0.75^2)$	10	20	10	10	10	10	10	10	10	10
		$N(-4.5, 0.5^2)$	20	20	10	10	20	20	10	10	20	20
		$N(-4.5, 0.75^2)$	20	20	10	10	10	10	10	10	10	10
		$N(-4.5, 1.0^2)$	20	20	10	10	10	10	10	10	10	10
		$N(-4.75, 0.75^2)$	20	20	10	10	20	20	10	10	20	20
	m1r1	$N(-4.25, 0.75^2)$	10	20	10	10	10	10	10	10	10	10
		$N(-4.5, 0.5^2)$	20	20	10	10	20	10	10	10	20	10
		$N(-4.5, 0.75^2)$	20	20	10	10	10	10	10	10	10	10
		$N(-4.5, 1.0^2)$	10	20	10	10	10	10	10	10	10	10
		$N(-4.75, 0.75^2)$	20	20	10	10	20	10	10	10	20	10

Table B.3. The number of plots needed to achieve overlap for a maximum of two of the repetitions.
As determined using the 2-tailed 95 or 99 % confidence intervals of the annual mortality rates of the first and second consolidated sets (M1M2_95, M1M2_99), or a maximum of two repetitions where zero was contained within the two-tailed and one-tailed 95 or 99 % confidence intervals of the absolute (in percentage points) and relative difference between the annual mortality rates of the second and the first consolidated sets (ppD_95(2), ppD_95(1), ppD_9592), ppD_99(1), relD_95(2), relD_95(1), relD_99(2), relD_99(1)), for the different consolidated interval lengths (consolLn), population dynamics variations (dynVar), and mortality rate distributions (mortDistr). Darker shading indicates more plots are needed, up to a simulated maximum of 100.

consolLn	dynVar	mortDistr	M1M2_95	M1M2_99	ppD_95(2)	ppD_95(1)	ppD_99(2)	ppDiff_99(1)	relD_95(2)	relD_95(1)	relD_99(2)	relD_99(1)
5	m3r4	$N(-4.25, 0.75^2)$	>100	>100	20	20	30	20	20	20	40	20
		$N(-4.5, 0.5^2)$	>100	>100	30	20	30	30	30	30	30	30
		$N(-4.5, 0.75^2)$	>100	>100	20	20	30	30	30	20	40	30
		$N(-4.5, 1.0^2)$	>100	>100	20	20	30	20	20	20	30	20
		$N(-4.75, 0.75^2)$	>100	>100	30	30	30	30	30	30	30	30
	m2r2	$N(-4.25, 0.75^2)$	>100	>100	50	50	80	70	50	50	80	60
		$N(-4.5, 0.5^2)$	>100	>100	60	60	80	80	80	60	80	80
		$N(-4.5, 0.75^2)$	>100	>100	60	60	60	60	60	50	70	70
		$N(-4.5, 1.0^2)$	>100	>100	40	40	70	80	60	40	70	60
		$N(-4.75, 0.75^2)$	>100	>100	60	60	>100	>100	>100	60	>100	>100
10	m3r4	$N(-4.25, 0.75^2)$	30	40	10	10	10	10	10	10	10	10
		$N(-4.5, 0.5^2)$	30	40	10	10	10	10	10	10	10	10
		$N(-4.5, 0.75^2)$	30	50	10	10	10	10	10	10	10	10
		$N(-4.5, 1.0^2)$	30	40	10	10	10	10	10	10	10	10
		$N(-4.75, 0.75^2)$	30	40	10	10	10	10	10	10	10	10
	m2r2	$N(-4.25, 0.75^2)$	30	50	10	10	20	20	10	10	20	10
		$N(-4.5, 0.5^2)$	40	50	10	10	20	20	10	10	20	20
		$N(-4.5, 0.75^2)$	30	50	10	10	20	20	10	10	20	20
		$N(-4.5, 1.0^2)$	30	50	10	10	20	10	10	10	20	10
		$N(-4.75, 0.75^2)$	40	50	20	10	20	20	20	10	20	20
	m1r2	$N(-4.25, 0.75^2)$	60	80	30	30	40	40	30	30	40	40
		$N(-4.5, 0.5^2)$	90	>100	40	40	60	40	40	40	60	40
		$N(-4.5, 0.75^2)$	80	>100	30	30	50	40	30	30	50	40
		$N(-4.5, 1.0^2)$	60	90	30	20	40	40	30	20	50	40
		$N(-4.75, 0.75^2)$	90	>100	60	40	70	60	60	40	70	70

Table B.3. (Continued) The number of plots needed to achieve overlap for a maximum of two of the repetitions.

consolLn	dynVar	mortDistr	M1M2_95	M1M2_99	ppD_95(2)	ppD_95(1)	ppD_99(2)	ppDiff_99(1)	relD_95(2)	relD_95(1)	relD_99(2)	relD_99(1)
10	m1r1	$N(-4.25, 0.75^2)$	60	90	40	30	40	40	40	30	40	40
		$N(-4.5, 0.5^2)$	90	>100	50	50	70	60	50	50	70	70
		$N(-4.5, 0.75^2)$	70	90	40	30	40	40	40	30	40	40
		$N(-4.5, 1.0^2)$	70	100	30	30	50	40	30	30	50	40
		$N(-4.75, 0.75^2)$	100	>100	40	40	50	50	40	40	50	50
20	m3r4	$N(-4.25, 0.75^2)$	10	10	10	10	10	10	10	10	10	10
		$N(-4.5, 0.5^2)$	10	10	10	10	10	10	10	10	10	10
		$N(-4.5, 0.75^2)$	10	10	10	10	10	10	10	10	10	10
		$N(-4.5, 1.0^2)$	10	10	10	10	10	10	10	10	10	10
		$N(-4.75, 0.75^2)$	10	10	10	10	10	10	10	10	10	10
	m2r2	$N(-4.25, 0.75^2)$	10	10	10	10	10	10	10	10	10	10
		$N(-4.5, 0.5^2)$	10	10	10	10	10	10	10	10	10	10
		$N(-4.5, 0.75^2)$	10	10	10	10	10	10	10	10	10	10
		$N(-4.5, 1.0^2)$	10	10	10	10	10	10	10	10	10	10
		$N(-4.75, 0.75^2)$	10	10	10	10	10	10	10	10	10	10
	m1r2	$N(-4.25, 0.75^2)$	10	20	10	10	10	10	10	10	10	10
		$N(-4.5, 0.5^2)$	20	20	10	10	20	10	10	10	20	10
		$N(-4.5, 0.75^2)$	10	20	10	10	10	10	10	10	10	10
		$N(-4.5, 1.0^2)$	20	20	10	10	10	10	10	10	10	10
		$N(-4.75, 0.75^2)$	20	20	10	10	20	20	10	10	20	20
	m1r1	$N(-4.25, 0.75^2)$	10	20	10	10	10	10	10	10	10	10
		$N(-4.5, 0.5^2)$	10	20	10	10	20	10	10	10	20	10
		$N(-4.5, 0.75^2)$	20	20	10	10	10	10	10	10	10	10
		$N(-4.5, 1.0^2)$	10	20	10	10	10	10	10	10	10	10
		$N(-4.75, 0.75^2)$	20	20	10	10	20	10	10	10	20	10

Table B.4. The number of plots needed to achieve overlap for a maximum of five of the repetitions.

As determined using the 2-tailed 95 or 99 % confidence intervals of the annual mortality rates of the first and second consolidated sets (M1M2_95, M1M2_99), or a maximum of five repetitions where zero was contained within the two-tailed and one-tailed 95 or 99 % confidence intervals of the absolute (in percentage points) and relative difference between the annual mortality rates of the second and the first consolidated sets (ppD_95(2), ppD_95(1), ppD_9592), ppD_99(1), relD_95(2), relD_95(1), relD_99(2), relD_99(1)), for the different consolidated interval lengths (consolLn), population dynamics variations (dynVar), and mortality rate distributions (mortDistr). Darker shading indicates more plots are needed, up to a simulated maximum of 100.

consolLn	dynVar	mortDistr	M1M2_95	M1M2_99	ppD_95(2)	ppD_95(1)	ppD_99(2)	ppDiff_99(1)	relD_95(2)	relD_95(1)	relD_99(2)	relD_99(1)
5	m3r4	$N(-4.25, 0.75^2)$	>100	>100	20	20	20	20	20	20	20	20
		$N(-4.5, 0.5^2)$	>100	>100	20	20	30	30	20	20	30	30
		$N(-4.5, 0.75^2)$	>100	>100	20	20	30	20	20	20	30	30
		$N(-4.5, 1.0^2)$	>100	>100	20	20	20	20	20	20	30	20
		$N(-4.75, 0.75^2)$	>100	>100	30	20	30	30	30	20	30	30
	m2r2	$N(-4.25, 0.75^2)$	>100	>100	40	40	60	70	50	40	60	60
		$N(-4.5, 0.5^2)$	>100	>100	40	40	80	70	60	40	80	70
		$N(-4.5, 0.75^2)$	>100	>100	40	40	60	60	50	40	60	60
		$N(-4.5, 1.0^2)$	>100	>100	40	40	70	40	40	40	60	40
		$N(-4.75, 0.75^2)$	>100	>100	50	50	70	60	50	50	90	70
10	m3r4	$N(-4.25, 0.75^2)$	30	40	10	10	10	10	10	10	10	10
		$N(-4.5, 0.5^2)$	30	40	10	10	10	10	10	10	10	10
		$N(-4.5, 0.75^2)$	30	40	10	10	10	10	10	10	10	10
		$N(-4.5, 1.0^2)$	30	40	10	10	10	10	10	10	10	10
		$N(-4.75, 0.75^2)$	30	40	10	10	10	10	10	10	10	10
	m2r2	$N(-4.25, 0.75^2)$	30	50	10	10	20	10	10	10	20	10
		$N(-4.5, 0.5^2)$	30	50	10	10	20	10	10	10	20	10
		$N(-4.5, 0.75^2)$	30	50	10	10	20	20	10	10	20	20
		$N(-4.5, 1.0^2)$	30	50	10	10	10	10	10	10	10	10
		$N(-4.75, 0.75^2)$	30	50	10	10	20	20	20	10	20	20
	m1r2	$N(-4.25, 0.75^2)$	50	80	30	20	40	30	30	20	40	30
		$N(-4.5, 0.5^2)$	80	100	40	30	40	40	40	40	40	40
		$N(-4.5, 0.75^2)$	70	100	30	20	50	40	30	20	50	40
		$N(-4.5, 1.0^2)$	60	80	20	20	40	40	20	20	40	40
		$N(-4.75, 0.75^2)$	80	>100	40	40	60	60	50	40	60	60

Table B.4. (Continued) The number of plots needed to achieve overlap for a maximum of five of the repetitions.

consolLn	dynVar	mortDistr	M1M2_95	M1M2_99	ppD_95(2)	ppD_95(1)	ppD_99(2)	ppDiff_99(1)	relD_95(2)	relD_95(1)	relD_99(2)	relD_99(1)
10	m1r1	$N(-4.25, 0.75^2)$	60	80	30	20	40	40	30	20	40	40
		$N(-4.5, 0.5^2)$	70	>100	40	40	60	50	40	40	60	50
		$N(-4.5, 0.75^2)$	70	80	30	20	40	40	30	20	40	40
		$N(-4.5, 1.0^2)$	60	90	30	20	40	30	30	20	40	30
		$N(-4.75, 0.75^2)$	70	100	40	30	50	40	40	30	50	50
20	m3r4	$N(-4.25, 0.75^2)$	10	10	10	10	10	10	10	10	10	10
		$N(-4.5, 0.5^2)$	10	10	10	10	10	10	10	10	10	10
		$N(-4.5, 0.75^2)$	10	10	10	10	10	10	10	10	10	10
		$N(-4.5, 1.0^2)$	10	10	10	10	10	10	10	10	10	10
		$N(-4.75, 0.75^2)$	10	10	10	10	10	10	10	10	10	10
	m2r2	$N(-4.25, 0.75^2)$	10	10	10	10	10	10	10	10	10	10
		$N(-4.5, 0.5^2)$	10	10	10	10	10	10	10	10	10	10
		$N(-4.5, 0.75^2)$	10	10	10	10	10	10	10	10	10	10
		$N(-4.5, 1.0^2)$	10	10	10	10	10	10	10	10	10	10
		$N(-4.75, 0.75^2)$	10	10	10	10	10	10	10	10	10	10
	m1r2	$N(-4.25, 0.75^2)$	10	20	10	10	10	10	10	10	10	10
		$N(-4.5, 0.5^2)$	10	20	10	10	10	10	10	10	10	10
		$N(-4.5, 0.75^2)$	10	20	10	10	10	10	10	10	10	10
		$N(-4.5, 1.0^2)$	10	20	10	10	10	10	10	10	10	10
		$N(-4.75, 0.75^2)$	20	20	10	10	20	10	10	10	20	10
	m1r1	$N(-4.25, 0.75^2)$	10	20	10	10	10	10	10	10	10	10
		$N(-4.5, 0.5^2)$	10	20	10	10	10	10	10	10	10	10
		$N(-4.5, 0.75^2)$	10	20	10	10	10	10	10	10	10	10
		$N(-4.5, 1.0^2)$	10	20	10	10	10	10	10	10	10	10
		$N(-4.75, 0.75^2)$	10	20	10	10	10	10	10	10	10	10

Table B.5. The number of plots needed to achieve overlap for a maximum of ten of the repetitions.
As determined using the 2-tailed 95 or 99 % confidence intervals of the annual mortality rates of the first and second consolidated sets (M1M2_95, M1M2_99), or a maximum of ten repetitions where zero was contained within the two-tailed and one-tailed 95 or 99 % confidence intervals of the absolute (in percentage points) and relative difference between the annual mortality rates of the second and the first consolidated sets (ppD_95(2), ppD_95(1), ppD_9592), ppD_99(1), relD_95(2), relD_95(1), relD_99(2), relD_99(1)), for the different consolidated interval lengths (consolLn), population dynamics variations (dynVar), and mortality rate distributions (mortDistr). Darker shading indicates more plots are needed, up to a simulated maximum of 100.

consolLn	dynVar	mortDistr	M1M2_95	M1M2_99	ppD_95(2)	ppD_95(1)	ppD_99(2)	ppDiff_99(1)	relD_95(2)	relD_95(1)	relD_99(2)	relD_99(1)
5	m3r4	$N(-4.25, 0.75^2)$	>100	>100	20	20	20	20	20	20	20	20
		$N(-4.5, 0.5^2)$	>100	>100	20	10	30	20	20	20	30	20
		$N(-4.5, 0.75^2)$	>100	>100	20	10	20	20	20	10	20	20
		$N(-4.5, 1.0^2)$	>100	>100	20	10	20	20	20	10	20	20
		$N(-4.75, 0.75^2)$	>100	>100	20	20	30	30	20	20	30	30
	m2r2	$N(-4.25, 0.75^2)$	>100	>100	40	30	60	50	40	30	60	50
		$N(-4.5, 0.5^2)$	>100	>100	40	40	60	40	40	40	60	60
		$N(-4.5, 0.75^2)$	>100	>100	40	30	50	50	40	30	50	50
		$N(-4.5, 1.0^2)$	>100	>100	30	30	70	40	30	30	40	40
		$N(-4.75, 0.75^2)$	>100	>100	40	50	60	60	50	40	70	60
	m1r2	$N(-4.5, 1.0^2)$	>100	>100	>100	100	>100	>100	>100	100	>100	>100
10	m3r4	$N(-4.25, 0.75^2)$	30	40	10	10	10	10	10	10	10	10
		$N(-4.5, 0.5^2)$	30	40	10	10	10	10	10	10	10	10
		$N(-4.5, 0.75^2)$	30	40	10	10	10	10	10	10	10	10
		$N(-4.5, 1.0^2)$	30	40	10	10	10	10	10	10	10	10
		$N(-4.75, 0.75^2)$	30	40	10	10	10	10	10	10	10	10
	m2r2	$N(-4.25, 0.75^2)$	30	50	10	10	10	10	10	10	10	10
		$N(-4.5, 0.5^2)$	30	50	10	10	20	10	10	10	20	10
		$N(-4.5, 0.75^2)$	30	50	10	10	20	10	10	10	20	10
		$N(-4.5, 1.0^2)$	30	50	10	10	10	10	10	10	10	10
		$N(-4.75, 0.75^2)$	30	50	10	10	20	10	10	10	20	20
	m1r2	$N(-4.25, 0.75^2)$	50	70	20	20	30	30	20	20	30	30
		$N(-4.5, 0.5^2)$	60	100	40	30	40	40	40	30	40	40
		$N(-4.5, 0.75^2)$	70	90	20	20	40	30	30	20	40	30
		$N(-4.5, 1.0^2)$	50	80	20	20	40	30	20	20	40	30
		$N(-4.75, 0.75^2)$	70	>100	40	30	50	50	40	30	60	50

Table B.5. (Continued) The number of plots needed to achieve overlap for a maximum of ten of the repetitions.

consolLn	dynVar	mortDistr	M1M2_95	M1M2_99	ppD_95(2)	ppD_95(1)	ppD_99(2)	ppDiff_99(1)	relD_95(2)	relD_95(1)	relD_99(2)	relD_99(1)
10	m1r1	$N(-4.25, 0.75^2)$	50	70	20	20	30	30	30	20	30	30
		$N(-4.5, 0.5^2)$	70	100	40	30	50	40	40	30	50	40
		$N(-4.5, 0.75^2)$	50	80	20	20	30	30	20	20	30	30
		$N(-4.5, 1.0^2)$	50	80	20	20	30	30	20	20	30	30
		$N(-4.75, 0.75^2)$	60	100	30	20	50	40	30	20	50	40
20	m3r4	$N(-4.25, 0.75^2)$	10	10	10	10	10	10	10	10	10	10
		$N(-4.5, 0.5^2)$	10	10	10	10	10	10	10	10	10	10
		$N(-4.5, 0.75^2)$	10	10	10	10	10	10	10	10	10	10
		$N(-4.5, 1.0^2)$	10	10	10	10	10	10	10	10	10	10
		$N(-4.75, 0.75^2)$	10	10	10	10	10	10	10	10	10	10
	m2r2	$N(-4.25, 0.75^2)$	10	10	10	10	10	10	10	10	10	10
		$N(-4.5, 0.5^2)$	10	10	10	10	10	10	10	10	10	10
		$N(-4.5, 0.75^2)$	10	10	10	10	10	10	10	10	10	10
		$N(-4.5, 1.0^2)$	10	10	10	10	10	10	10	10	10	10
		$N(-4.75, 0.75^2)$	10	10	10	10	10	10	10	10	10	10
	m1r2	$N(-4.25, 0.75^2)$	10	10	10	10	10	10	10	10	10	10
		$N(-4.5, 0.5^2)$	10	20	10	10	10	10	10	10	10	10
		$N(-4.5, 0.75^2)$	10	20	10	10	10	10	10	10	10	10
		$N(-4.5, 1.0^2)$	10	20	10	10	10	10	10	10	10	10
		$N(-4.75, 0.75^2)$	10	20	10	10	10	10	10	10	10	10
	m1r1	$N(-4.25, 0.75^2)$	10	10	10	10	10	10	10	10	10	10
		$N(-4.5, 0.5^2)$	10	20	10	10	10	10	10	10	10	10
		$N(-4.5, 0.75^2)$	10	20	10	10	10	10	10	10	10	10
		$N(-4.5, 1.0^2)$	10	20	10	10	10	10	10	10	10	10
		$N(-4.75, 0.75^2)$	10	20	10	10	10	10	10	10	10	10

Appendix C. A comparison of the trend result metrics

Of the various trend result metrics used for determining the minimum number of plots required for each given set of parameters (consolidated interval length, dynamics variation, mortality distribution), the absence of an overlap with zero of the confidence intervals of the absolute (ppDiff) and relative (relDiff) differences between the two sets were found to be the most efficient at detecting an increase in annual mortality rates between two consecutive sets of census intervals across all parameters.

When there was minimal or no overlap between the first and second consolidated sets, as was the case for the 20 year consolidated interval length (which samples 40 consecutive years out of a total 50-year period), the lack of overlap between the 95 % confidence intervals of the annual mortality rates of the first and second set proved nearly as efficient as the absence of overlap of the two-tailed 99 % confidence interval of ppDiff and relDiff with zero, but at shorter interval lengths the former trend result metric required on average 10-30 more plots to detect an increase of the same magnitude.

Since the 99 % confidence interval is wider than the 95 % confidence interval, and a two-tailed interval has a lower lower bound, compared to a one-tailed confidence interval, in general the least amount of plots needed to detect an increase was found for the one-tailed 95 % confidence interval, followed by the two-tailed 95 %, one-tailed 99 %, and finally the two-tailed 99 % confidence interval.

For some population dynamics variations or mortality distributions, the number of plots required to detect an increase was the same across all these confidence interval measures (e.g. 20 plots for both ppDiff and relDiff for no repetitions overlapping for variation m2r2, distributions $N(-4.5, 0.75^2)$ and $N(-4.75, 0.75^2)$, 10 year consolidated length). In other cases, a difference of 40 plots or greater was required for detecting the same increase between the one-tailed 95 % confidence interval and the two-tailed 99 % confidence interval (e.g. 60+ plots for ppDiff and 70+ plots for relDiff for no overlap under variation m2r2, distribution $N(-4.5, 0.5^2)$, 5 year consolidated length).

In addition to the different levels of uncertainty associated with the confidence intervals, there are different significance levels associated with the proportion of repetitions where the confidence intervals did overlap with each other (when comparing the annual mortality rates of the consecutive sets) or zero (for ppDiff and relDiff).

In the strictest case, which has been applied here, the number of plots chosen was such that no overlap being found for any of the repetitions was stable, also at greater numbers of plots. In some cases this resulted in the required number of plots being 20 higher, since no overlap was found at e.g. 40 plots (one-tailed 95 % confidence interval of ppDiff,

variation m2r2, distribution $N(-4.5, 0.75^2)$, 5 year consolidated interval length), but overlap was found again for three of the repetitions at 50 plots, before dropping back down permanently to no overlap for 60 plots and over. Consequently, when allowing the confidence intervals of 3 % of repetitions to contain zero, only 40 plots were required to detect the 2 % increase in annual mortality rates in this scenario.

Appendix D. Plots for short-term mortality rate increases

Table D.1. The number of plots required to detect a short-term increase in mortality rates.
Confidence from high to low: none (0 %; top left), one (1 %; top right), two (2 %; lower left) or five (5 %; lower right) of the total 100 repetitions' 95 % confidence intervals contain zero, using the percentage points difference between mortality rates drawn from distributions with a mean of -4.5 or -4.25 (SD 0.75 for both) in logistic space and the relative increase in annual mortality rates ("Incr."; in%), for events lasting one or two years ("Dur."; in years), at a census interval length of two years, under various population dynamics scenarios (m denotes relative increase in annual mortality rates, r relative increase in recruitment).

0 % overlap		-4.5				-4.25
Dur.	**Incr.**	**m0r0**	**m2r2**	**m2r3**	**m4r4**	**m0r0**
1	**5**	>250	*NA*	*NA*	*NA*	>250
	7.5	>250	*NA*	*NA*	*NA*	*NA*
	10	250	190	170	130	>250
	15	>250	*NA*	*NA*	*NA*	*NA*
	20	190	100	140	80	100
	30	80	*NA*	*NA*	*NA*	*NA*
	40	40	*NA*	*NA*	*NA*	*NA*
	50	30	20	30	20	40
	75	20	*NA*	*NA*	*NA*	20
	100	10	10	*NA*	*NA*	*NA*
2	**5**	250	*NA*	*NA*	*NA*	200
	7.5	190	*NA*	*NA*	*NA*	*NA*
	10	130	50	50	30	80
	15	40	*NA*	*NA*	*NA*	*NA*
	20	20	20	20	20	20
	30	10	*NA*	*NA*	*NA*	*NA*
	40	10	*NA*	*NA*	*NA*	*NA*
	50	10	10	*NA*	*NA*	*NA*
	75	10	*NA*	*NA*	*NA*	*NA*
	100	10	10	*NA*	*NA*	*NA*

1 % overlap		-4.5				-4.25
Dur.	**Incr.**	**m0r0**	**m2r2**	**m2r3**	**m4r4**	**m0r0**
1	**5**	>250	*NA*	*NA*	*NA*	>250
	7.5	>250	*NA*	*NA*	*NA*	*NA*
	10	190	190	160	130	>250
	15	200	*NA*	*NA*	*NA*	*NA*
	20	160	100	110	80	100
	30	80	*NA*	*NA*	*NA*	*NA*
	40	30	*NA*	*NA*	*NA*	*NA*
	50	30	20	30	20	30
	75	20	*NA*	*NA*	*NA*	20
	100	10	10	*NA*	*NA*	*NA*
2	**5**	250	*NA*	*NA*	*NA*	160
	7.5	140	*NA*	*NA*	*NA*	*NA*
	10	100	50	50	30	80
	15	40	*NA*	*NA*	*NA*	*NA*
	20	20	20	20	20	20
	30	10	*NA*	*NA*	*NA*	*NA*
	40	10	*NA*	*NA*	*NA*	*NA*
	50	10	10	*NA*	*NA*	*NA*
	75	10	*NA*	*NA*	*NA*	*NA*
	100	10	10	*NA*	*NA*	*NA*

2 % overlap		-4.5				-4.25
Dur.	**Incr.**	**m0r0**	**m2r2**	**m2r3**	**m4r4**	**m0r0**
1	**5**	>250	*NA*	*NA*	*NA*	>250
	7.5	>250	*NA*	*NA*	*NA*	*NA*
	10	180	190	140	100	>250
	15	190	*NA*	*NA*	*NA*	*NA*
	20	160	90	100	70	100
	30	70	*NA*	*NA*	*NA*	*NA*
	40	30	*NA*	*NA*	*NA*	*NA*
	50	30	20	20	20	30
	75	20	*NA*	*NA*	*NA*	20
	100	10	10	*NA*	*NA*	*NA*
2	**5**	230	*NA*	*NA*	*NA*	160
	7.5	140	*NA*	*NA*	*NA*	*NA*
	10	100	40	50	30	60
	15	30	*NA*	*NA*	*NA*	*NA*
	20	20	20	20	20	20
	30	10	*NA*	*NA*	*NA*	*NA*
	40	10	*NA*	*NA*	*NA*	*NA*
	50	10	10	*NA*	*NA*	*NA*
	75	10	*NA*	*NA*	*NA*	*NA*
	100	10	10	*NA*	*NA*	*NA*

5 % overlap		-4.5				-4.25
Dur.	**Incr.**	**m0r0**	**m2r2**	**m2r3**	**m4r4**	**m0r0**
1	**5**	>250	*NA*	*NA*	*NA*	>250
	7.5	>250	*NA*	*NA*	*NA*	*NA*
	10	160	150	110	90	250
	15	180	*NA*	*NA*	*NA*	*NA*
	20	160	90	90	70	80
	30	60	*NA*	*NA*	*NA*	*NA*
	40	30	*NA*	*NA*	*NA*	*NA*
	50	20	20	20	20	20
	75	10	*NA*	*NA*	*NA*	10
	100	10	10	*NA*	*NA*	*NA*
2	**5**	220	*NA*	*NA*	*NA*	130
	7.5	140	*NA*	*NA*	*NA*	*NA*
	10	80	40	40	30	50
	15	30	*NA*	*NA*	*NA*	*NA*
	20	20	10	20	10	20
	30	10	*NA*	*NA*	*NA*	*NA*
	40	10	*NA*	*NA*	*NA*	*NA*
	50	10	10	*NA*	*NA*	*NA*
	75	10	*NA*	*NA*	*NA*	*NA*
	100	10	10	*NA*	*NA*	*NA*

Appendix E. All pan-tropical hierarchical model descriptions

Plots with fewer censuses should still yield reliable distributions due to the hierarchical nature of HL2 models, but the effect of specifying a minimum number of censuses per plot and a minimum number of plots satisfying this condition per spatial region is tested for, using no minimum (models with suffix '_min0'), a minimum of three (suffix '_min3'), of five (suffix '_min5') and of seven (suffix '_min7') censuses per plot and the specified minimum number of plots, with this minimum number of plot censuses, per region. Since the mean and standard deviation of the plots' logit-normal distributions are assumed to exhibit logit-normal distributions for all plots combined on a regional scale, and regions with a higher mean annual mortality rate could be expected to also have a higher variation in annual mortality rates, HL2 models are tested using both the assumption of correlation between these regional distributions (suffix '_bivar') or independence (suffix '_noBivar').

In the higher-level models (HL1 & HL2) the assumption of not only the average mortality differing per region, but also the variation of regional mortality rates, is tested by having one set of models where the mean and standard deviation parameters are estimated separately for each bio-geographical or continental region (suffix '_indivSd') and one set where the mean of the regional distributions is estimated per individual region, but a single standard deviation value is estimated for all the regions (suffix '_regSd'). For each model we obtain estimates, and uncertainty, for all relevant model parameters (Table E.1, Table E.2) using three chains with an appropriate number of burn-in iterations to ensure convergence (increasing with number of observations per region and model complexity).

When the regional mean and standard deviation distributions are assumed to be correlated, since plots with a higher mean mortality rate might be expected to have a higher standard deviation, k_x and $\log(\sigma_x)$ are drawn from a regional scale bivariate normal distribution, with the subscript 'μ, c' relating to the mean and standard deviation of the long term spatial mean on a regional scale, and 'σ, c' to the mean and standard deviation of the long term spatial standard deviation on a regional scale; ρ_c denotes the correlation between these two

$$\{k_x,\ \log(\sigma_x)\} \sim N(k_{\mu,c}, k_{\sigma,c},\ \sigma_{\mu,c}, \sigma_{\sigma,c}, \rho_c) \qquad \text{(E-1)}$$

Table E.1. All hierarchical pan-tropical models and their properties.
The region represented at the first and second hierarchical level (if present), the minimum number of plot censuses per plot/plots per region and whether the bivariate normal distribution was used.

Model Code	1st Hier. level	2nd Hier. level	Min. pc/p	Incl. bivar.
HL0	-	-	-	-
HL1BGR	Biogeographical	-	-	-
HL1C	Continental	-	-	-
HL1PT	Pan-tropical	-	-	-
HL2BGR_min0_bivar	Plot	Biogeographical	0	Y
HL2BGR_min0_noBivar	Plot	Biogeographical	0	N
HL2BGR_min3_bivar	Plot	Biogeographical	3	Y
HL2BGR_min3_noBivar	Plot	Biogeographical	3	N
HL2BGR_min5_bivar	Plot	Biogeographical	5	Y
HL2BGR_min5_noBivar	Plot	Biogeographical	5	N
HL2BGR_min7_bivar	Plot	Biogeographical	7	Y
HL2BGR_min7_noBivar	Plot	Biogeographical	7	N
HL2C_min0_bivar	Plot	Continental	0	Y
HL2C_min0_noBivar	Plot	Continental	0	N
HL2C_min3_bivar	Plot	Continental	3	Y
HL2C_min3_noBivar	Plot	Continental	3	N
HL2C_min5_bivar	Plot	Continental	5	Y
HL2C_min5_noBivar	Plot	Continental	5	N
HL2C_min7_bivar	Plot	Continental	7	Y
HL2C_min7_noBivar	Plot	Continental	7	N
HL2PT_min0_bivar	Plot	Pan-tropical	0	Y
HL2PT_min0_noBivar	Plot	Pan-tropical	0	N
HL2PT_min3_bivar	Plot	Pan-tropical	3	Y
HL2PT_min3_noBivar	Plot	Pan-tropical	3	N
HL2PT_min5_bivar	Plot	Pan-tropical	5	Y
HL2PT_min5_noBivar	Plot	Pan-tropical	5	N
HL2PT_min7_bivar	Plot	Pan-tropical	7	Y
HL2PT_min7_noBivar	Plot	Pan-tropical	7	N

Table E.2. All hierarchical pan-tropical model parameters and their descriptions.

Par.	Description
N_0	Number of trees with dbh > 10 cm alive in region (HL1 models) or plot (HL2 models) x at start of census interval t of length T years
N_1	Number of trees out of N_0 in region (HL1 models) or plot (HL2 models) x that have survived the census interval t of length T years
x	Region (HL1 models) or plot (HL2 models) identification number
t	Census interval identification number
T	Census interval length (years)
$m_{x,t}$	The observed mortality rate in region/plot x during census interval t of length T years (years^{-1})
$k_{x,t}$	Estimated mortality rate in region/plot x during census interval t of length T years, in logistic parameter space (years^{-1})
$\mu_{x,t}$	Logistic transformation of $k_{x,t}$ (years^{-1})
k_x	Estimated overall mean mortality rate in region/plot x (across all census intervals), in logistic parameter space (years^{-1})
μ_x	Logistic transformation of k_x (years^{-1}); median of the back-transformed logit-normal distribution
σ_x	Estimated overall standard deviation in mortality rates in region/plot x (across all census intervals; years^{-1})
$k_{\mu,c}$	Estimated overall mean of mean mortality rates in region c (across all plots in that region), in logistic parameter space (years^{-1})
$k_{\sigma,c}$	Estimated overall standard deviation in mean mortality rates in region c (across all plots in that region; years^{-1})
$\sigma_{\sigma,c}$	Estimated overall mean of standard deviations in mortality rates in region c (across all plots in that region), in logarithmic parameter space (years^{-1})
$\sigma_{\sigma,c}$	Estimated overall standard deviation in standard deviations of mortality rates in region c (across all regions in that continent), in logarithmic parameter space (years^{-1})
ρ_c	Correlation coefficient between mean and standard deviation distributions in region c (across all plots in that region)